PSD8

8TH INTERNATIONAL CONFERENCE ON POSITION SENSITIVE DETECTORS

Gas Pixel Detector and beyond

R. Bellazzini

INFN - sez. Pisa, Pisa, Italy

8th International Conference on Position Sensitive Detectors

Glasgow, Scotland, 1st to the 5th of September

Polarimetry: The Missing Piece of the Puzzle

Imaging: Chandra

Timing: RXTE

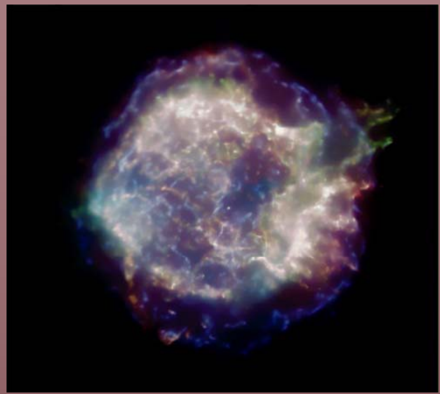

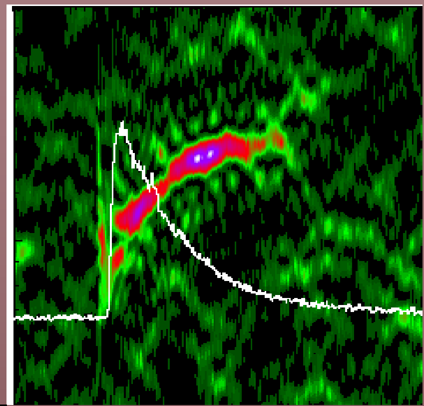

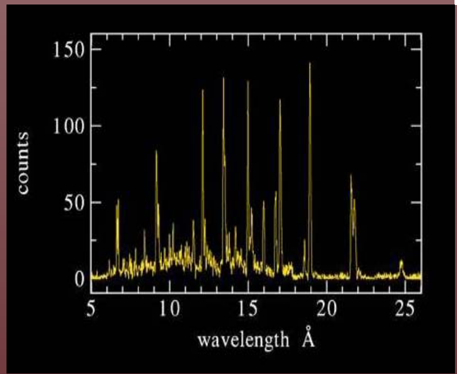

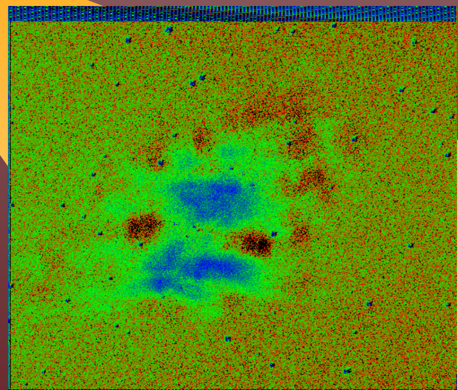

Spectroscopy: AstroE2, Constellation-X, Chandra

Polarimetry: ?

The only polarized source already known

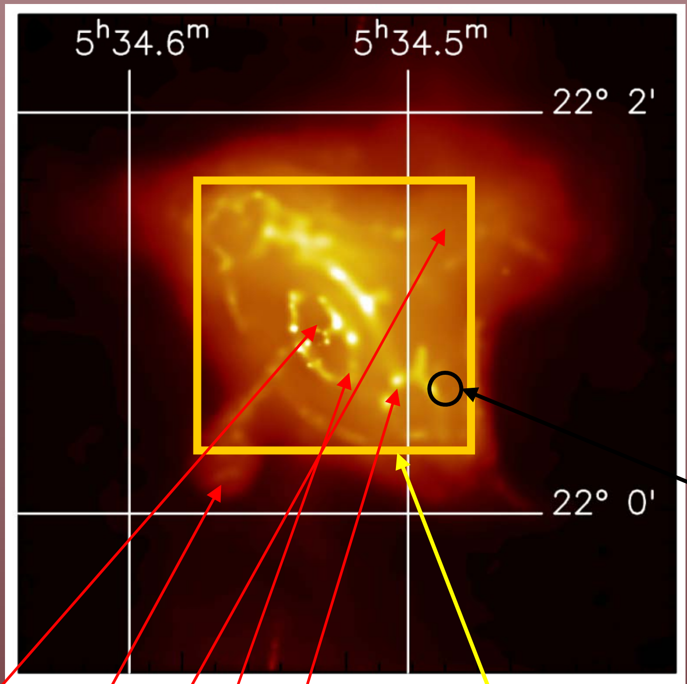

p.s.f.

f.o.v.

PSR

NW jet

SE jet

Inner torus

Outer torus

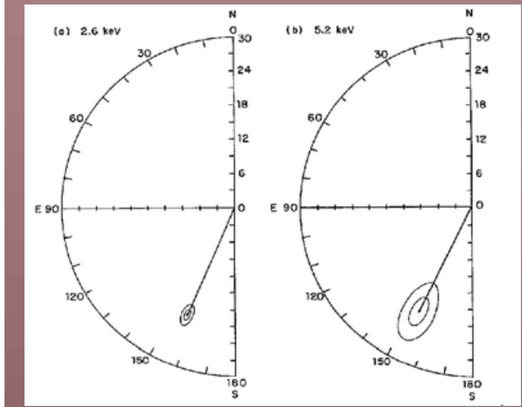

Positive measurement: of X-ray polarization of the Crab Nebula without pulsar contamination (by lunar occultation, Weisskopf et al., 1978).

$P = 19.2 \pm 1.0$ %

$\theta = 156.4^o \pm 1.4^o$

But this is only the average measurement. The structure is much more complex!

With XPOL we can perform the separate polarimetry, imaging, spectroscopy and timing of details of the major structures

The principle of detection

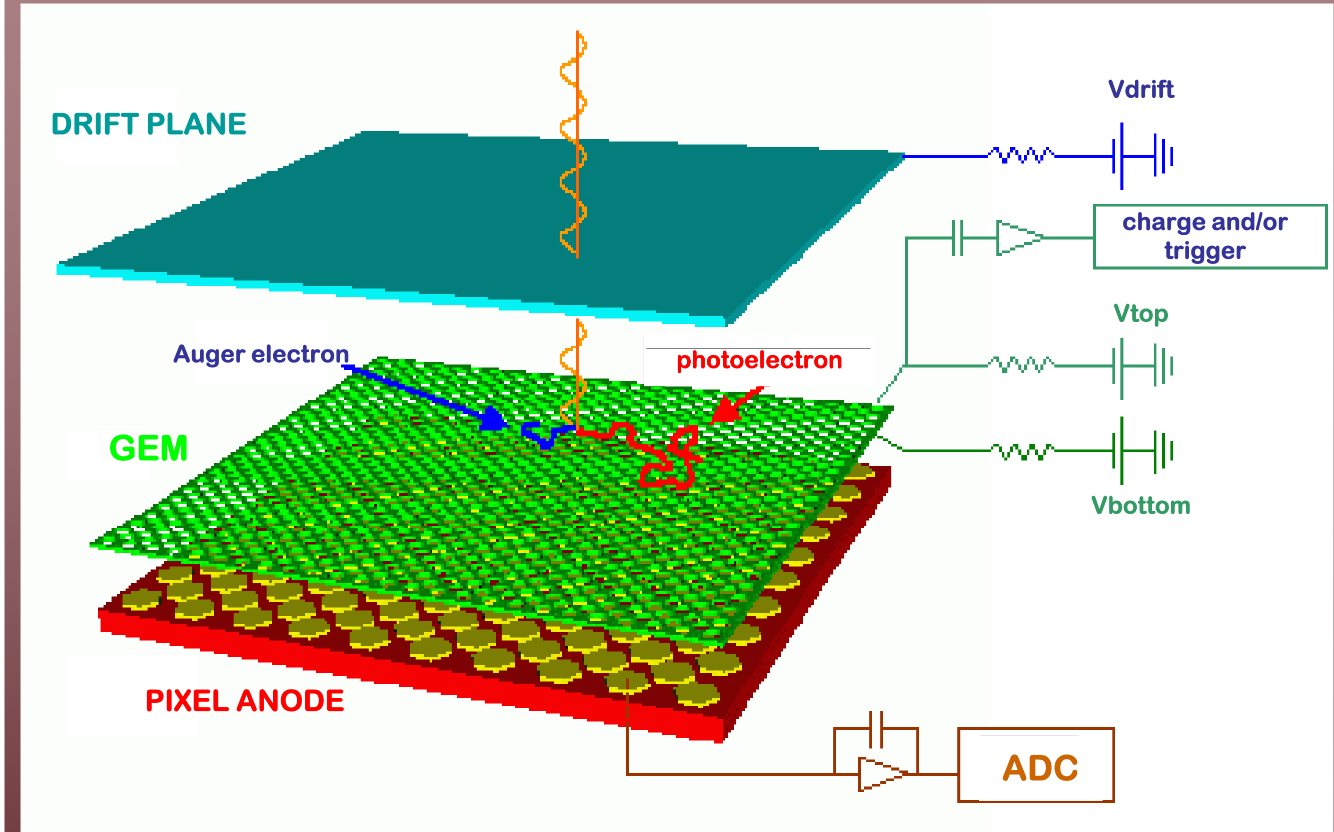

GEM electric field

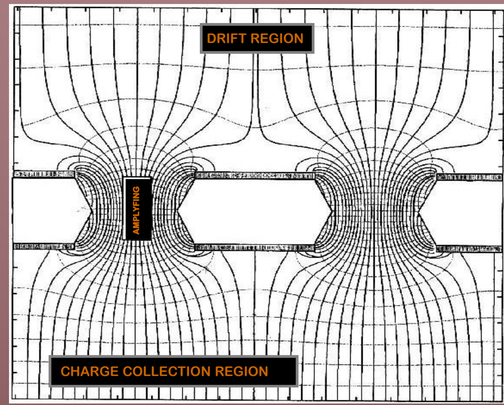

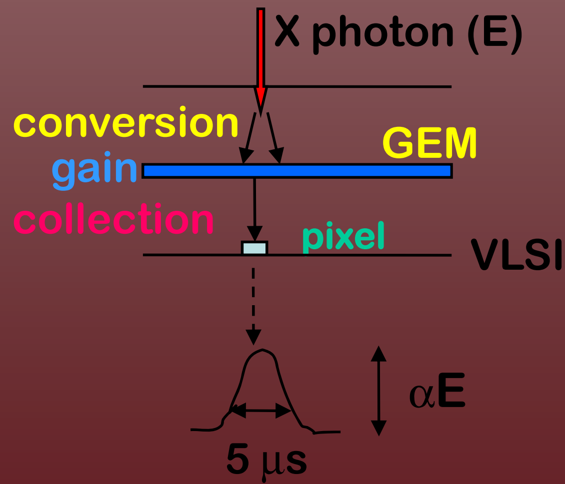

A custom CMOS analog chip is at the same time the pixelized charge collecting electrode and the amplifying, shaping and charge measuring front-end electronics of Micropattern Gas Detectors (MPGD) or other suitable charge multiplier

Table 1 Physical characteristics and performances of the micro-pattern detector

	Present prototype (2–10 keV)	Improved configuration (3.5–10 keV)
Drift/absorption gap	6 mm	30 mm
Drift field	3,000 V cm^{-1}	1,500 V cm^{-1}
Gas filling and pressure	(Ne 80%–DME 20%); 1 atm	(Ne 40%–DME 60%); 4 atm
Gas grain	5,000	2,500
Transverse diffusion in drift	80 μm	<100 μm
GEM thickness		kapton foil
GEM hole geometry		-μm pitch
GEM voltage		
Detection efficiency at 5.4 keV		
Read-out pixel size		
Number of pixels		
Read-out plane technology		
Track length/pixel size (6 keV)		= 10%
Sensitivity to Her X1		P = 1%
Sensitivity to 3C-273		P = 1%
Sensitivity to MCG-6-30-15		0 (over Bragg)
Gain in the integration time over SXRP (strong sources)		00 (over Bragg)
Gain in the integration time over SXRP (faint sources)		

We show also the observing time needed to measure (at 99% ... micro-pattern gas chamber (MPGC) is placed at the focus of th ... use only photons above 3.5 keV to compute the sensitivity. ... modulation. Her X-1 is a galactic ... polarimetry, a direct measure of ... Seyfert-1 galaxy for which a broa ... polarimeter foreseen in a future X ... polarization of Thomson scattering ... multiplier. VLSI, very large scale i ... sical sources if the ... proved design we ... antly reduces the ... d, by ... is a ... sitive ... e on ... tron

letters to nature

... of a new generation of photoelectric polarimeters in the 2–10 keV band. The device can simultaneously also produce good images (50–100 μm), moderately good spectroscopy (16% full-width at half-maximum, at 5.4 keV), and fast, high-rate timing down to 150 eV. Moreover, being truly two-dimensional, it is non-dispersive and does not require rotation.

We also tested our capability to model the polarization detection processes. As absorption, slowing down, scattering and transverse diffusion of electrons in the drift are well known quantities, we may reliably predict the performance of another detector configuration that would be better optimized for astrophysical applications. It is based on an existing[31] VLSI (Very Large Scale Integration) readout chip combined with other well established detector technology. We can derive the polarimetric sensitivity of such detectors when installed at the focus of a real X-ray telescope. In Table 1 we compare the sensitivity of the present and final configuration of the MPGC with SXRP.

The MPGC requires integration periods that are about 100 times shorter than those of the SXRP to detect the same polarization in bright sources. With integrations of the order of one day we could perform polarimetry of active galactic nuclei at the 1% level, a breakthrough in this fascinating window of high-energy astrophy-

9. Connors, P. A. & Stark, R. F. Observable gravitational effects on polarized radiation coming from near a black hole. *Nature* 269, 128–129 (1977).
10. Stark, R. F. & Connors, P. A. Observational test for the existence of a rotating black hole in Cyg X-1. *Nature* 266, 429–430 (1977).
11. Connors, P. A., Piran, T. & Stark, R. Polarization features of X-ray radiation emitted near a black hole. *Astrophys. J.* 235, 224–244 (1980).
12. Bao, G., Wiita, P. & Hadrava, P. Energy-dependent polarization variability as a black hole signature. *Phys. Rev. Lett.* 77, 12–15 (1996).
13. Celotti, A. & Matt, G. Polarization properties of synchrotron self-Compton emission. *Mon. Not. R. Astron. Soc.* 268, 451–458 (1994).
14. Poutanen, J. Relativistic jets in blazars: polarization of radiation. *Astrophys. J. Suppl. Ser.* 92, 607–609 (1994).
15. Tanaka, Y. *et al.* Gravitationally redshifted emission implying an accretion disk and massive black-hole in the active galaxy MCG-6-30-15. *Nature* 375, 659–661 (1995).
16. Ogura, J., Nobuyori, O. & Kojima, Y. Profiles and polarization properties of emission lines from relativistic disks. *Publ. Astron. Soc. Jpn* 52, 841–845 (2000).
17. Matt, G., Fabian, A. C. & Ross, R. R. X-ray photoionized accretion discs: UV and X-ray continuum spectra and polarization. *Mon. Not. R. Astron. Soc.* 264, 839–852 (1993).
18. Novick, R., Weisskopf, M. C., Berthelsdorf, R., Linke, R. & Wolff, R. S. Detection of X-ray polarization of the Crab Nebula. *Astrophys. J.* 174, L1–L8 (1972).
19. Weisskopf, M. C., Silver, E. H., Kestenbaum, H. L., Long, K. S. & Novick, R. A precision measurement of the X-ray polarization of the Crab Nebula without pulsar contamination. *Astrophys. J.* 220, L117–L122 (1978).
20. Kaaret, P. *et al.* SXRP: a focal plane stellar X-ray polarimeter for the Spectrum-X-Gamma mission. *Opt. Eng.* 29, 773–783 (1990).
21. Schnopper, H. W. & Kalata, K. Polarimeter for celestial X-rays. *Astron. J.* 74, 854–858 (1969).
22. Novick, R. in *Planets, Stars and Nebulae Studied with Photopolarimetry* (ed. Gerehls, T.) 262–317 (Univ. Arizona Press, Tucson, 1972).

30. Sauli, F. GEM: a new concept for electron amplification in gas detectors. *Nucl. Instrum. Methods A* 386, 531–534 (1997).
31. Campbell, M. *et al.* A pixel readout chip for 10–30 Mrad in standard 0.25μm CMOS. *IEEE Trans. Nucl. Sci.* 46, 156–160 (1999).
32. Bavdaz, M. *et al.* Status of the X-ray evolving universe spectroscopy mission (XEUS). *Proc. SPIE* 4138, 69–78 (2000).
33. Christensen, F. E. *et al.* X-ray calibration of the SODART flight telescope. *Proc. SPIE* 3113, 69–78 (1997).

An efficient photoelectric X-ray polarimeter for the study of black holes and neutron stars

E. Costa, P. Soffitta, R. Bellazzini, A. Brez, N. Lumb, G. Spandre

Nature, Vol. 411 (2001) 662.

Three ASIC generations of increasing size, reduced pitch and improved functionality have been realized

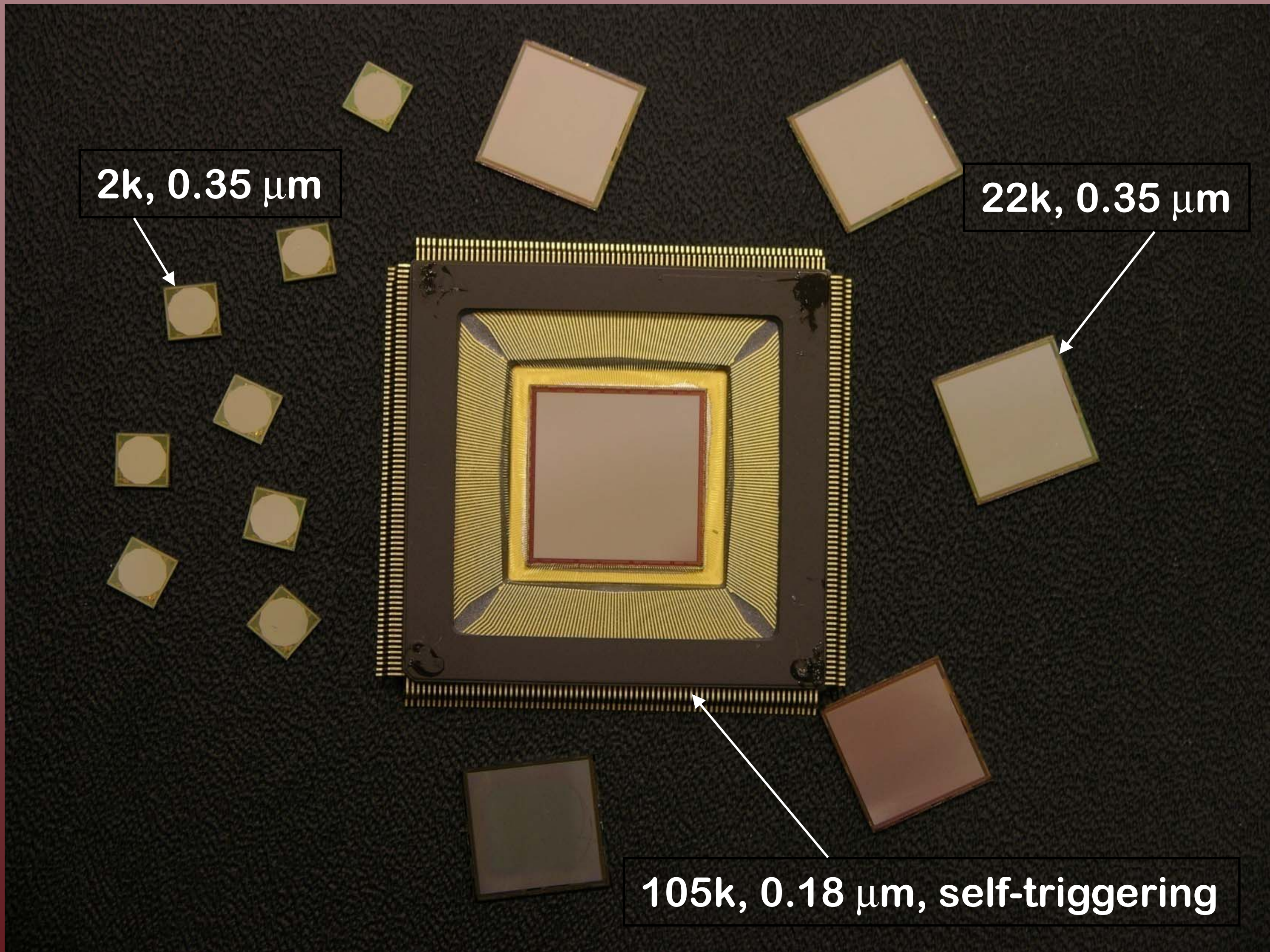

The collecting anode/read-out VLSI chip

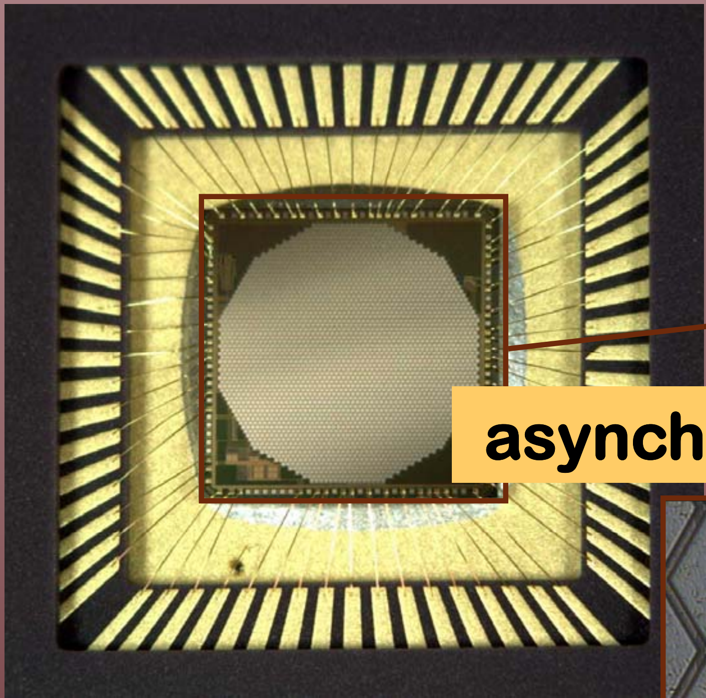

First ASIC prototype

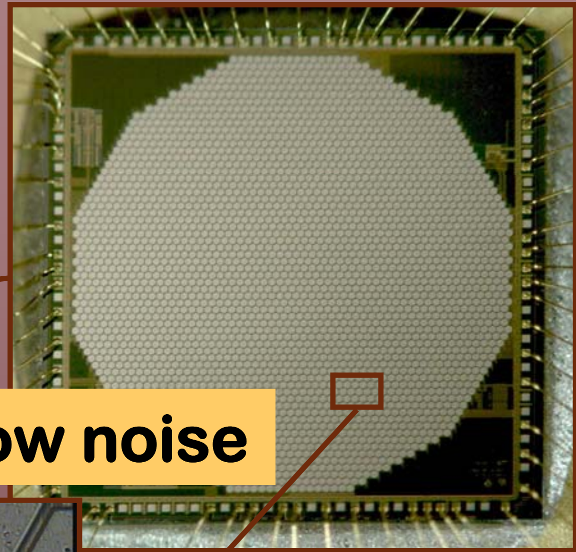

asynchronous, fast, low noise

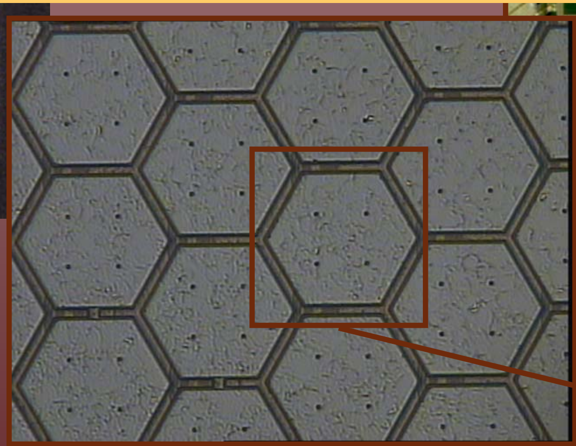

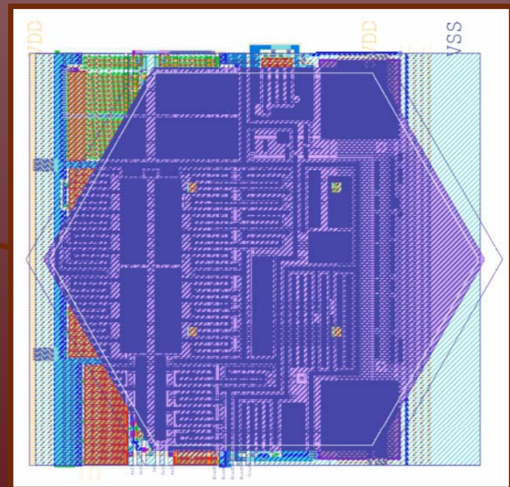

pixel electronics dimension:
80 μm x 80 μm in an hexagonal array,
comprehensive of preamplifier/shaper, S/H and routing (serial read-out) for each pixel
number of pixels: 2101

~3.5 μs shaping time
100 e- ENC
100 mv/fC input sensitivity
20 fC dynamic range

Last technological step: a 0.18 μm CMOS VLSI

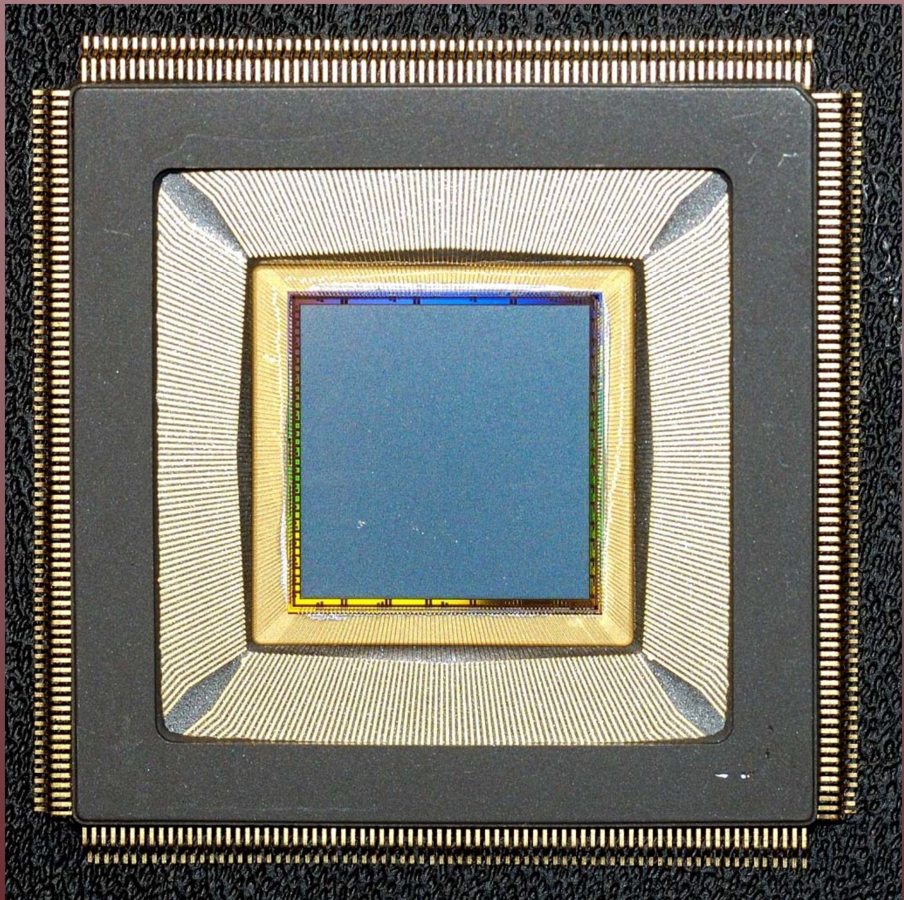

Matrix organization: 300 x 352 pixels
width=300x50μm=15mm,
height=352x43.3μm=15.24mm

The chip integrates more than 16.5 million transistors.
It has a15mm x 15mm active area of 105’600 pixels organized in a honeycomb matrix

470 pixels/mm^2
Pixel noise: 50 electrons ENC
Total power dissipation ~ 0.5 Watt

Detector assembly

- GEM pitch: 50 μm
- GEM holes diameters: 33 μm, 15 μm
- Read out pitch: 50 μm
- Absorption gap thickness: 10 mm
- Collection gap thickness: 1 mm

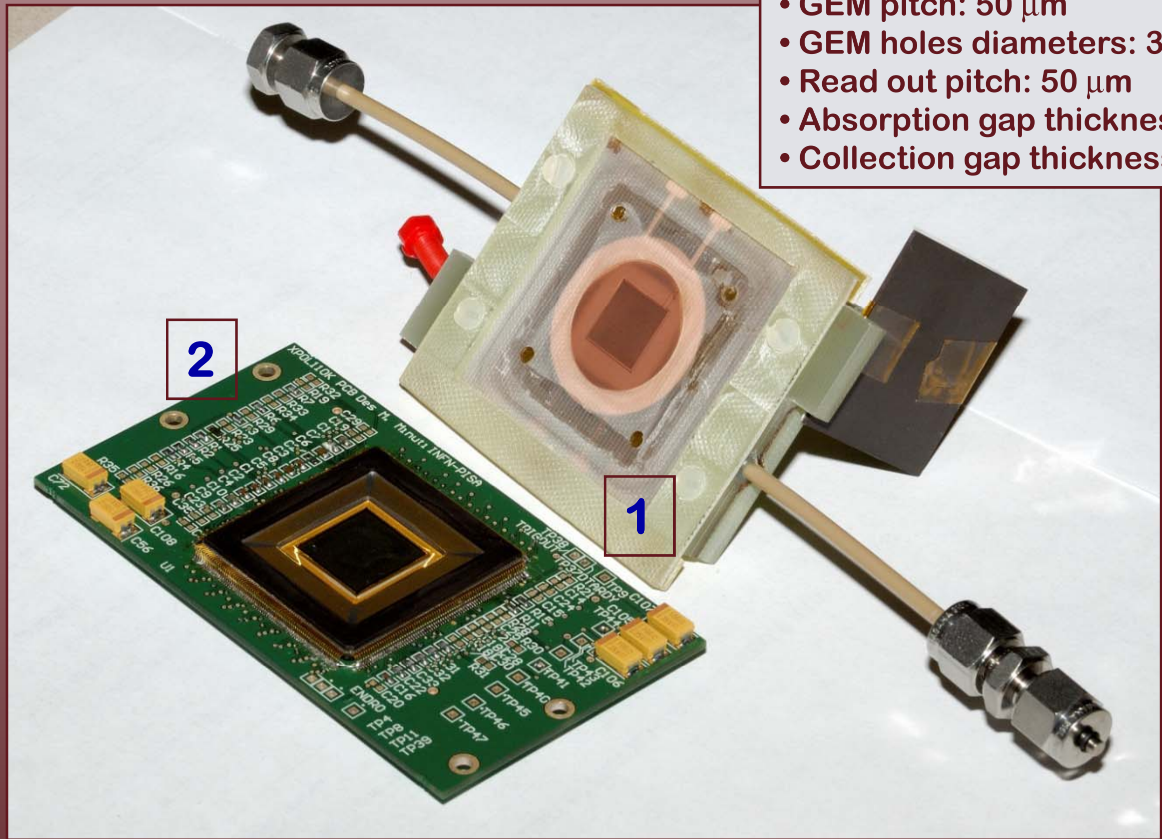

1 - The GEM glued to the bottom of the gas-tight enclosure
2 - The large area ASIC mounted on the control motherboard

Large effective gas gain around 1000 @450V in Ne(50%)-DME(50%)
(at least 70 V less than in our standard 90 μm pitch GEM)

GEM specs

pitch: 50 μm

holes outer Ø: 35 μm / inner Ø: 15 μm

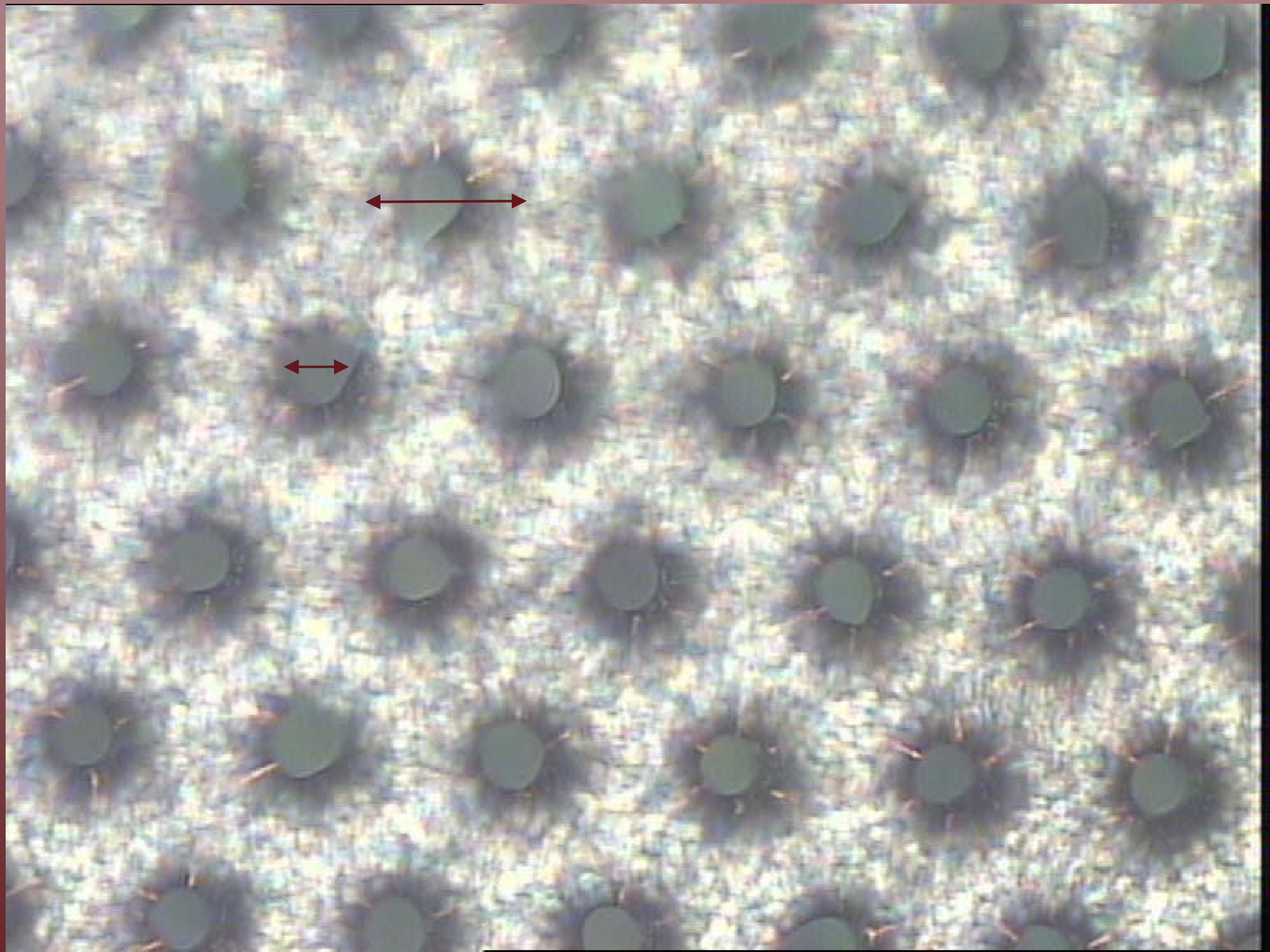

The matching of readout and gas amplification (GEM) pitch allows getting optimal results and to fully exploit the very high granularity of the device

Tracks reconstruction

1) The track is recorded by the PIXel Imager

2) Baricenter evaluation

3) Reconstruction of the principal axis of the track: maximization of the second moment of charge distribution

4) Reconstruction of the conversion point: major second moment (track length) + third moment along the principal axis (asymmetry of charge release)

5) Reconstruction of emission direction: pixels are weighted according to the distance from conversion point.

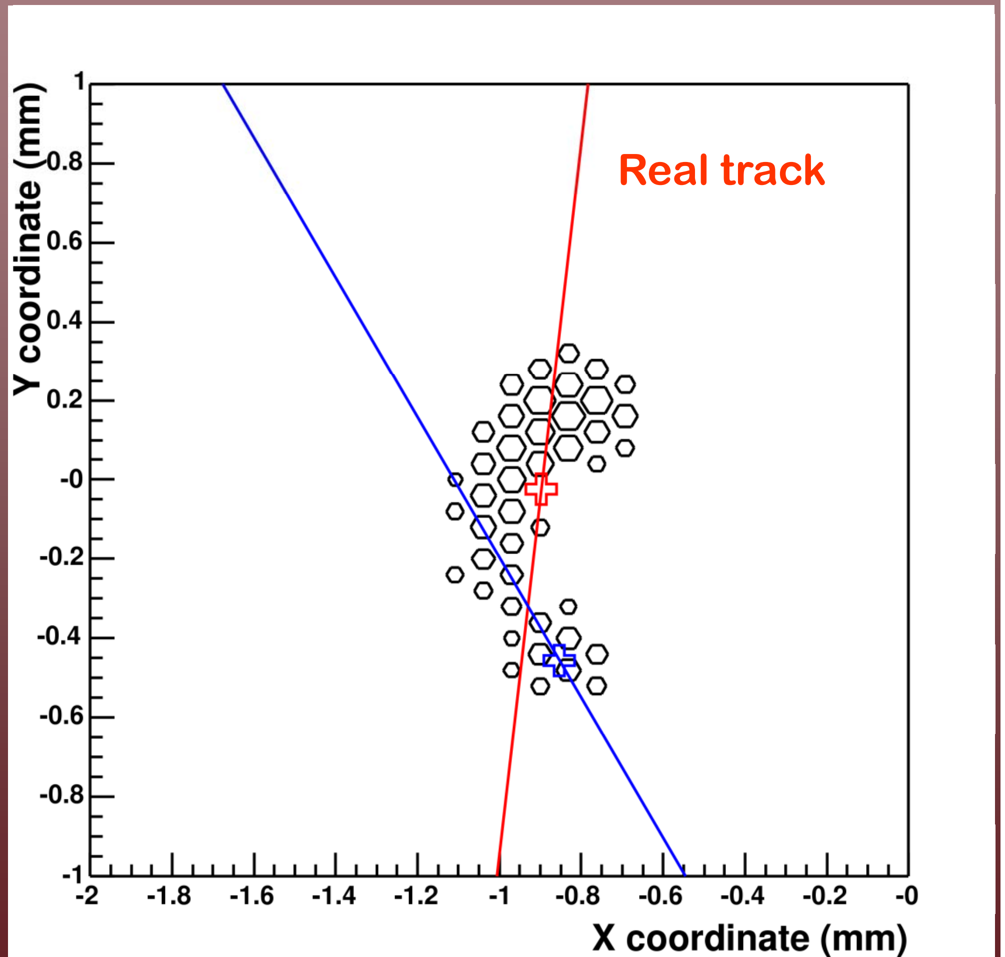

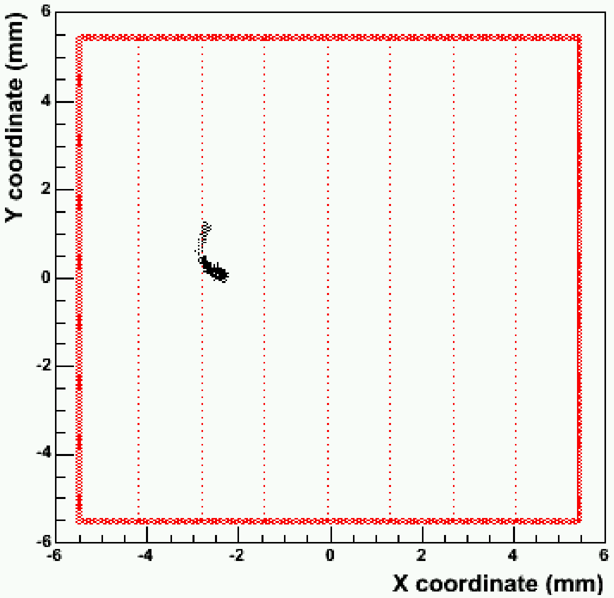

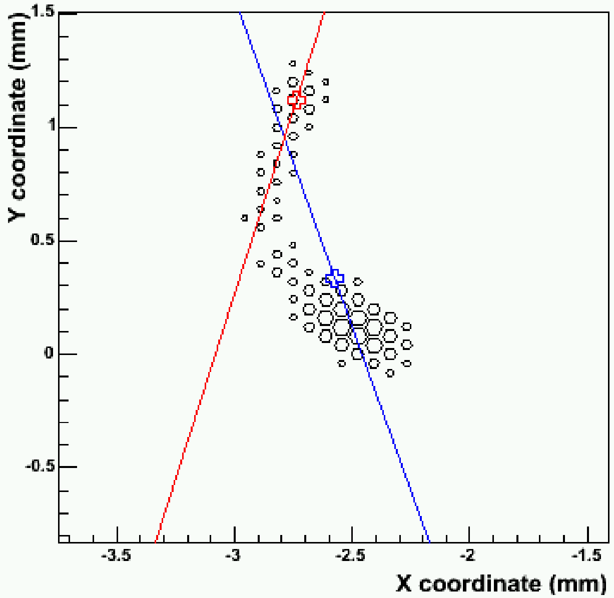

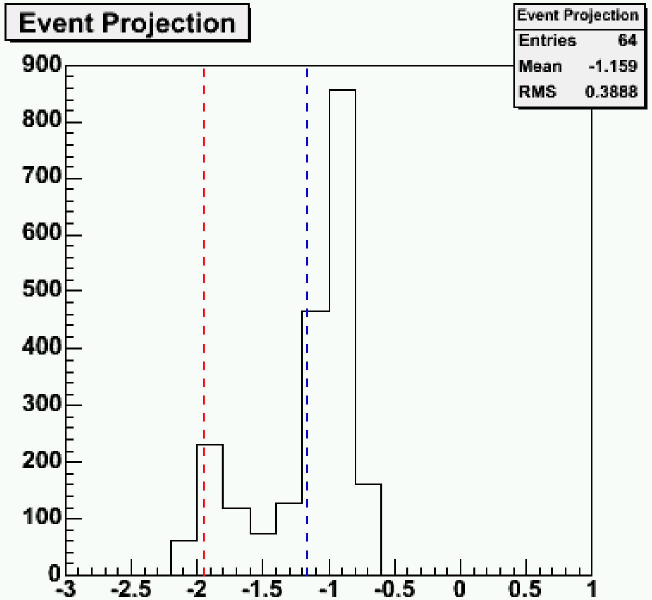

Event Number:	1
Number of Clusters:	1
Cluster Size (largest):	64
Pulse Height:	2097.1
Signal to Noise:	136.3
Baricenter:	-2.58 0.34
Conversion Point:	-2.73 1.12
Second Mom Max:	0.1511
Second Mom Min:	0.0128
Shape (ratio of moments):	11.85
Third Mom Max:	-6.5e-02
Phi (iteration 1)	-1.2381
Phi (iteration 2)	-1.8707

✚ Reconstructed Baricenter
✚ Reconstructed Impact Pt.

Track morphology and angle reconstruction

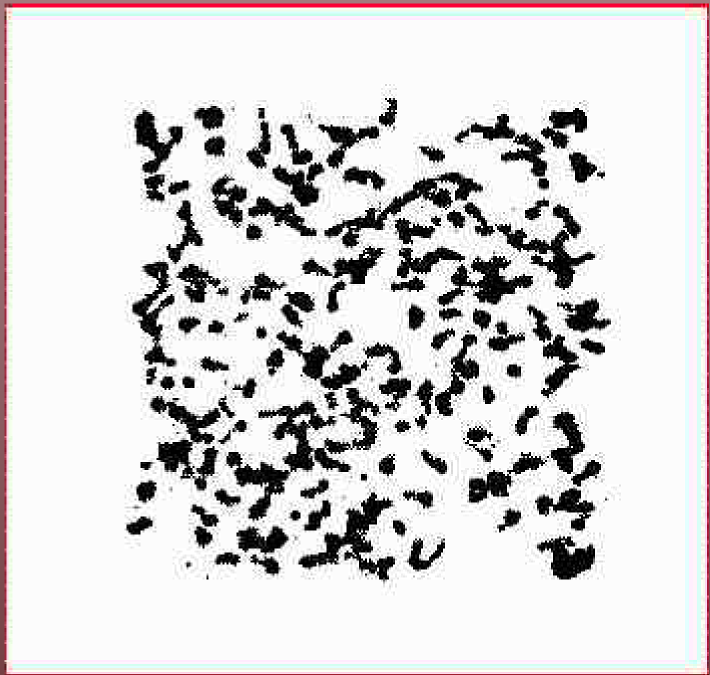

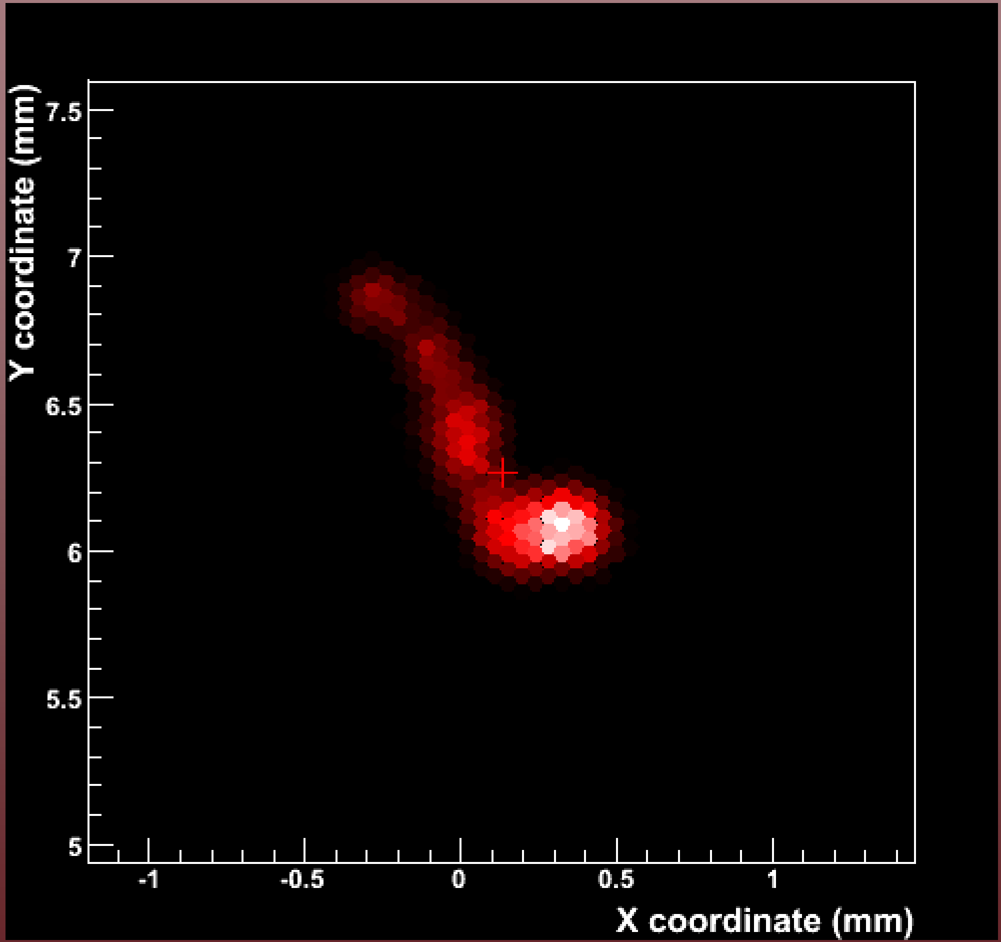

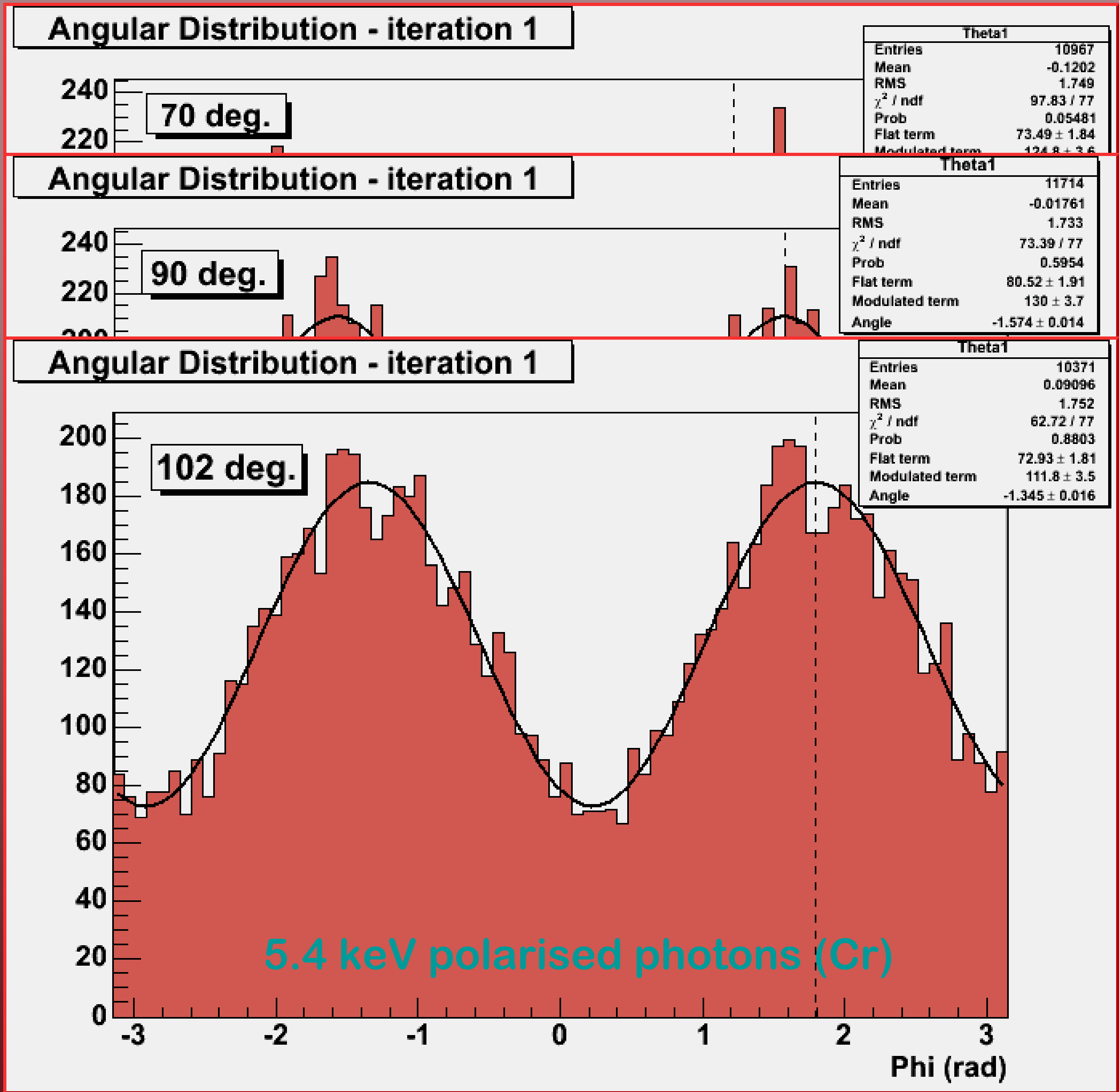

Angular Distribution - iteration 1
70 deg.
Theta1
Entries 10967
Mean -0.1202
RMS 1.749
χ² / ndf 97.83 / 77
Prob 0.05481
Flat term 73.49 ± 1.84
Angular Distribution - iteration 1
90 deg.
Theta1
Entries 11714
Mean -0.01761
RMS 1.733
χ² / ndf 73.39 / 77
Prob 0.5954
Flat term 80.52 ± 1.91
Modulated term 130 ± 3.7
Angle -1.574 ± 0.014
Angular Distribution - iteration 1
102 deg.
Theta1
Entries 10371
Mean 0.09096
RMS 1.752
χ² / ndf 62.72 / 77
Prob 0.8803
Flat term 72.93 ± 1.81
Modulated term 111.8 ± 3.5
Angle -1.345 ± 0.016
Phi (rad)
5.4 keV polarised photons (Cr)

Imaging capability

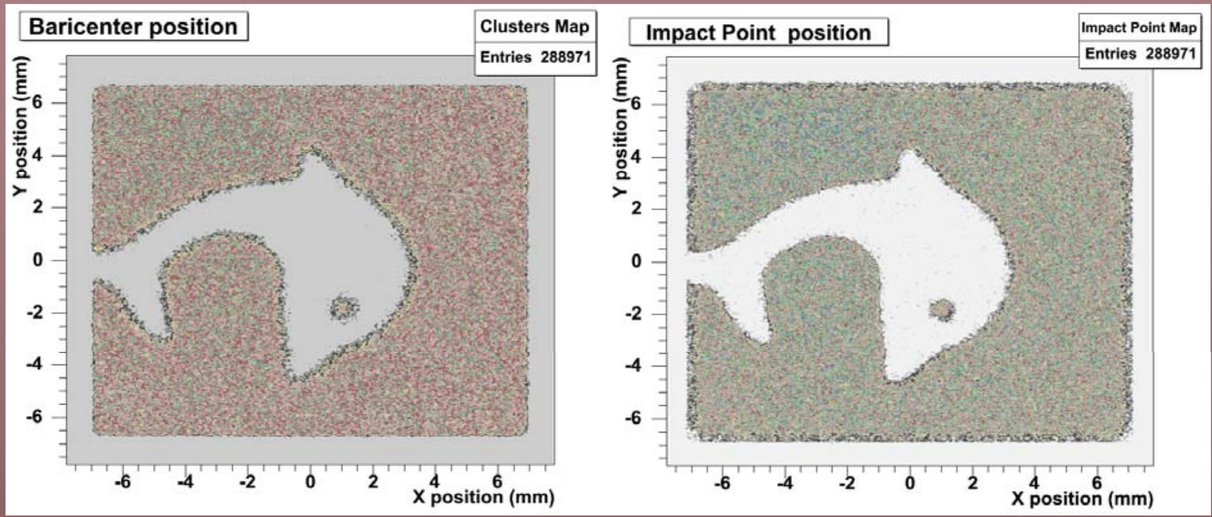

55Fe source Ne(50%)-DME(50%)

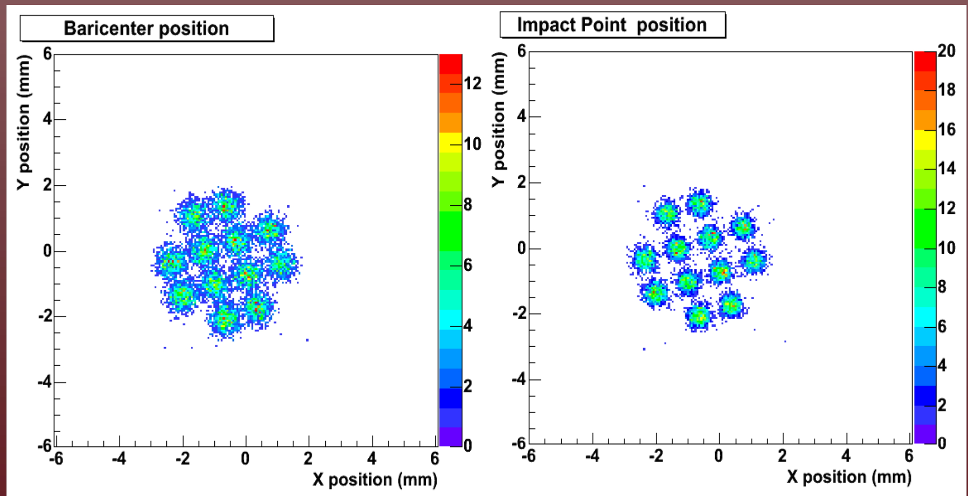

Holes: 0.6 mm diameter, 2 mm apart.

Imaging and spectroscopic capability

Argon (50%)-DME(50%)

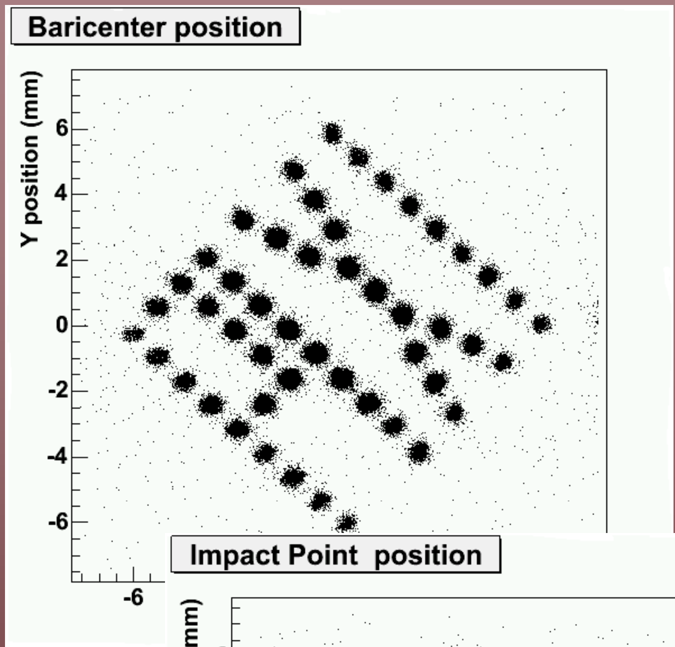

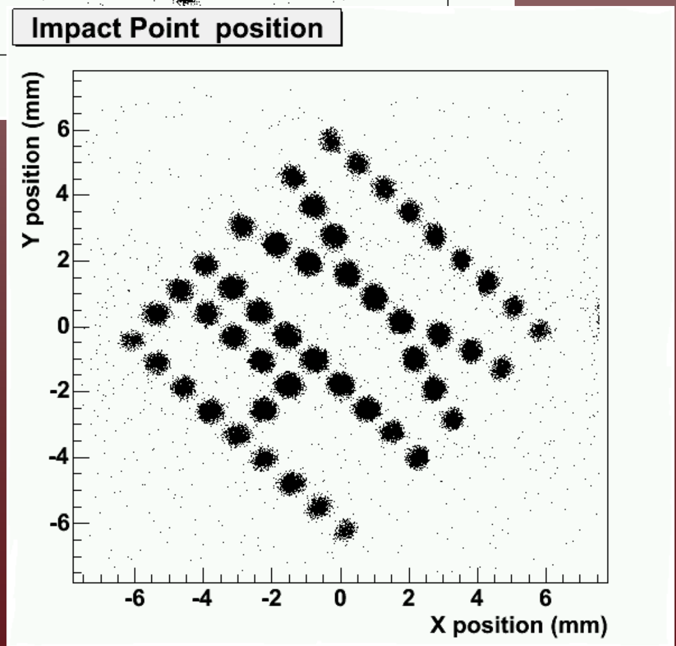

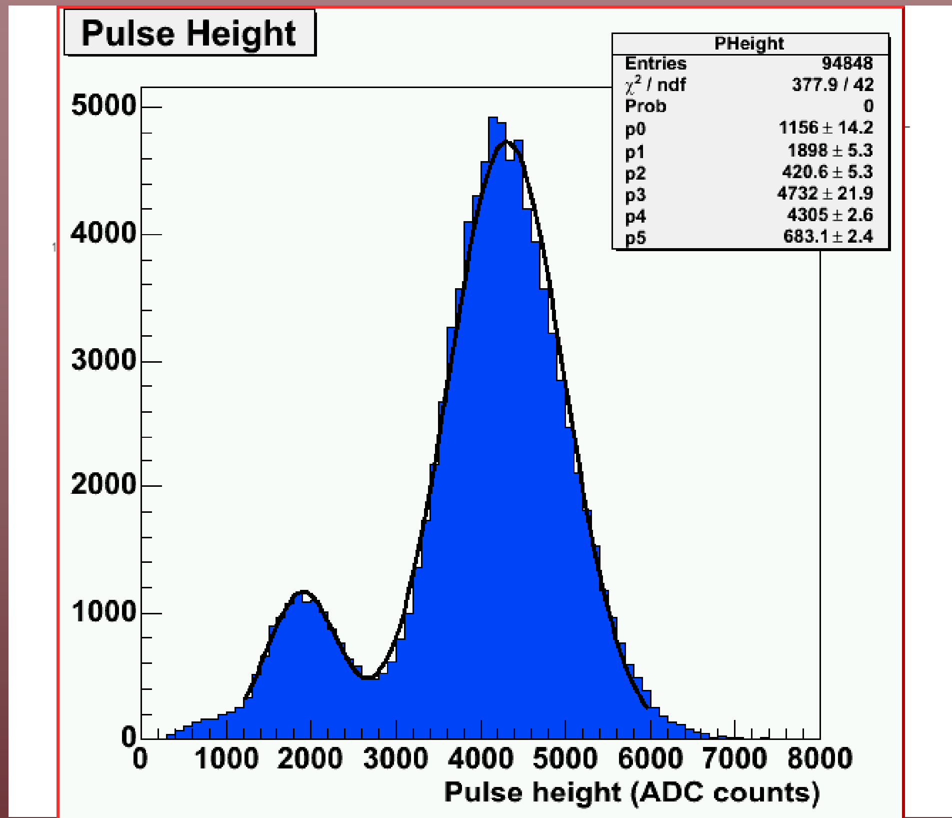

Holes:
Ø 0.5 mm
pitch 1 mm

Residual modulation

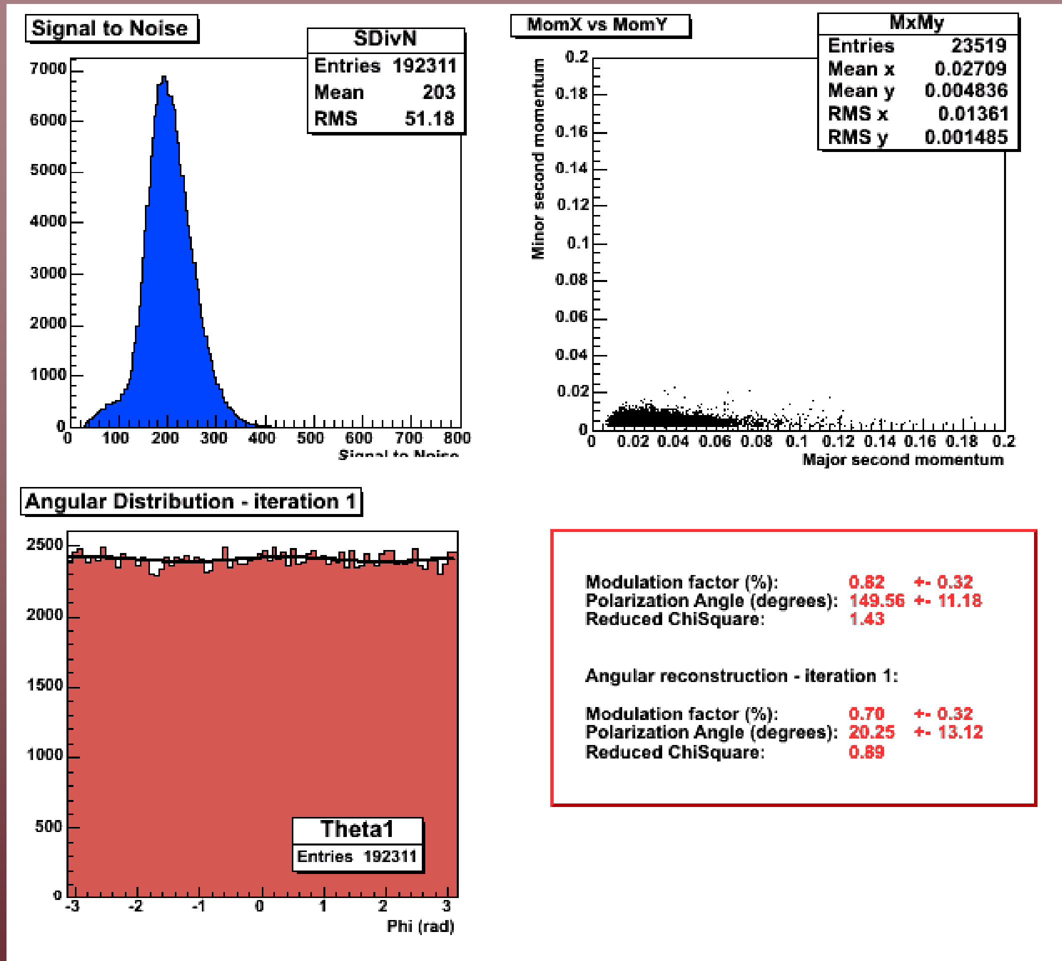

S/N distribution, scatter plot of the two principal axes of the cluster charge and residual modulation, obtained with 55Fe source in Ne(50%)-DME(50%)

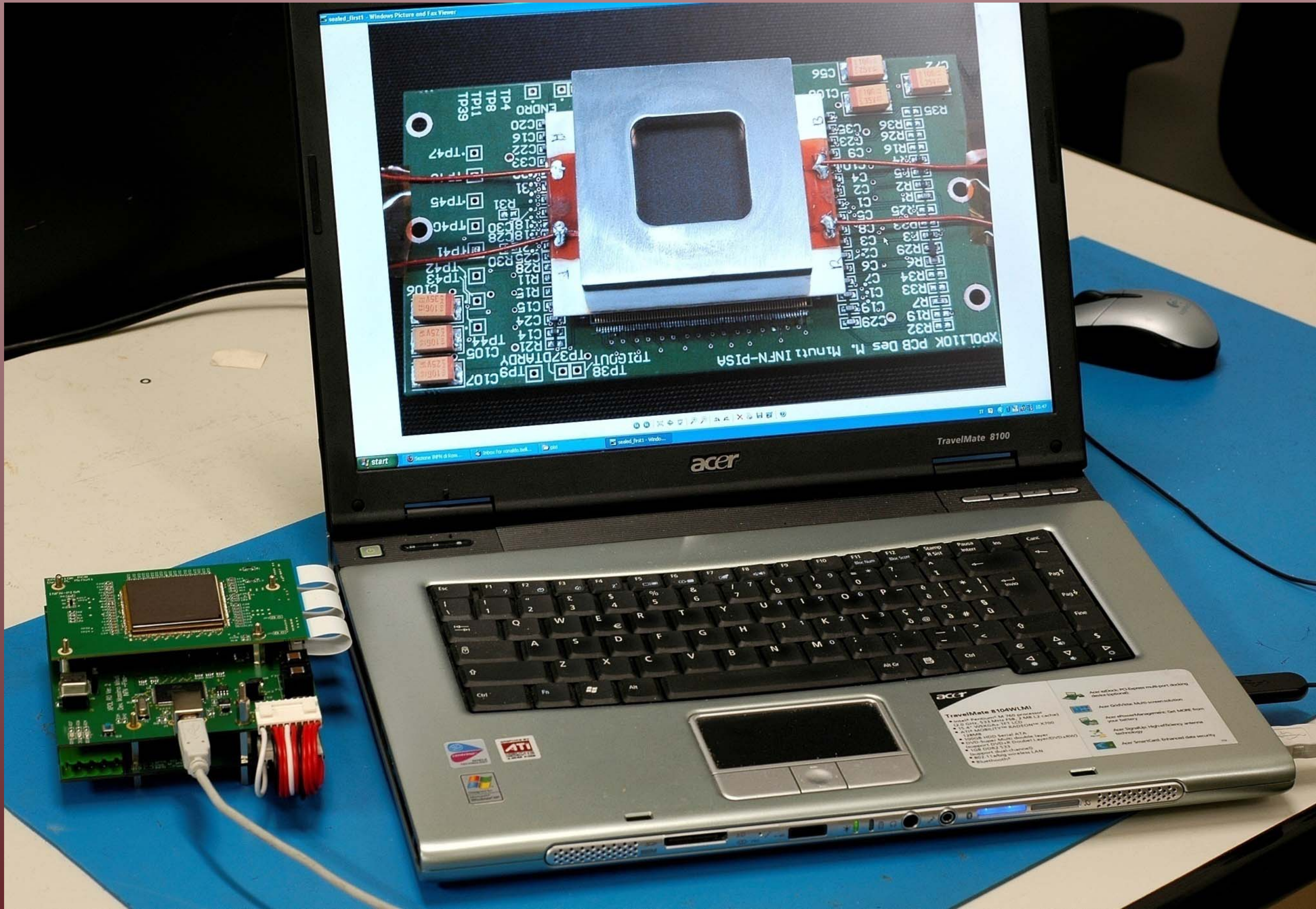

. The level of integration, compactness and operational simplicity of this device is comparable to solid state detectors

Semitransparent Photocathode

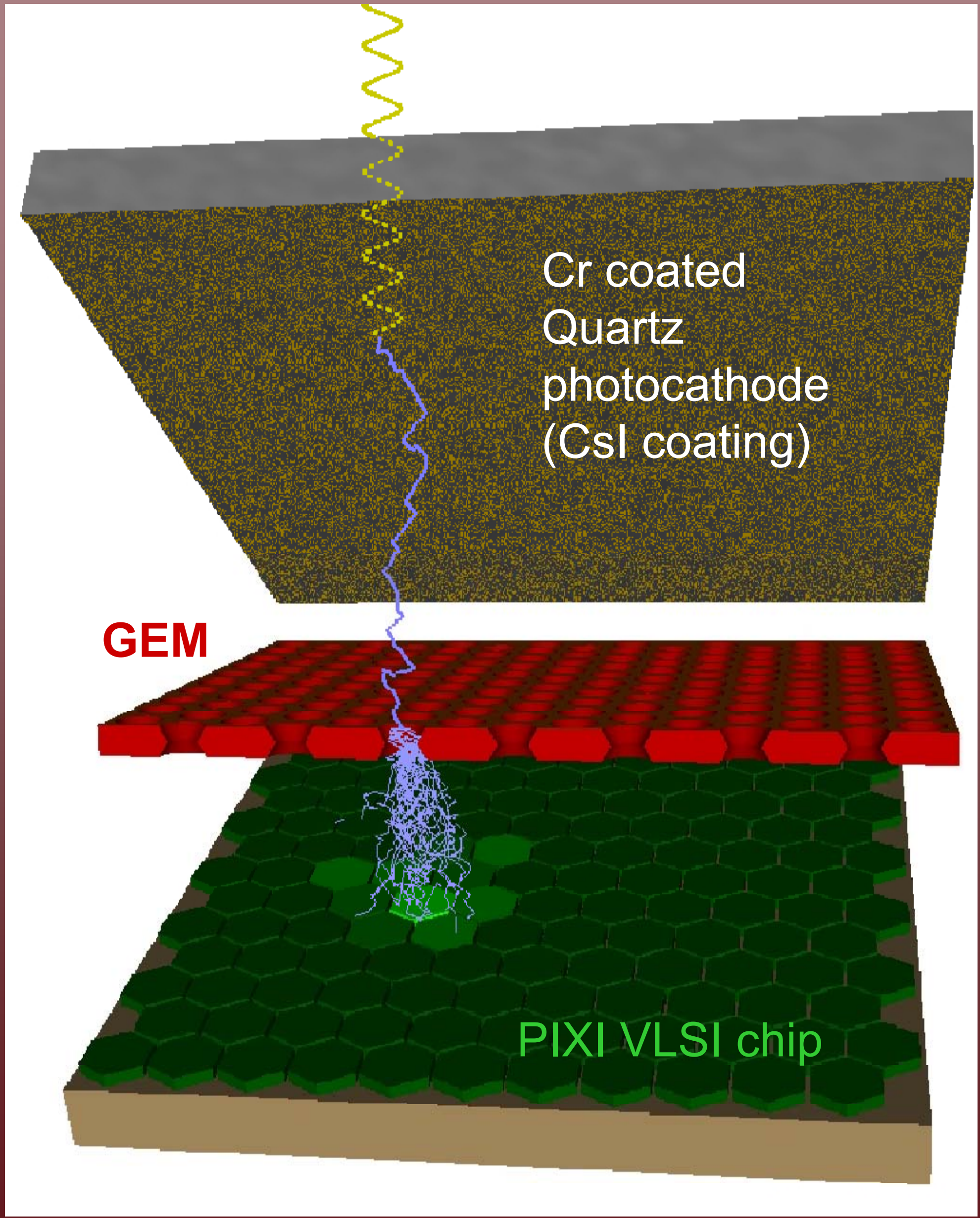

Drift gap = 1 mm
Transfer gap = 1mm
GEM thickness = 50 μm
GEM pitch = 50 μm

Pros:

- Simple
- High gain
- High geometrical efficiency

Cons:

- Low thickness → Low Q.E.
- Extra diffusion in the gas layer above the GEM

Reflective Photocathode

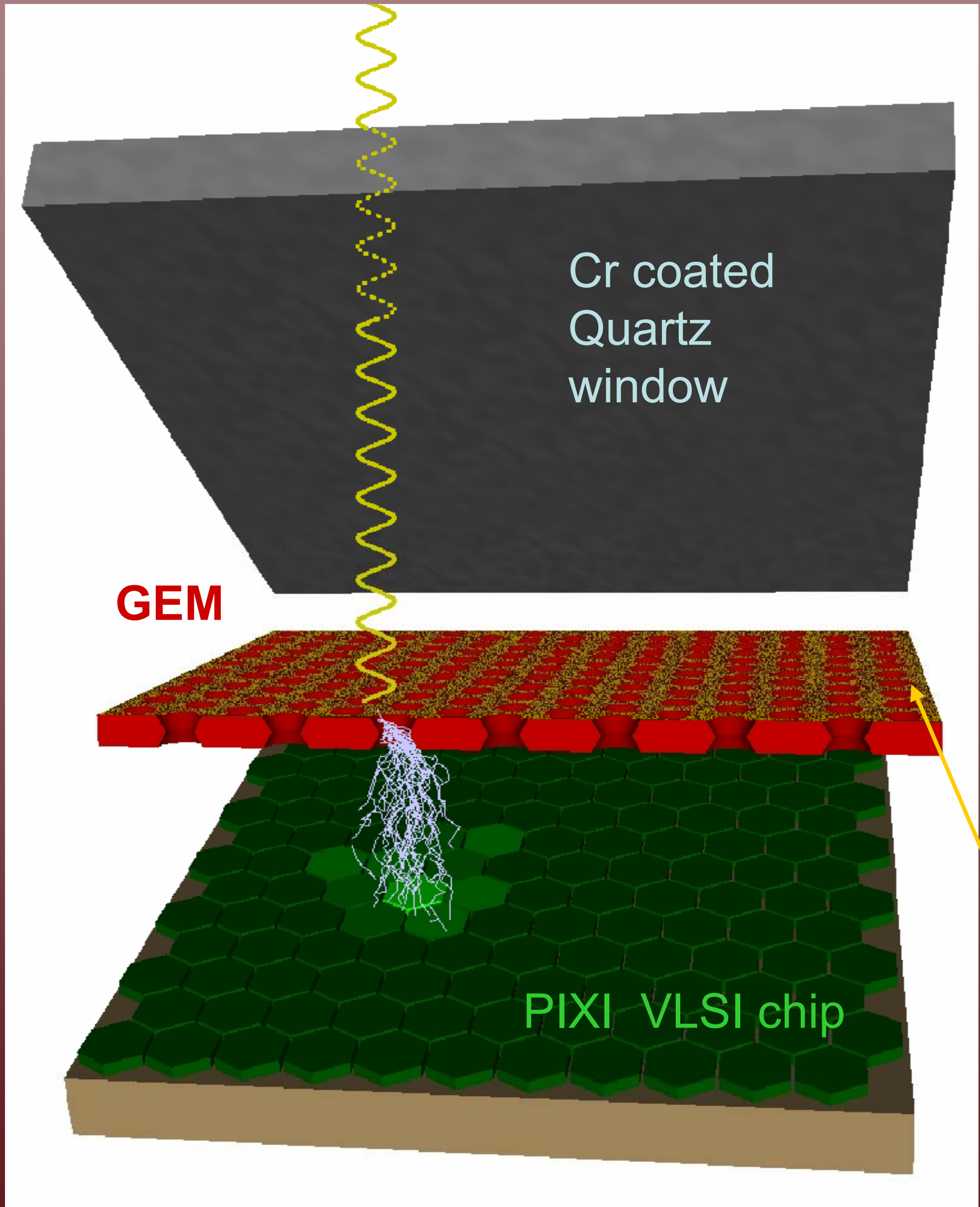

Drift gap = 1 mm
Transfer gap = 1mm
GEM thickness = 50 mm
GEM pitch = 50 mm

Pros:
- Thick film → high Q.E. (10-20%)

Cons:
- More complicated to build
- Special gold coating on the GEM
- Low geometrical efficiency (in our case 50%)
- Lower gas gain

CsI photocathode

UV photo-detector with *single electron* sensitivity

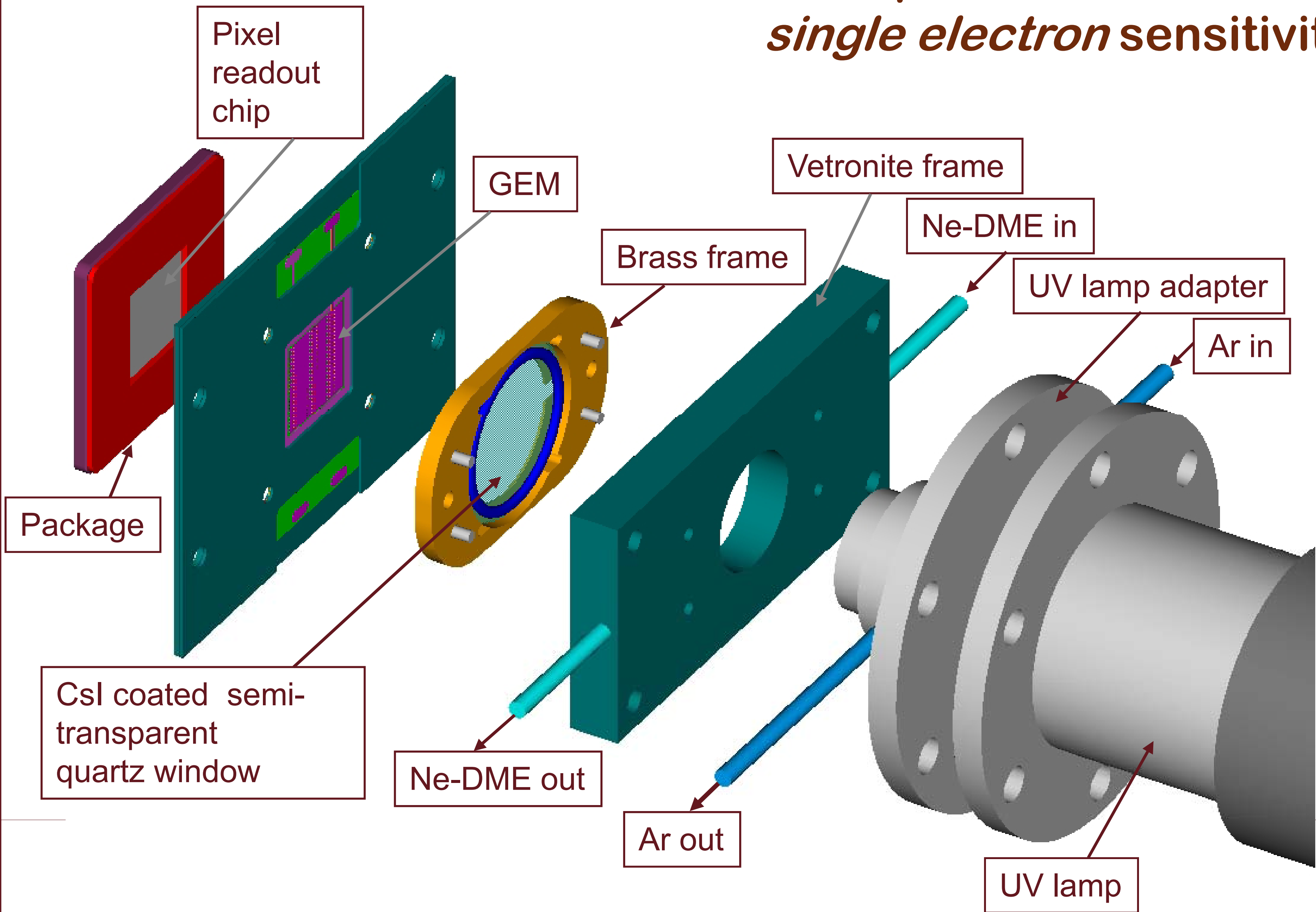

Single photon operation

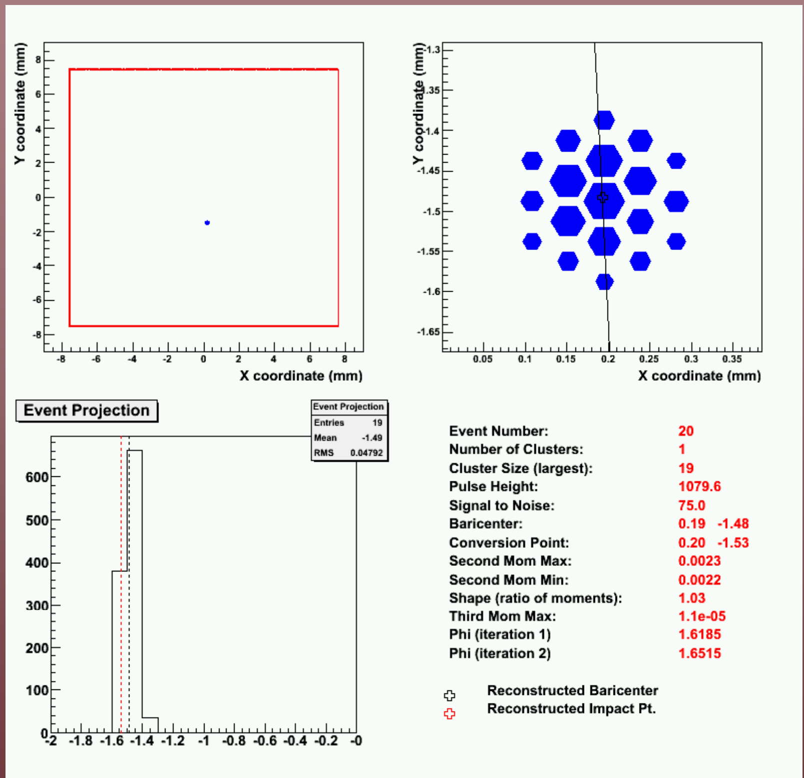

Single photon event topology

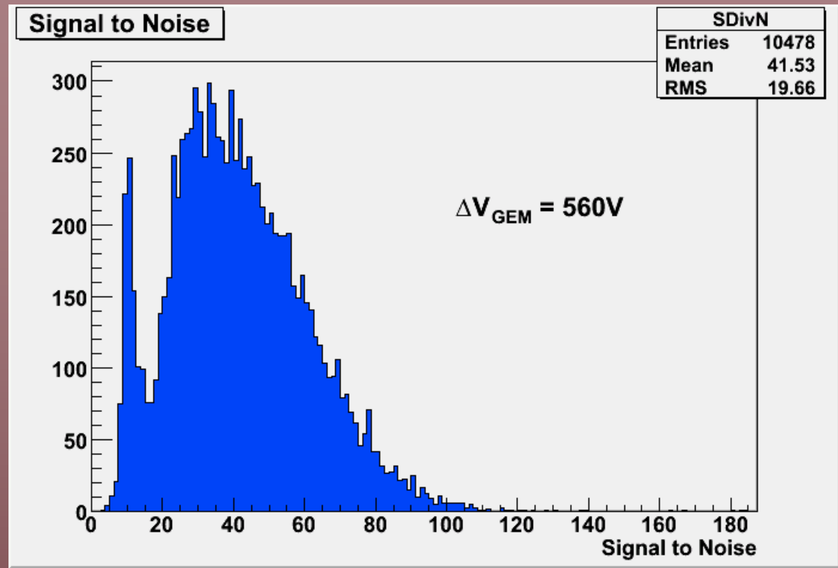

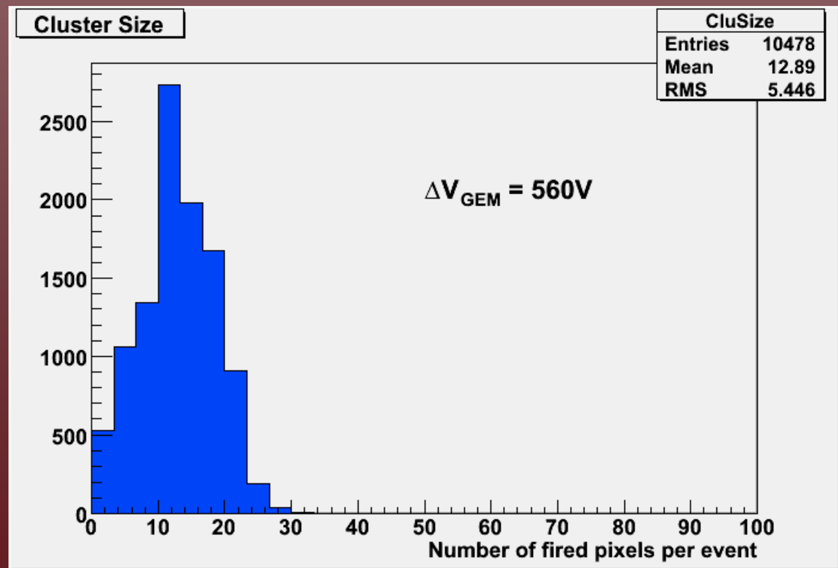

Semitransparent Photocathode

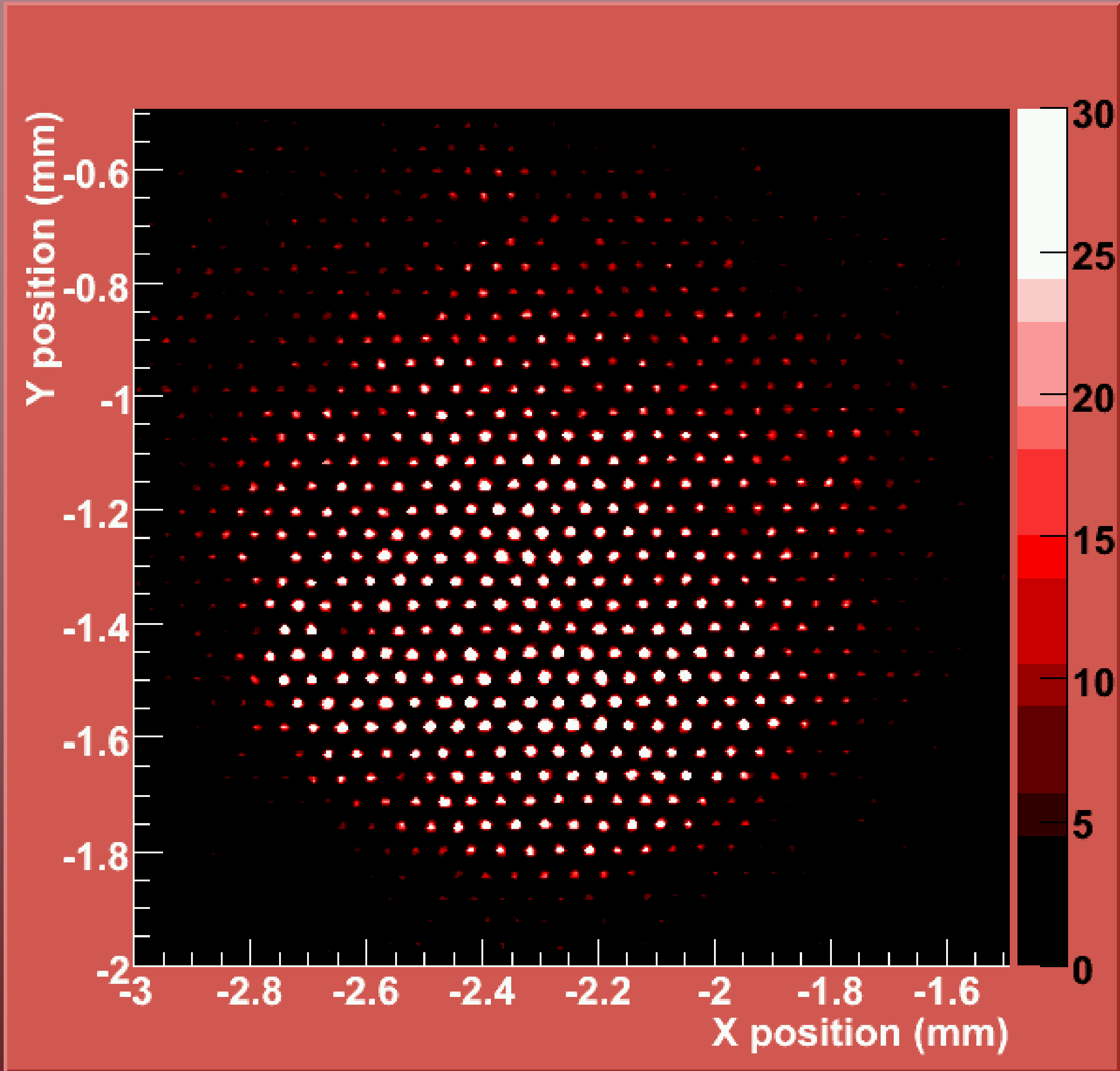

"Self-portrait" of the GEM amplification structure

Intrinsic resolution
of the read-out system

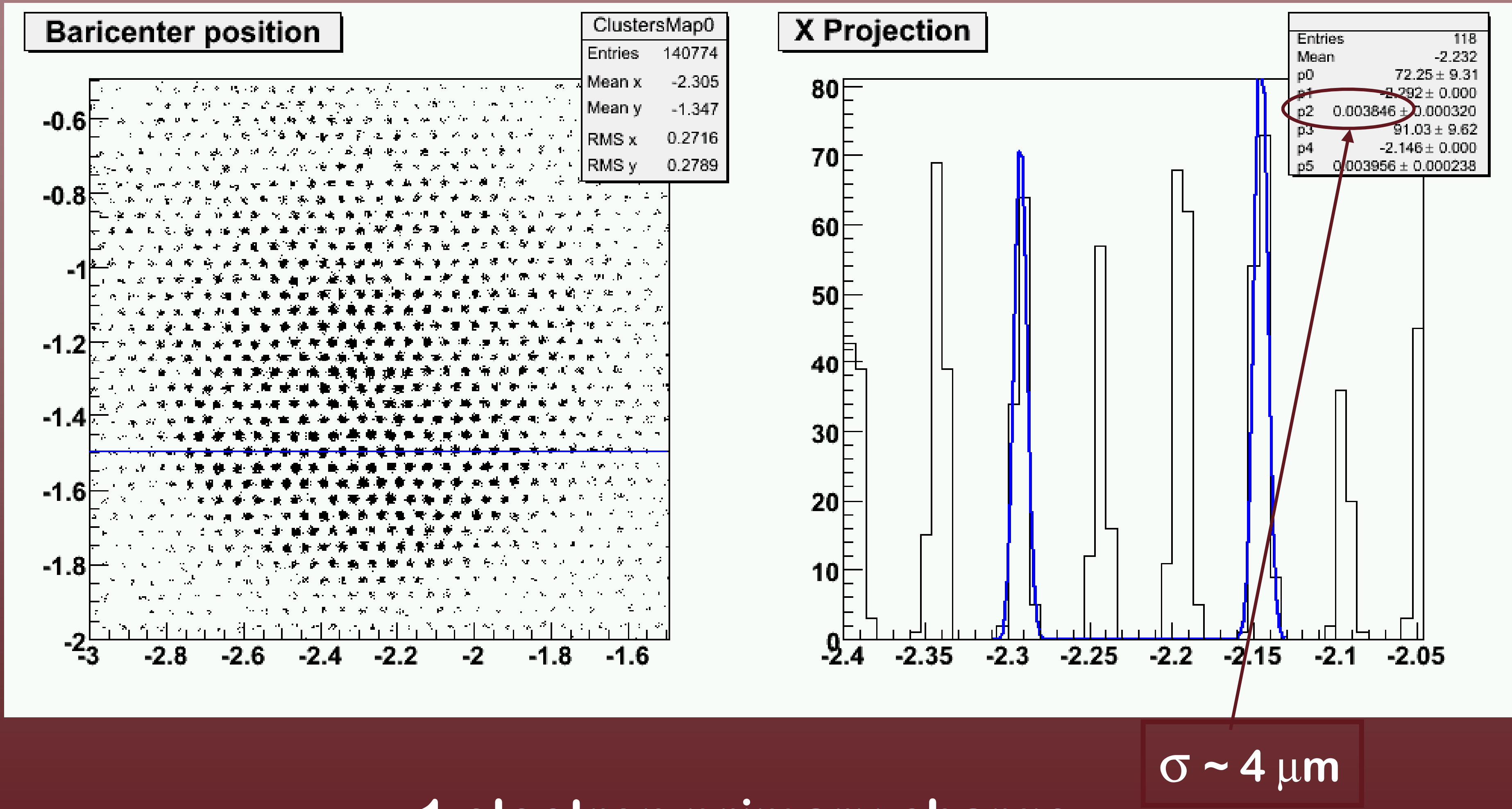

1 electron primary charge

Semitransparent Photocathode

From gas to vacuum

The use of Xpol as readout plane of a Micro Channel Plate coupled to a suitable photocathode in vacuum

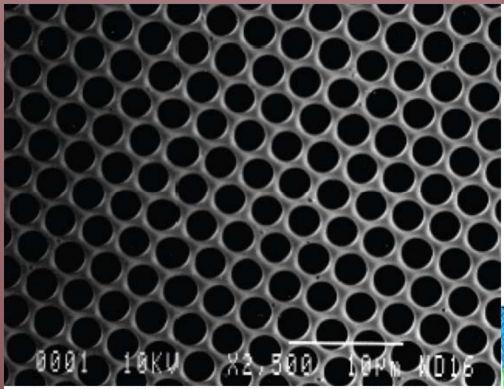

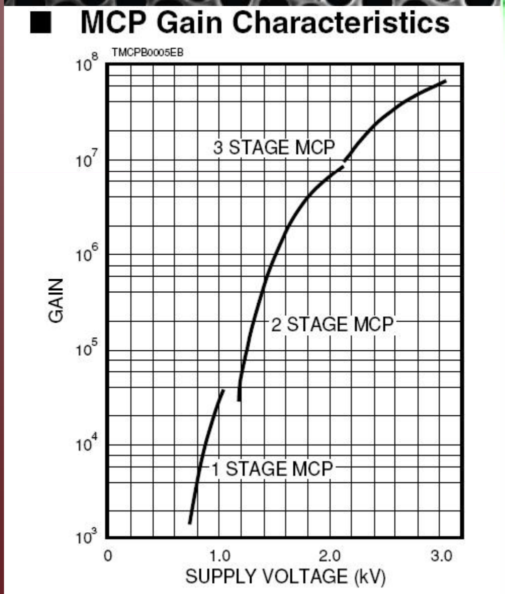

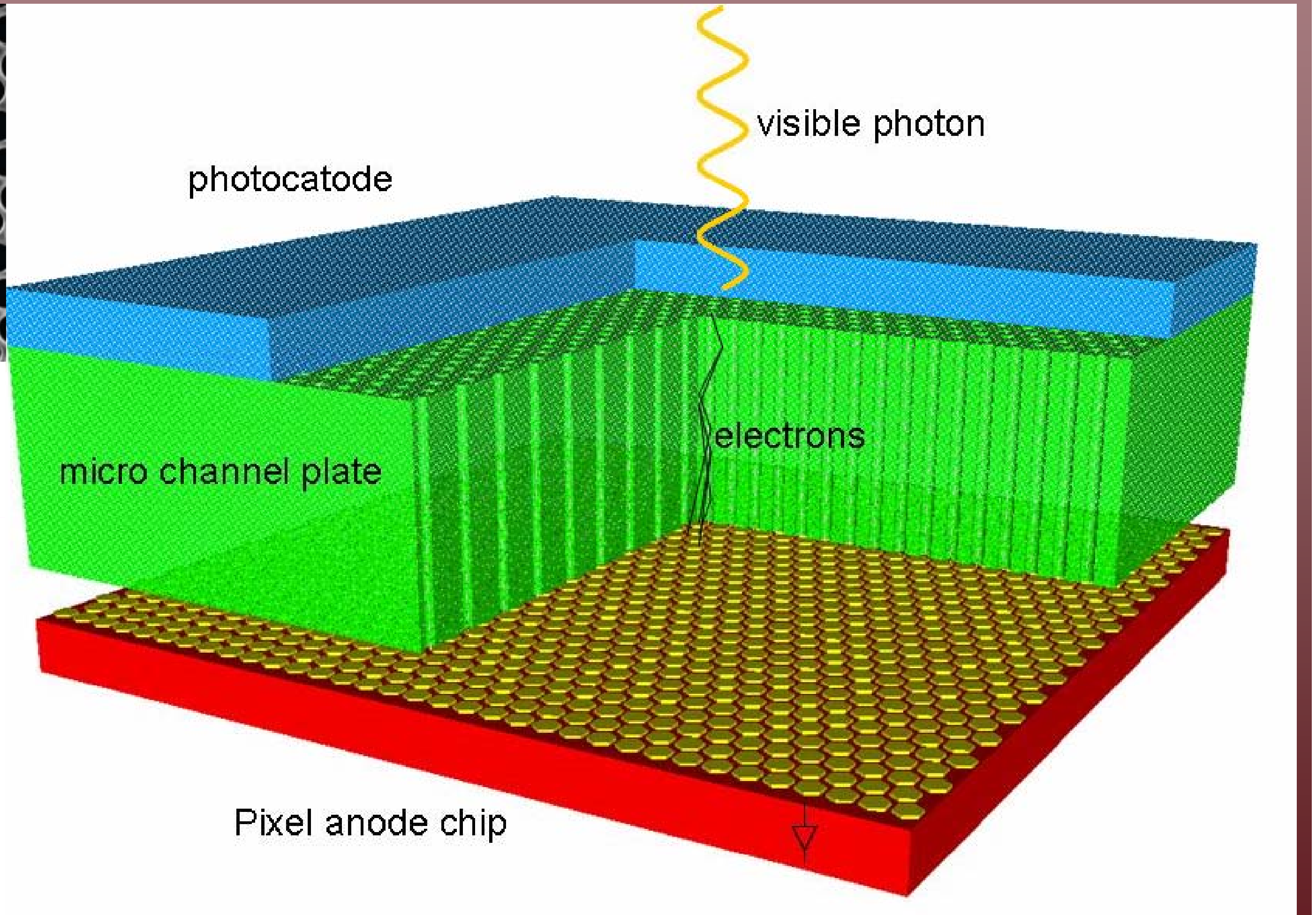

First test in collaboration with Space Science Laboratory, Berkeley

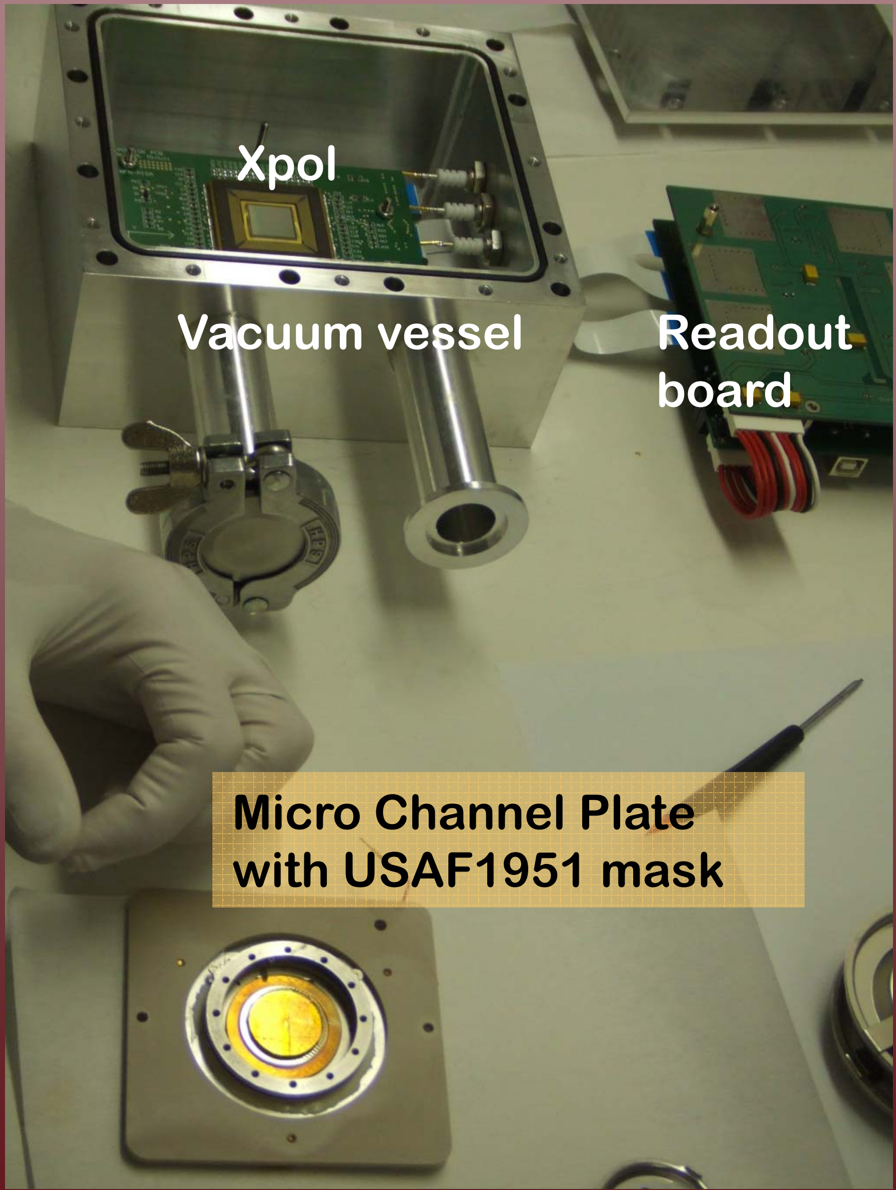

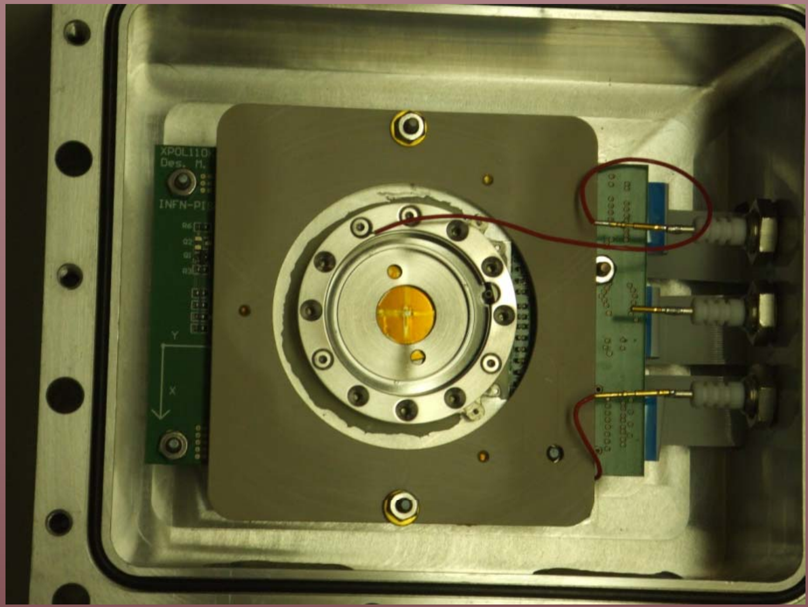

The events

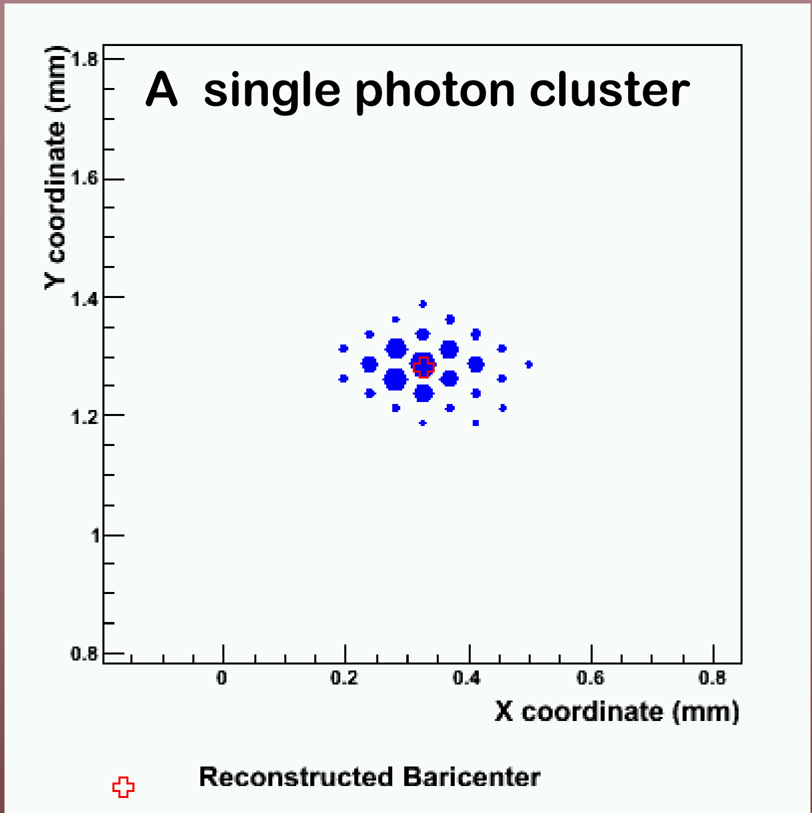

At low rate the detector records single photon events in window mode (<1K channels/frame, frame rate up to 10KHz).

A multi photon (18) event

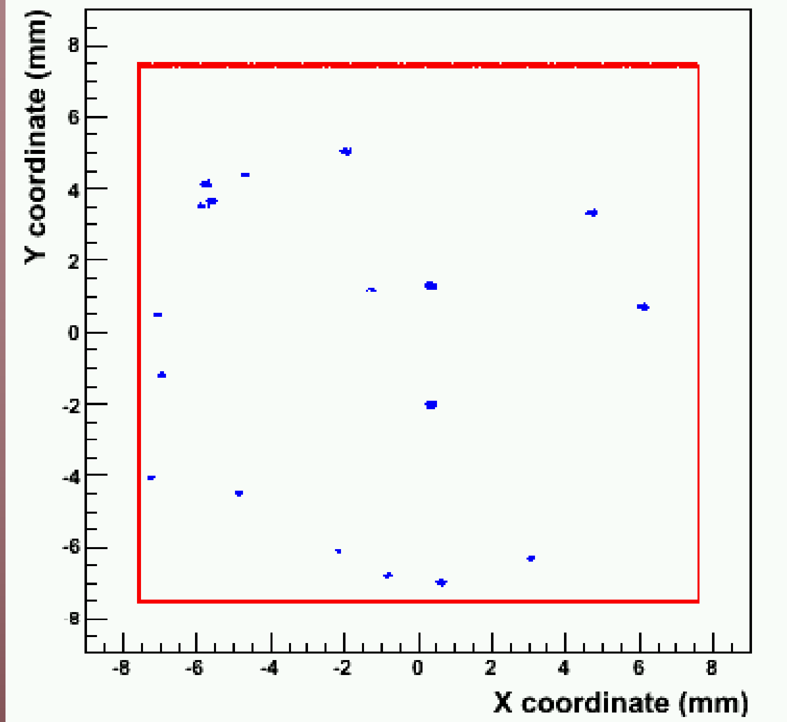

Event Number:	1543
Number of Clusters:	18
Cluster Size (largest):	26
Pulse Height:	1662.7
Baricenter Coord.(mm):	0.32 1.28
Average Rate (D.T.included, Hz):	inf

Thanks to the high granularity, at high rate the detector can resolve up to few hundreds of photons/frame in full frame readout mode (1KHz frame rate, up to ~200KHz photon rate)

MCP 12.5μm aperture 15μm pitch

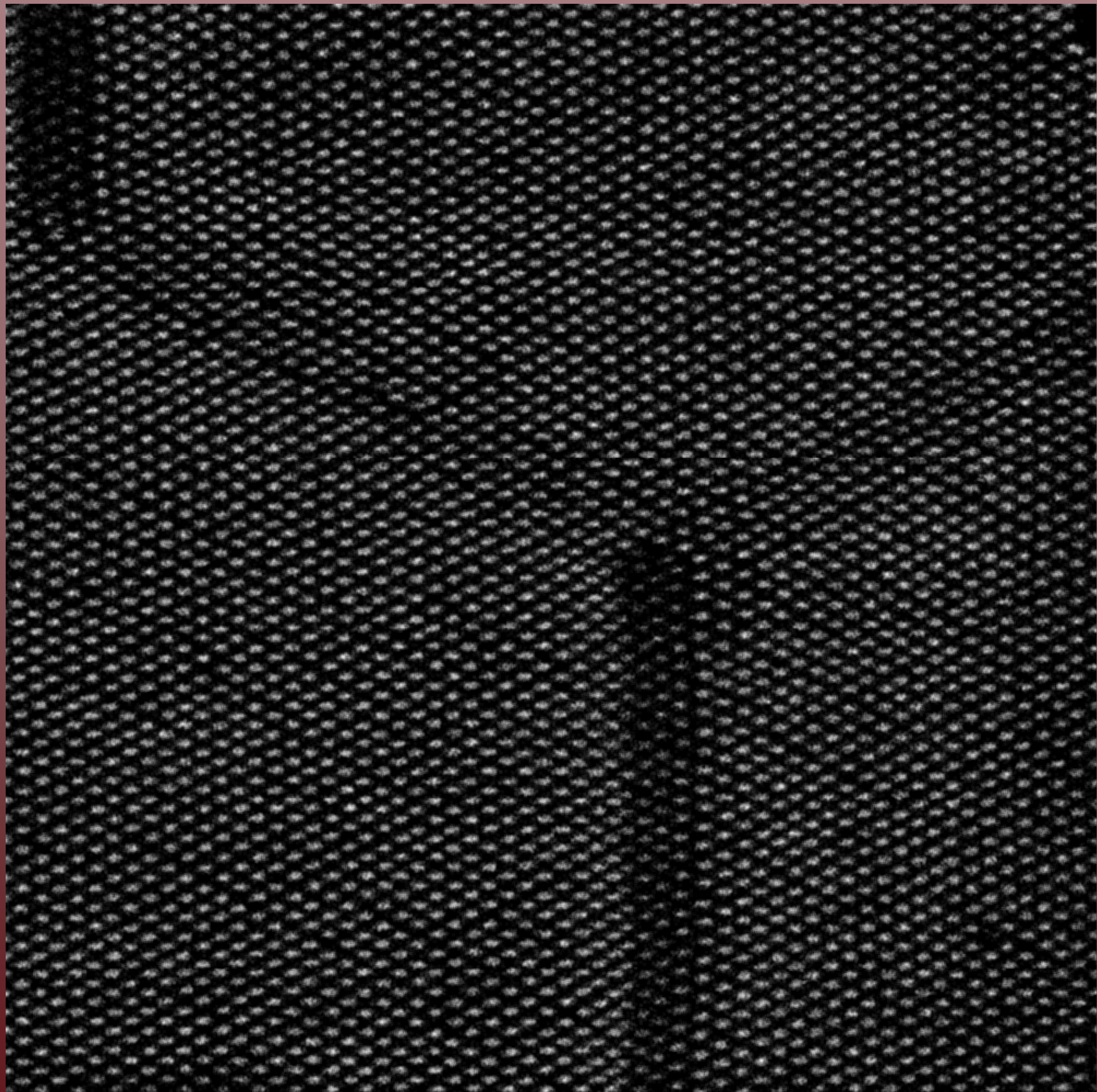

1mm^2 flat field image

The USAF1951 3-Bar Resolving Power Test Chart

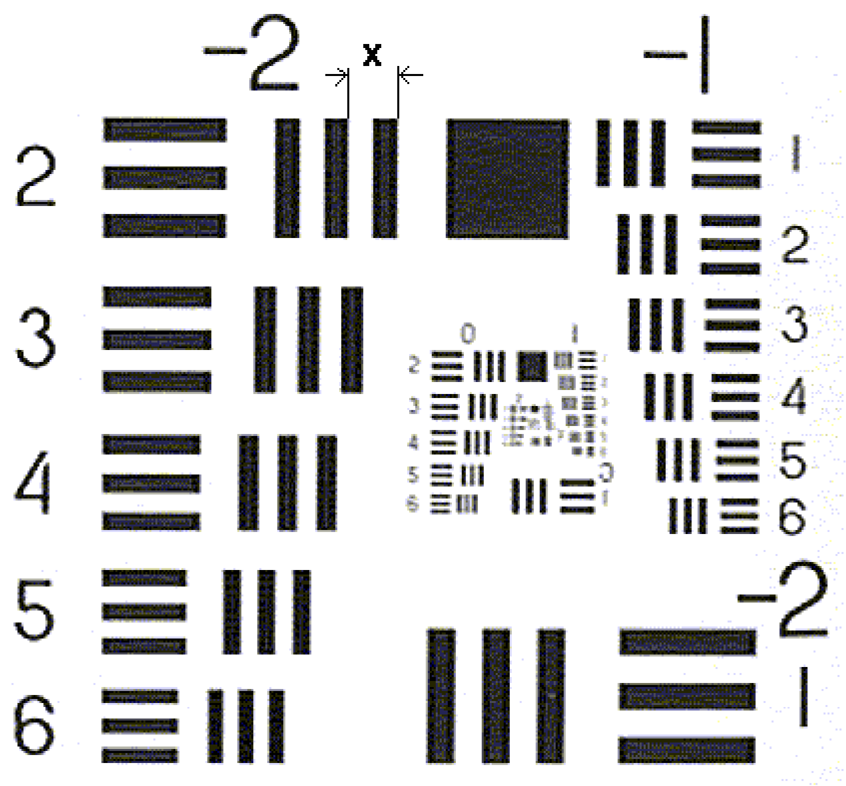

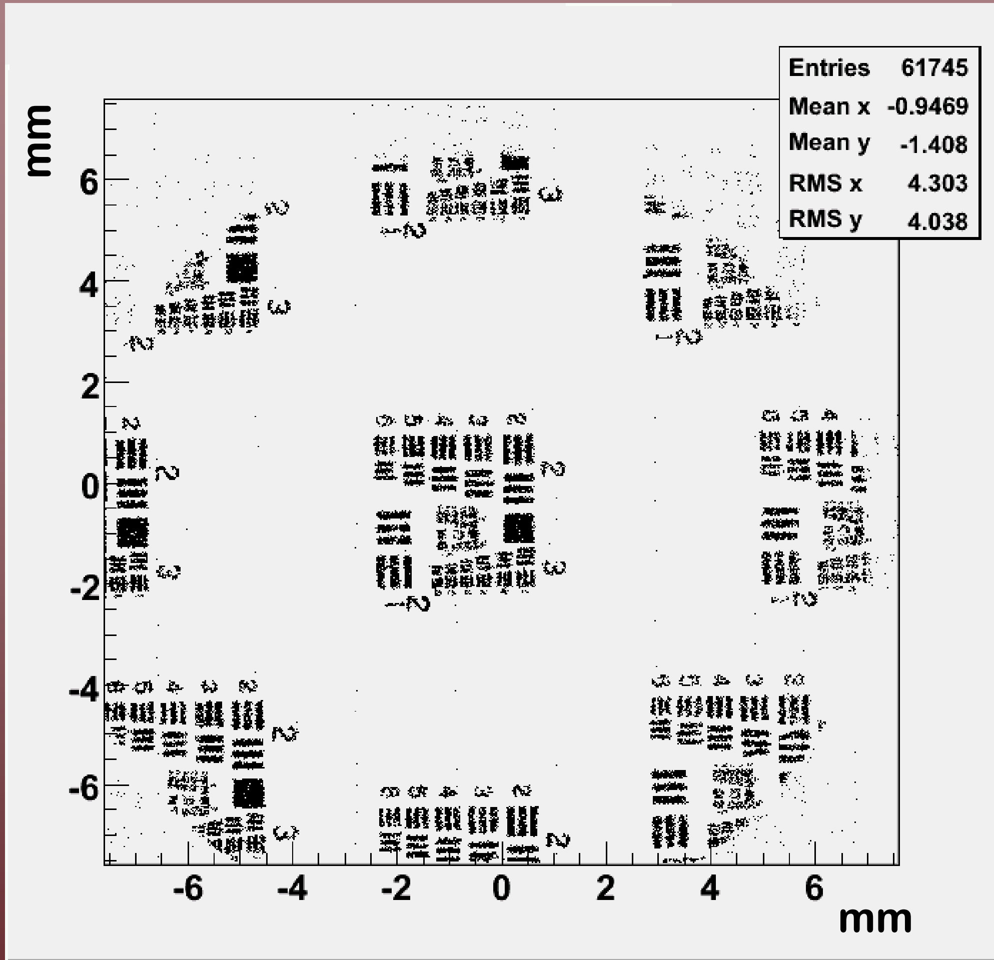

Line pairs/mm = $2^{n+(m-1)/6}$

X (mm) = $2^{-n-(m-1)/6}$

Es. n=6, m=1, X=2^{-6}=1/64=15.6μm

n=6, m=2, X=$2^{-(6+1/6)}$=1/72=14μm

n=6, m=6, X=$2^{-(6+5/6)}$=1/114=8.7μm

n=7, m=1, X=2^{-7}=1/128=7.8μm

Full detector image

MCP 10μm aperture 12μm pitch

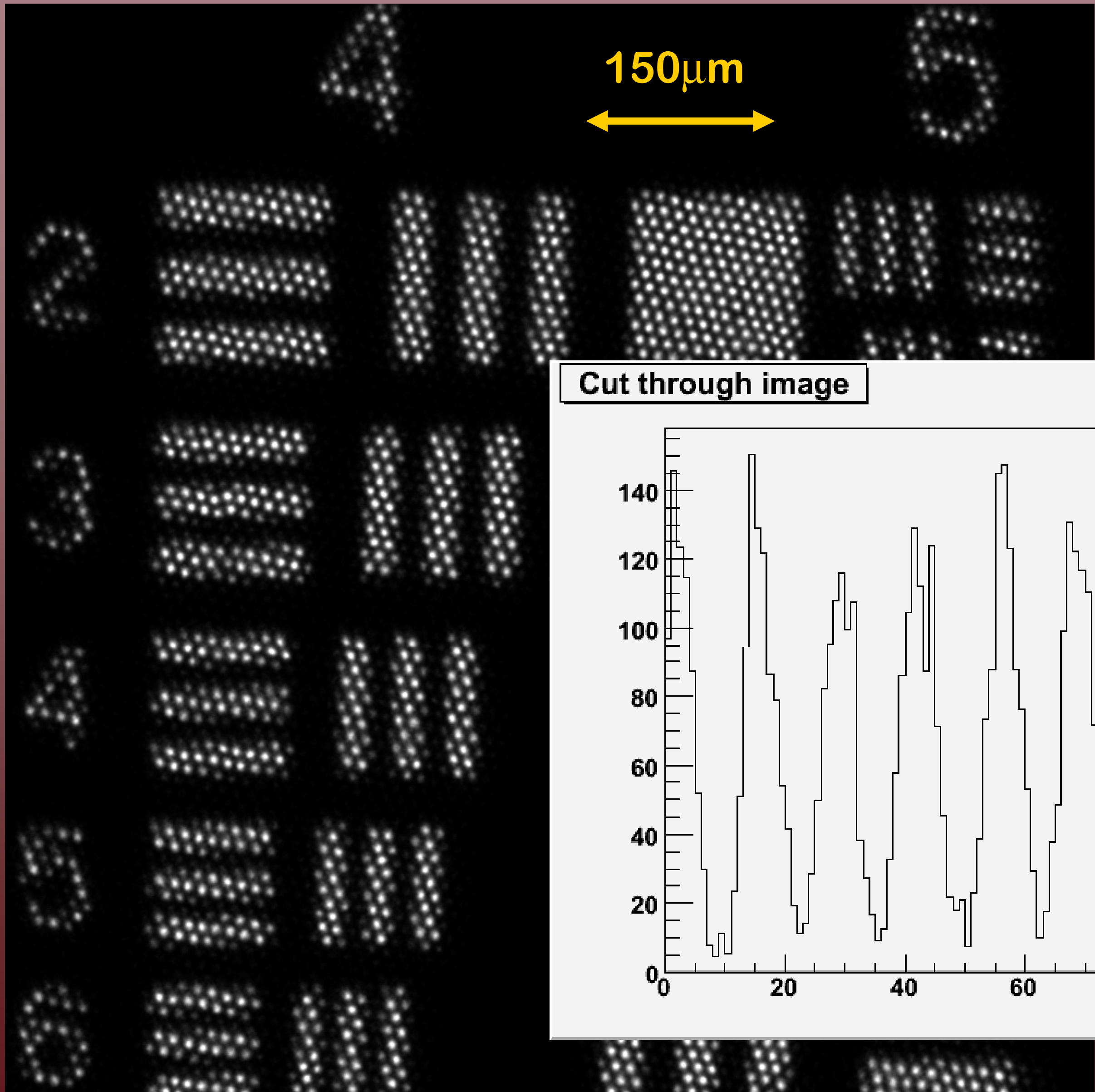

In a 140μm square easily resolved 150 spots.
The peak width includes the electron cloud width.

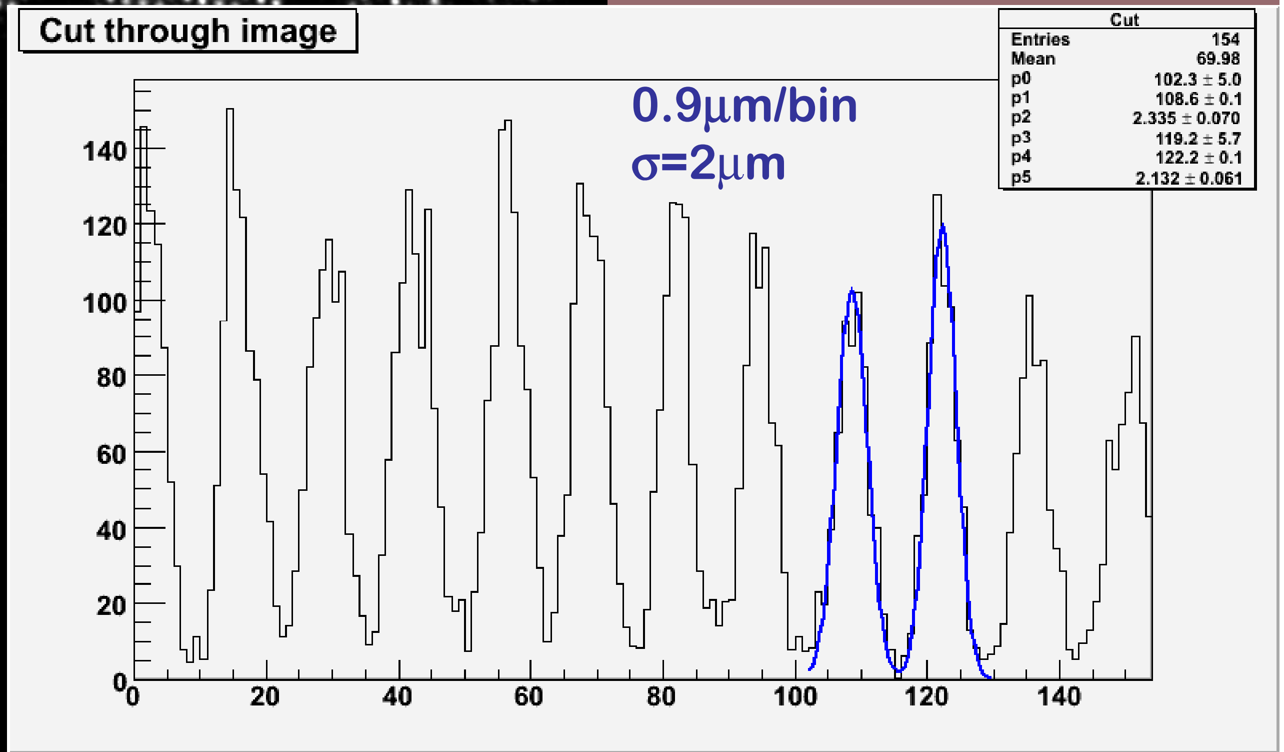

MCP 4μm aperture 5.5μm pitch

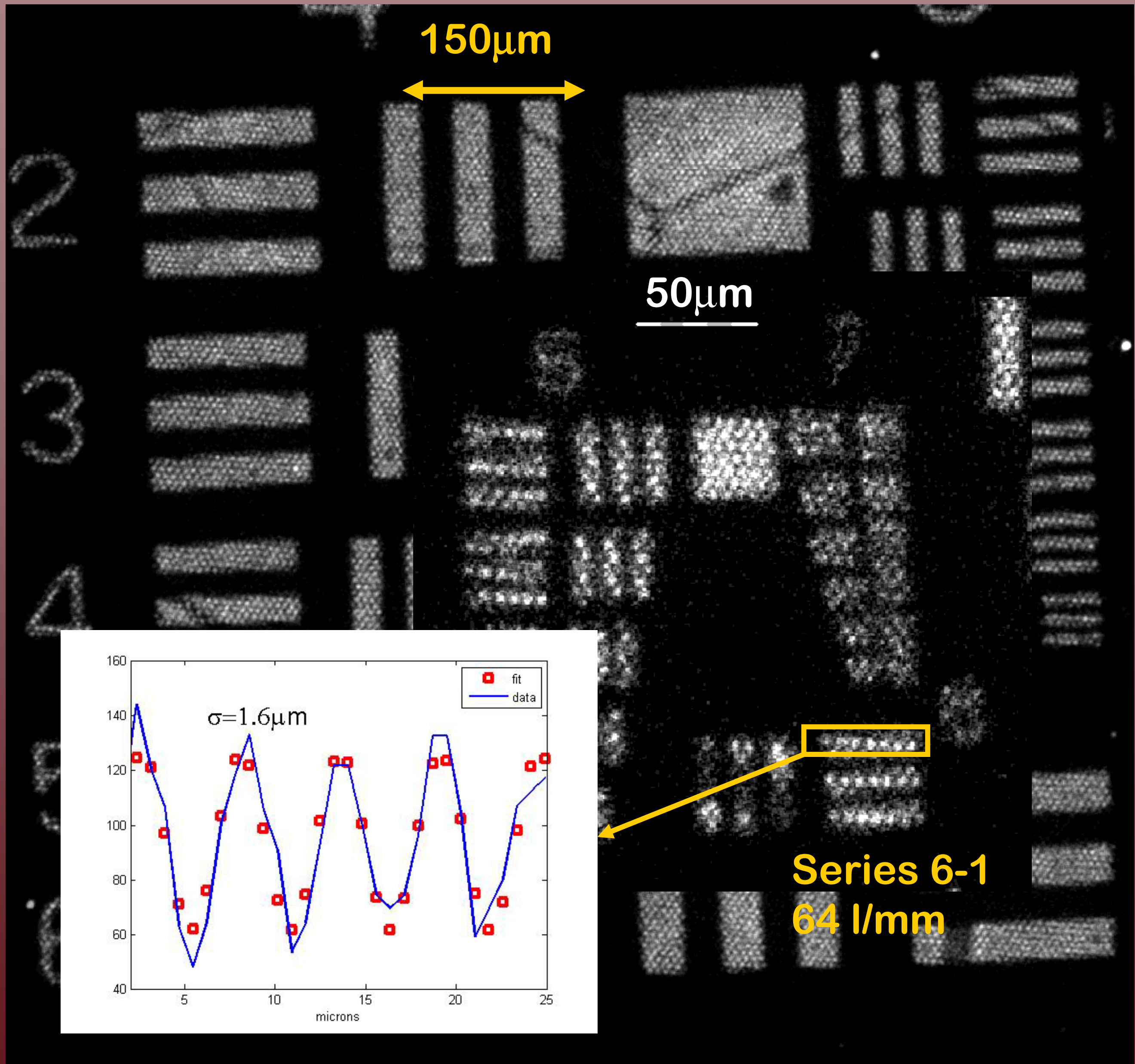

ANALOG → COUNTING:
an extremelay large area CMOS counting ASIC

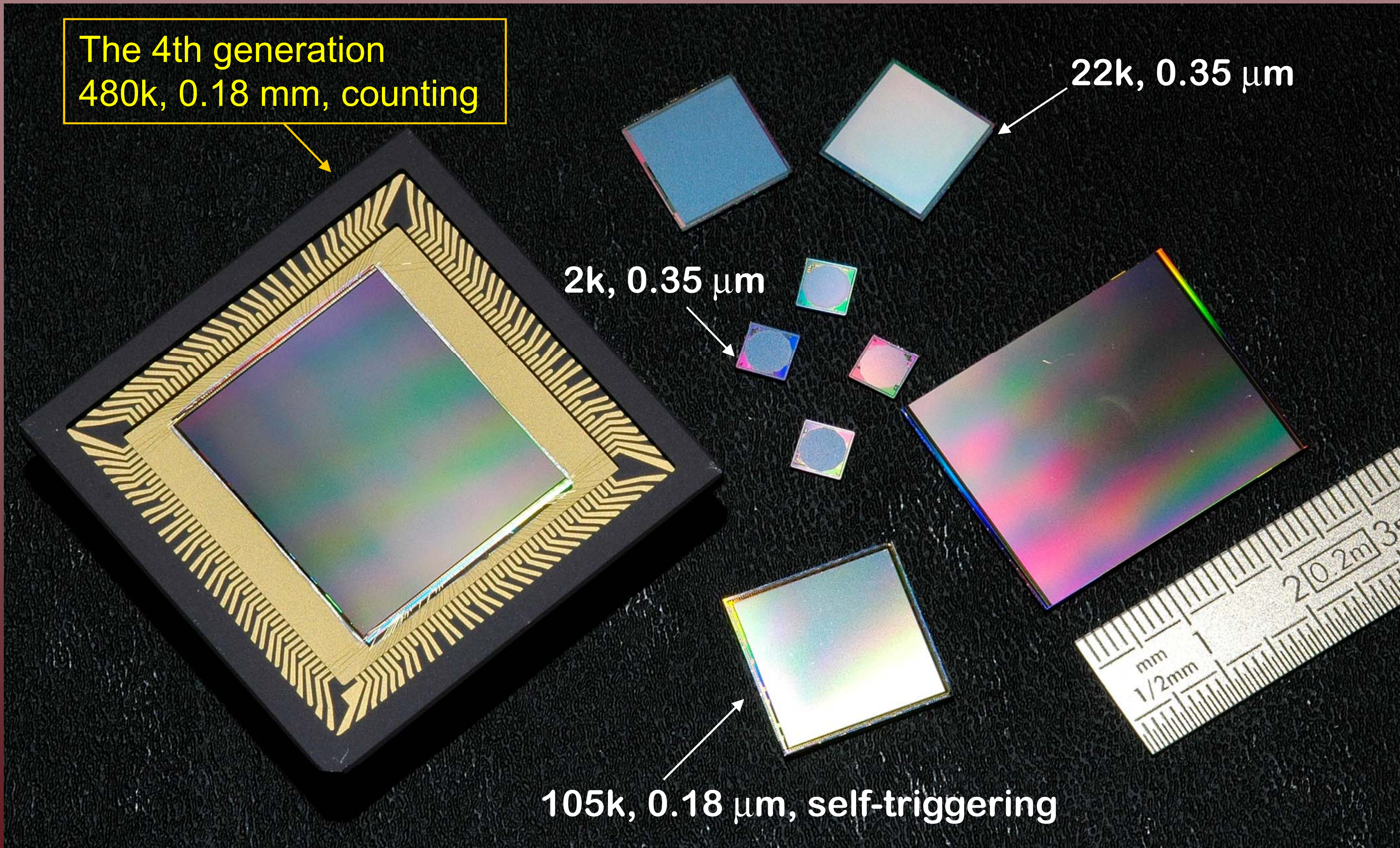

The chip layout

Bonding pads only on two opposite sides

↓

Two side buttable chip

With just 2 chip side by side we get a 5 cm x 3 cm sensor

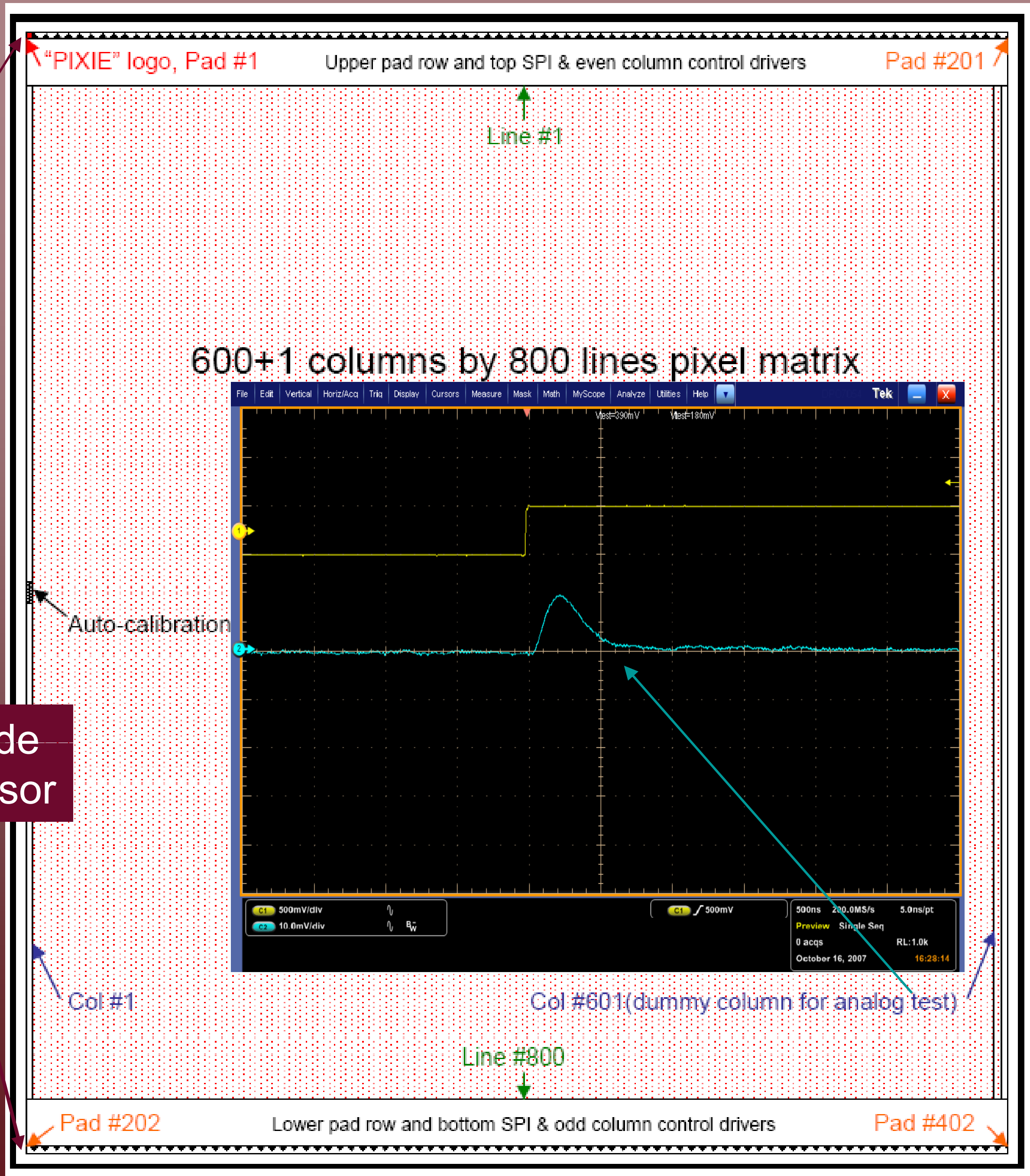

The CMOS counting ASIC

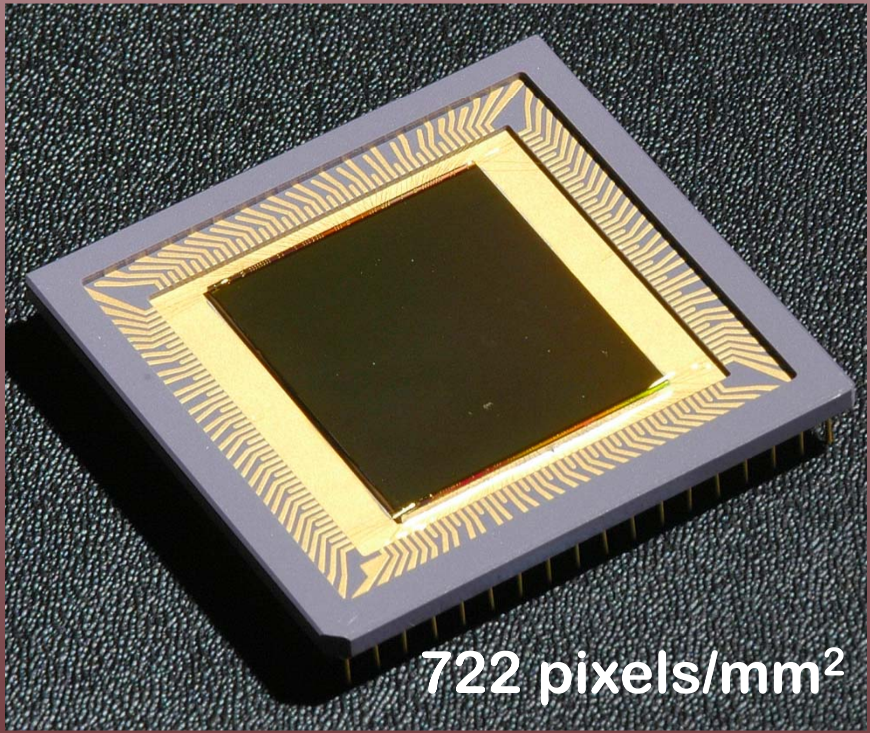

The chip integrates more than 259 million transistors.
It has **480k** pixels organized in a honeycomb matrix of **600 columns×800 lines** corresponding to an active area of
24mm (600x40μm) ×27.7mm (800x34.64μm)

Each pixel is connected to a charge-sensitive shaping amplifier followed by a discriminator and a 15-bit shift register.

A self-calibration circuit is implemented in each pixel to reduce unavoidable DC offset variations from pixel to pixel →
a *global threshold* can be applied to the whole matrix.

Each pixel column can be individually configured for:

- counting the number of events during a given time slot or
- providing, with an external clock, a timestamp to the event or the time over threshold

Work program

This chip has been or will be used as the basic building block of several detector configurations:

- coupled to gas ionization chamber
- coupled to charge multipliers (MCP, GEM …)
- coupled to solid state semiconductors (CdTe, CZT, ….)

Thin ,High Pressure, Parallel Plate Ionization Chamber

- Gas Pressure:12 bar
- Gas Filling Xe(95)-CO2(5), W=25 eV
- Gas Gap:700 microns
- Entrance Window:1.5 mm Beryllium
- Working Mode:counting
- Illumination:X Rays 5-20keV
- Signal charge/photon:300-800 electrons
- Conceptually identical to a solid state pixel device, but with gas as absorbing medium

Working in gas ionization counting mode (G=1) at 8 keV

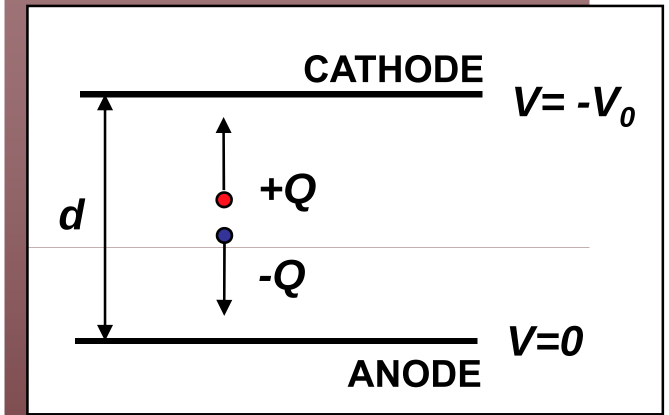

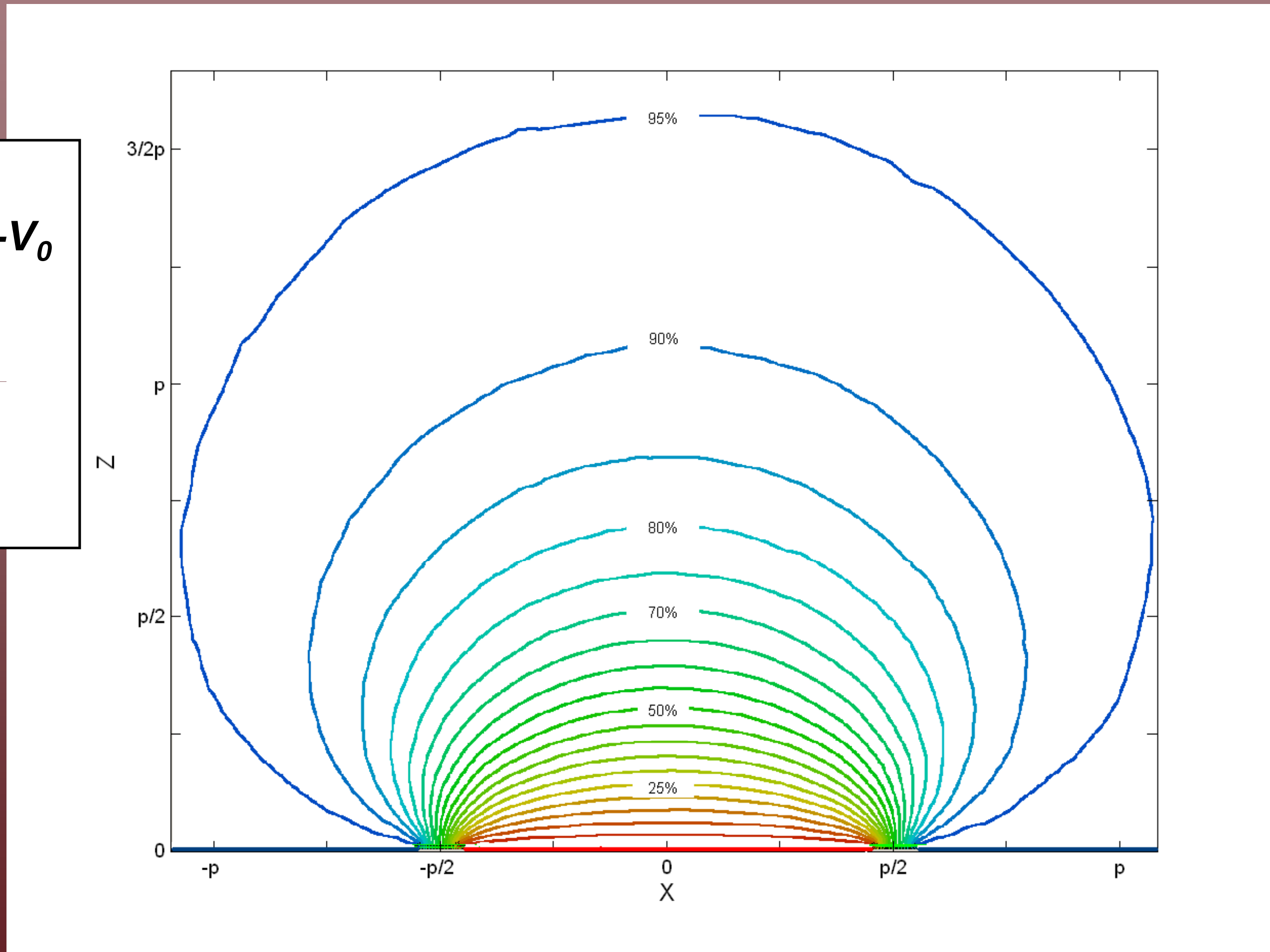

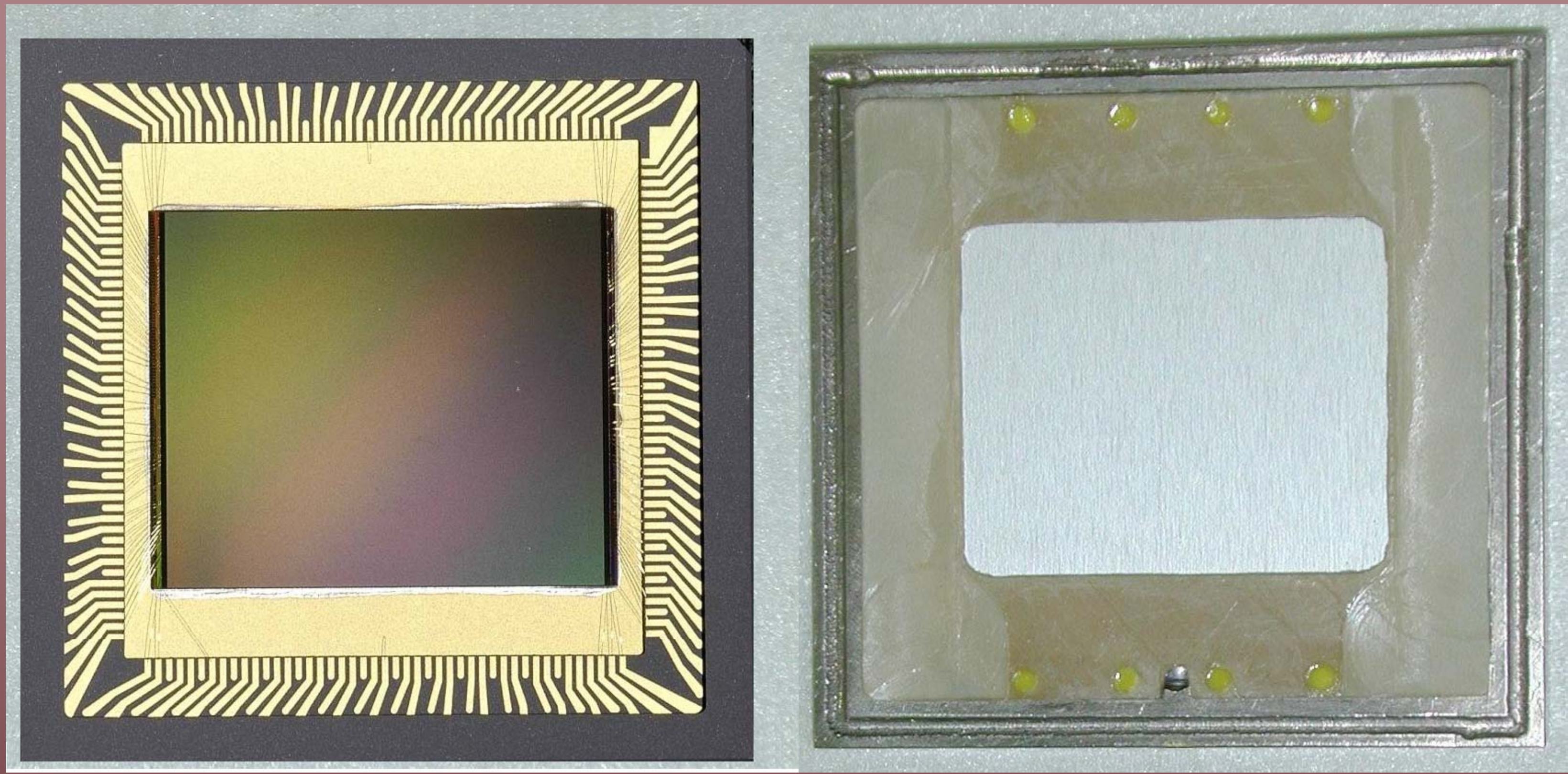

The simplest possible detector concept:

just a pixelized collection plane and a window

No gas system, no complex bump bonding

Ideal solution for photon energy around 10keV

Collaboration with
Oxford Instruments Analytical Oy (Finland)

IMAGE GALLERY

Imaging at 8 keV in pulse ionization mode

Source: copper tube @ 10 kV high voltage

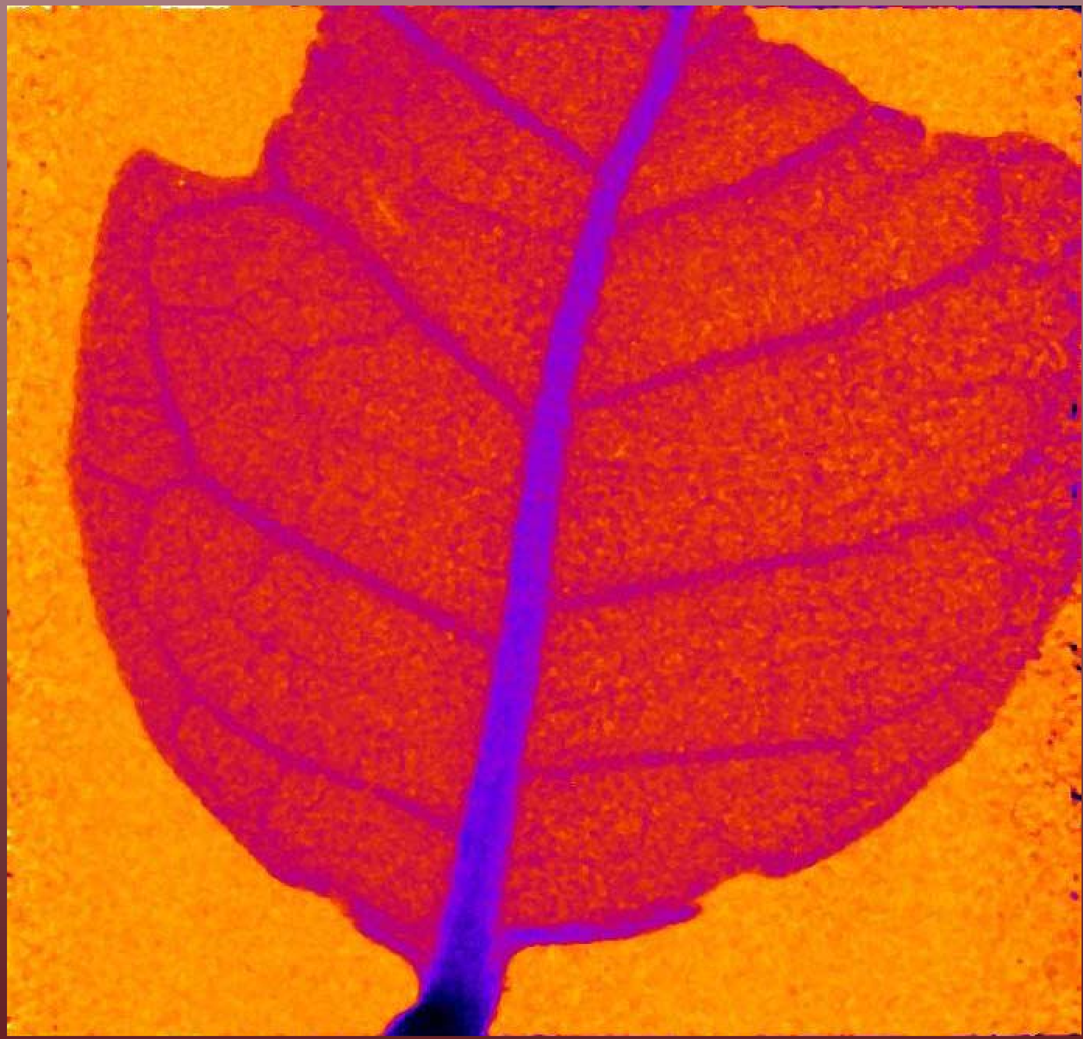

IMAGE GALLERY

High resolution image of high contrast object

IMAGE GALLERY
High resolution image of a high contrast biological sample

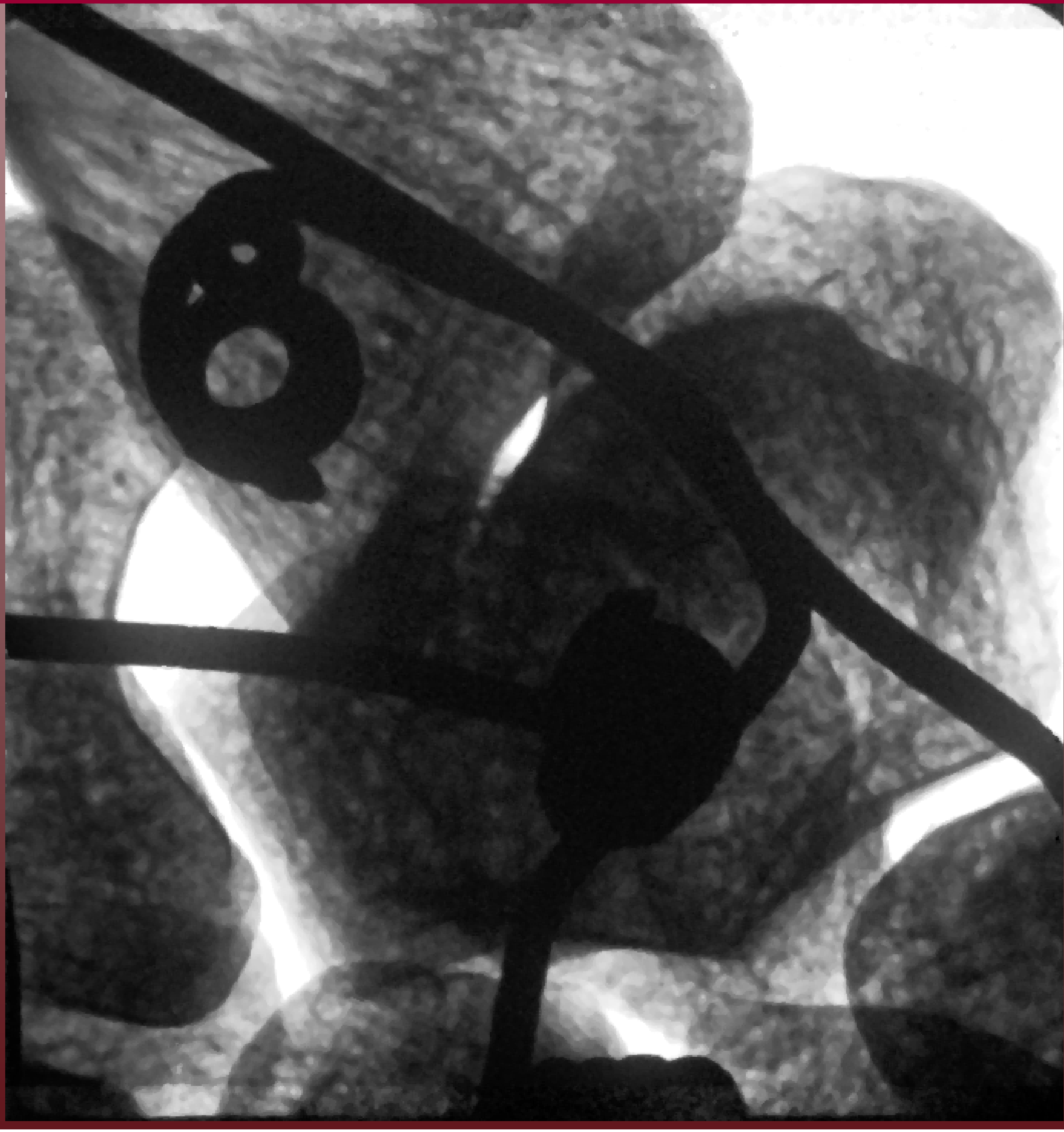

IMAGE GALLERY
High resolution image of
low contrast biological sample

	Xpol	MEDIPIX2	PIXIE
Technology:	CMOS 0.18 μm	CMOS 0.25 μm	CMOS 0.18 μm
Type:	analog	digital (counting)	digital (counting+ ToT+Time stamp)
Area:	15x15=225mm^2(1.1X)	14x14=196mm^2(1X)	24x28=672mm^2(3.4X)
Pixel no.:	105.600 (1.6X)	65.536 (1X)	480.000 (7.3X)
Pixel density:	470/mm^2 (1.4X)	330/mm^2 (1X)	720/mm^2 (2.2X)
Pixel noise:	50 electrons *ENC*	110 electrons *ENC*	50 electrons *ENC*
Read-out scheme:	asynchronous, synchronous	synchronous	synchronous
Read-out trigger:	self-trigger, internal, external	internal, external	internal, external
Read-out mode:	single pixel, window, full frame (8-16 nodes)	full frame (1 node)	Full frame (up to 200 nodes)
Global threshold:	2000 el. (unadjusted)	1000 el. (adjusted)	200 el. (auto-adjusted)
Frame rate:	10 kHz	1 kHz	5 kHz
Event rate:	~10^5/s (10^2 ev. / frame)	~ 10^9/s	> 10^9/s
Resolution:	~ 1μm (analog int.)	~15μm (55/√12)	~11μm (38/√12)
Metal fraction:	90%	13%	47%

Conclusions

Analog and counting pixel ASICs of *very large area* and *high granularity* have been designed, fabricated, packaged and used.
These chips have been and will be the basic building block of several detector configurations when coupled to:

- charge multipliers (MCP,GEM,…)
- solid state semiconductors (CdTe, CZT, ….)
- gas ionization chambers working in pulse counting mode

The *high granularity and low noise* of the read-out plane of the XPOL analog chip and the possibility to reconstruct the centroid of the single electron avalanche from UV photon conversion, has allowed to reach ultra-high intrinsic spatial resolution: 4μm in gas and 1.6μm in vacuum.

The possibility to work in ionization mode with high pressure gas fillings coupled to the PIXIE counting chip has been demonstrated and high resolution images at high events rate have been acquired.
Depending on type of charge supplier, pixel and die size, electronics shaping time, analog vs. digital read-out, counting vs. integrating mode, many applications can be envisaged for this class of detectors.

Spares slides

From gas to solid state

Collaboration with
ACRORAD (Japan) & AJAT Oy (Finland)

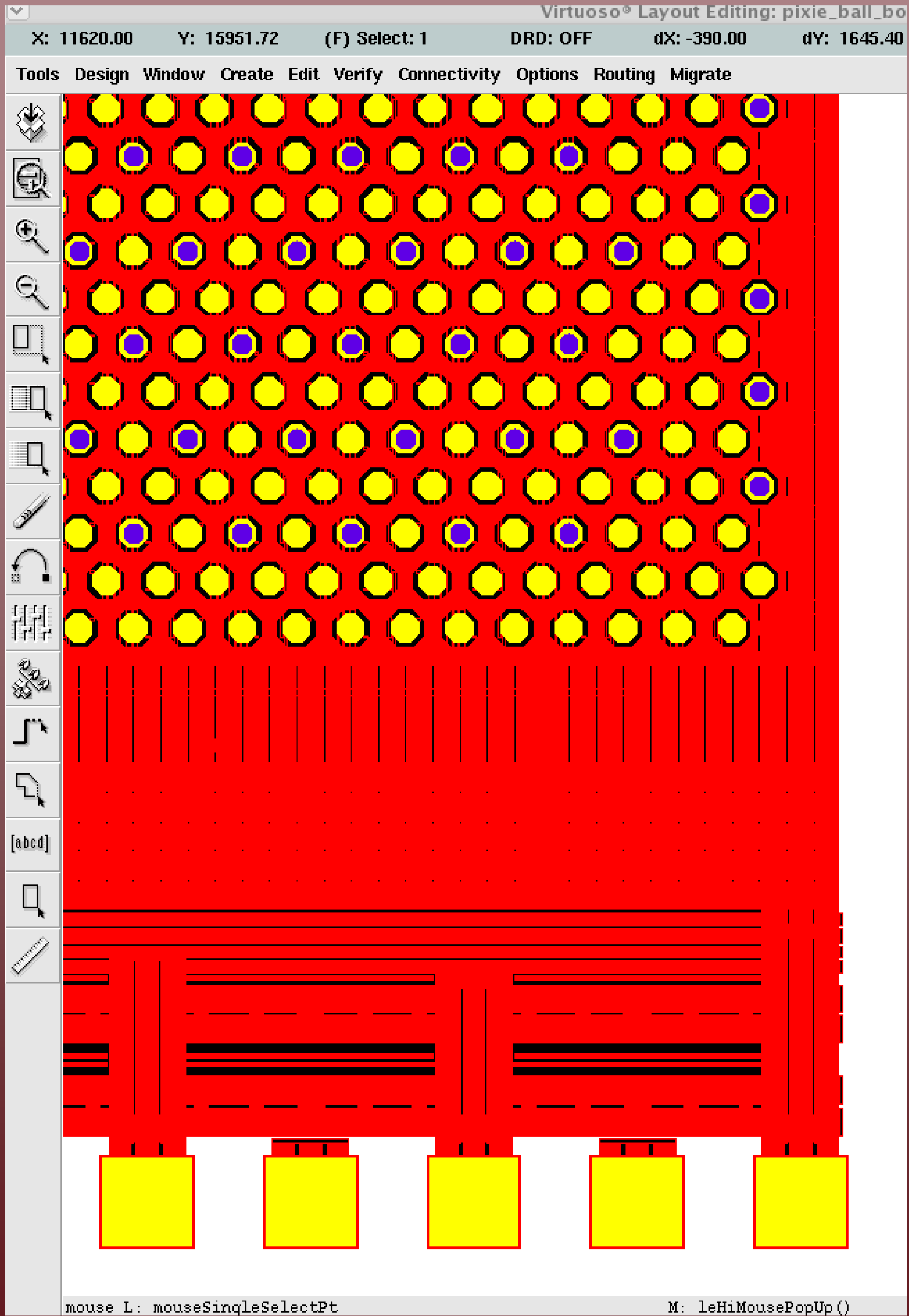

Large area CdTe Schottky type
(27.7 x 24.2 x 0.5 mm)
(ACRORAD)

Electrode structure:
- AlN
- Au-Ni-Au
- Pt
- Cdte
- In
- Ti

Pixel pitch
CdTe crystal = 80 µm
ASIC = 40µm
⇓
Only 1 out of 4 pixel is bump bonded to the crystal (AJAT)

Extremely low dark current @ operating voltages (400-700V)

Stability under HV obtained by switching HV off for a few seconds every half an hour.

Resolution pattern

Image size: 24mm ×27.7mm

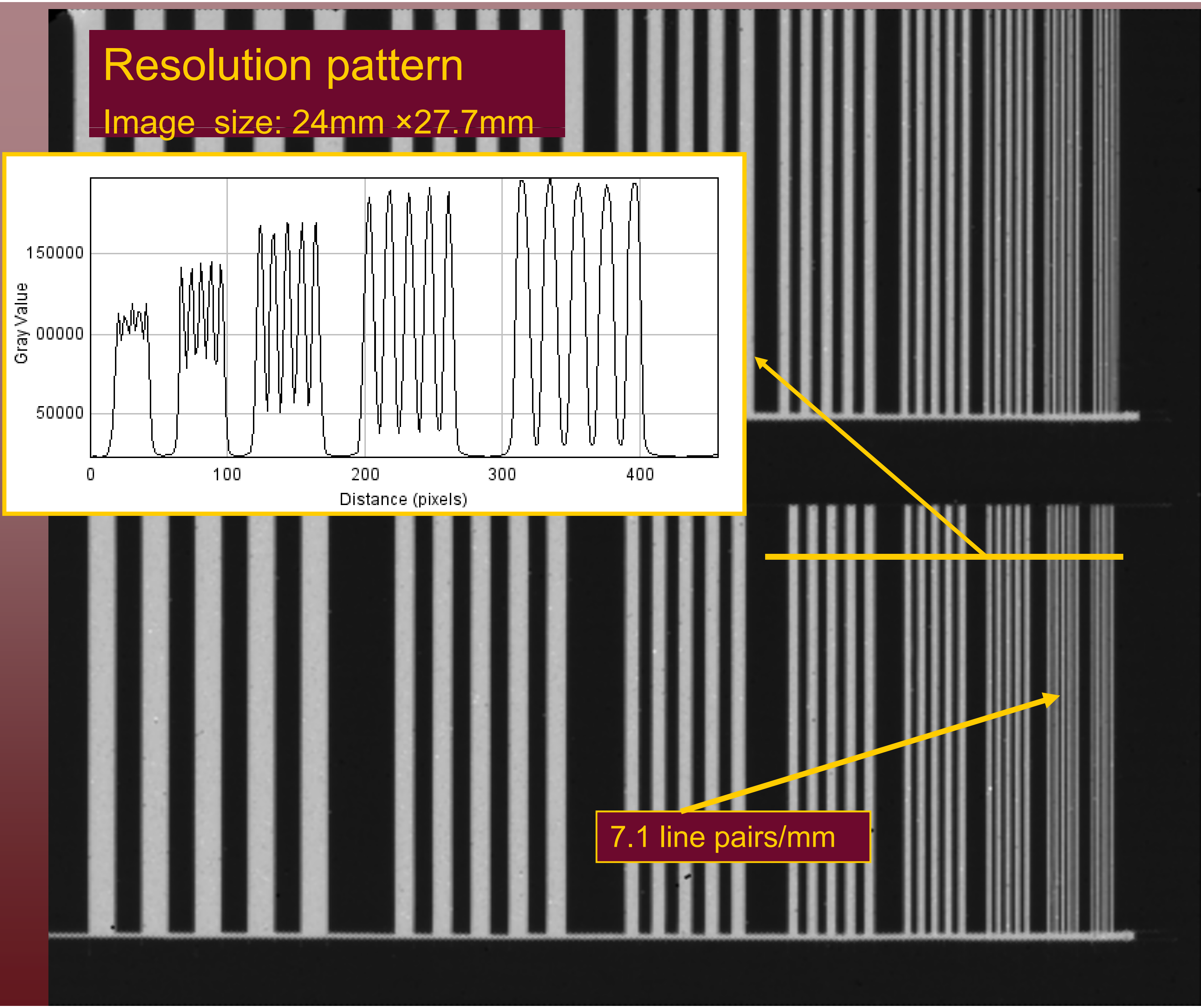

Resolution pattern

Image size: 24mm ×27.7mm

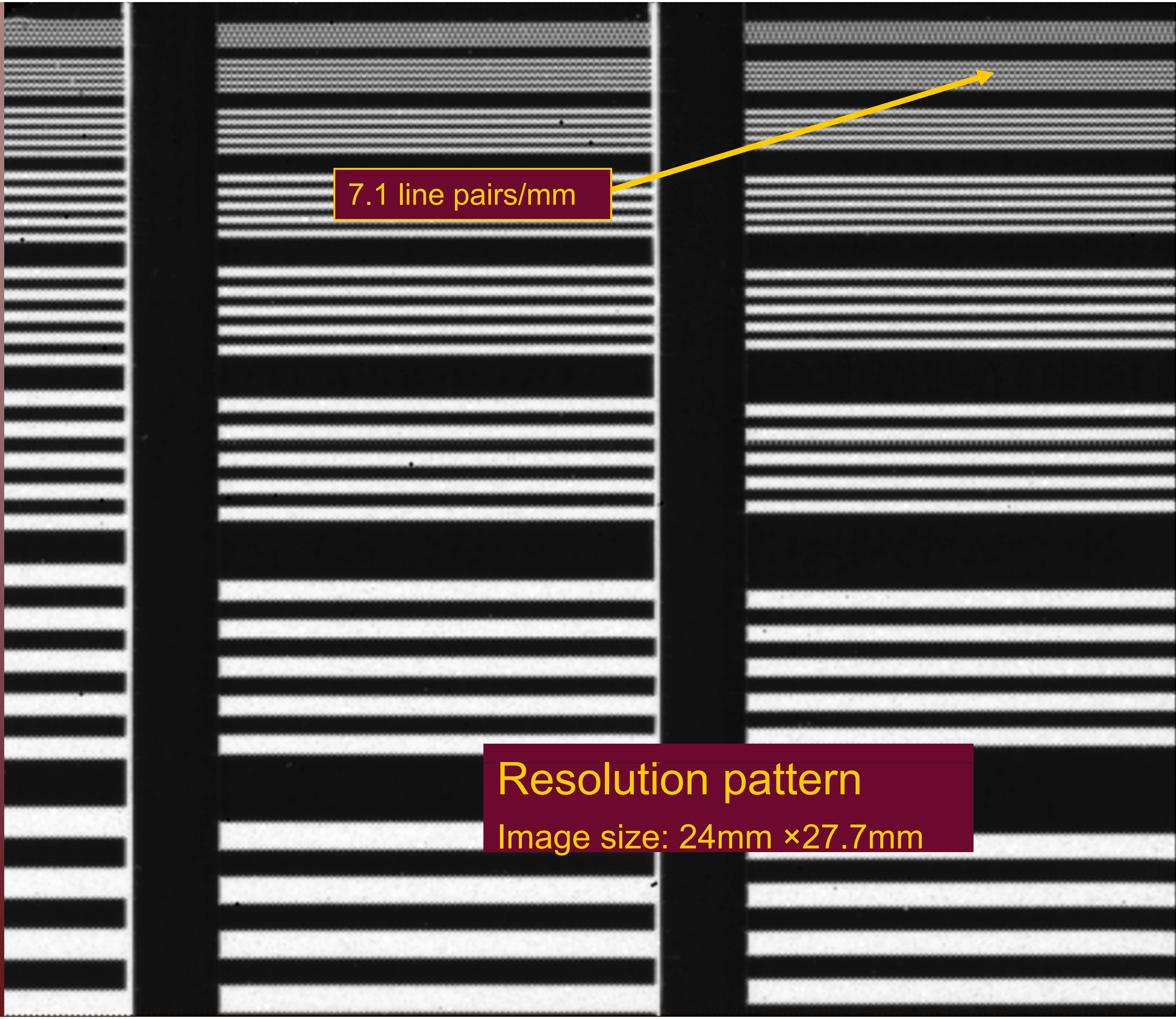

Resolution pattern

Image size: 24mm ×27.7mm

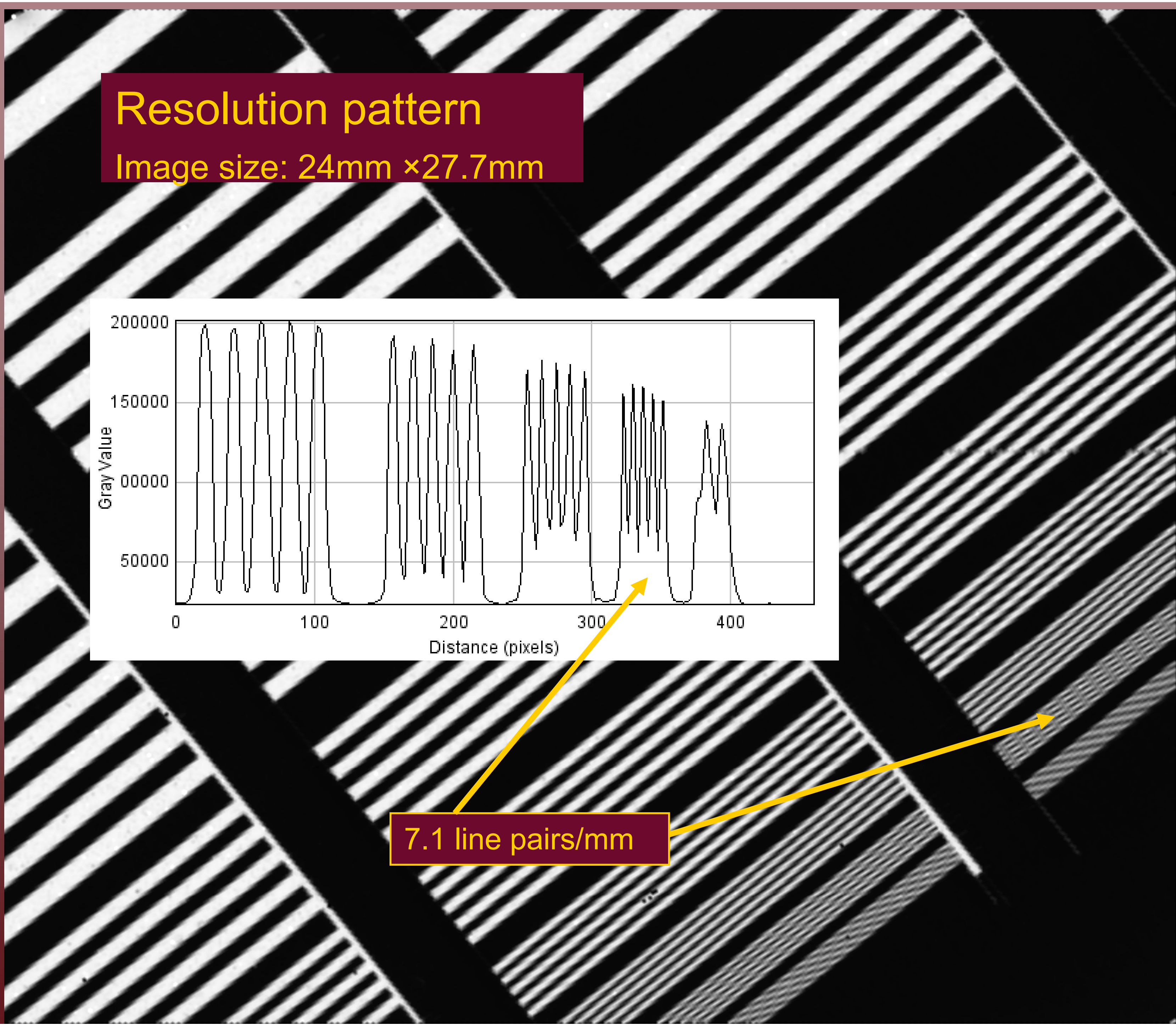

IMAGE GALLERY

Integrated circuit on a plastic package

High and very low contrast structures visible on the same image

35 kV Cr-tube

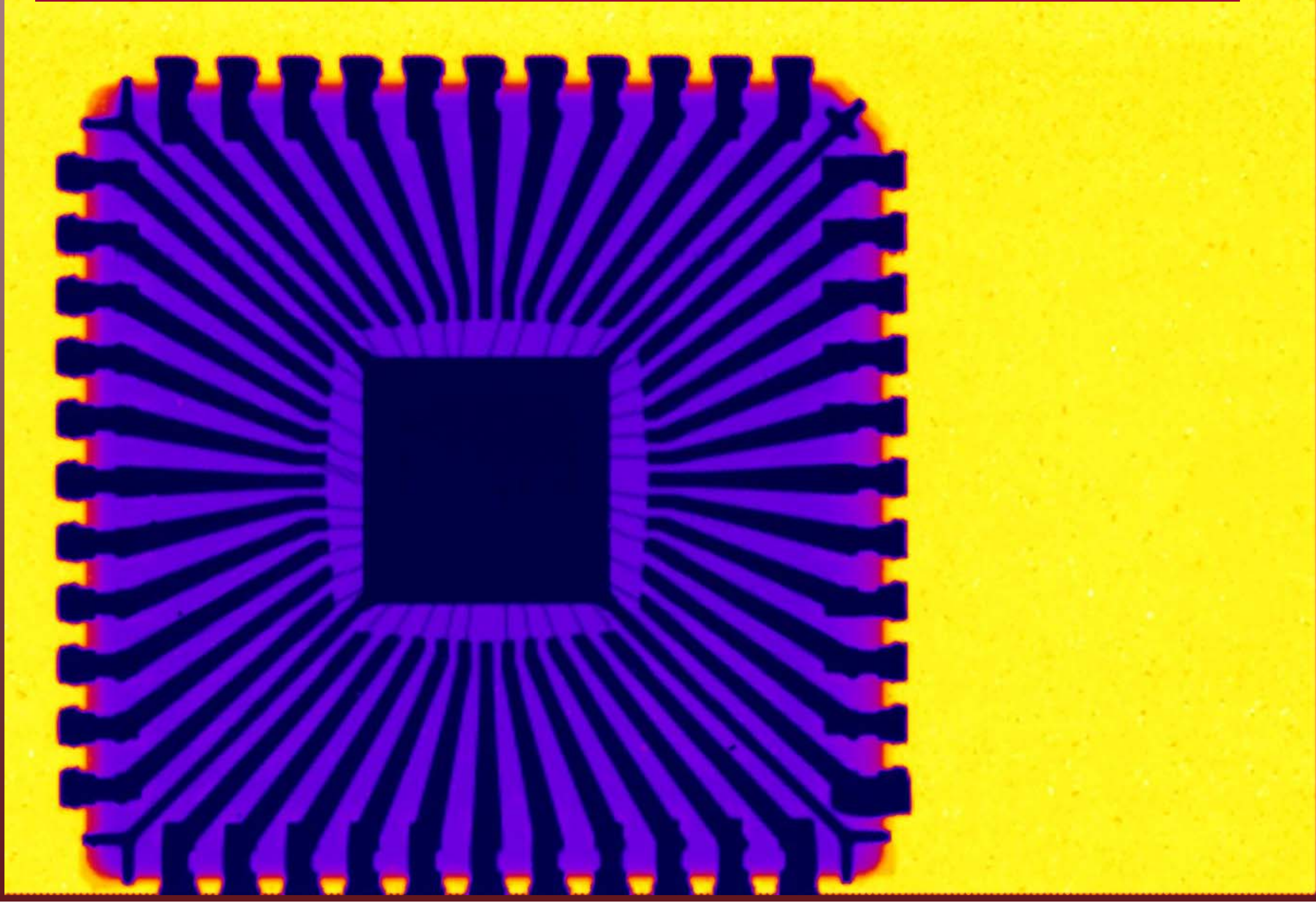

IMAGE GALLERY

Large area ASIC in ceramic package

High and extremely low contrast structures visible on the same image

35 kV Cr-tube

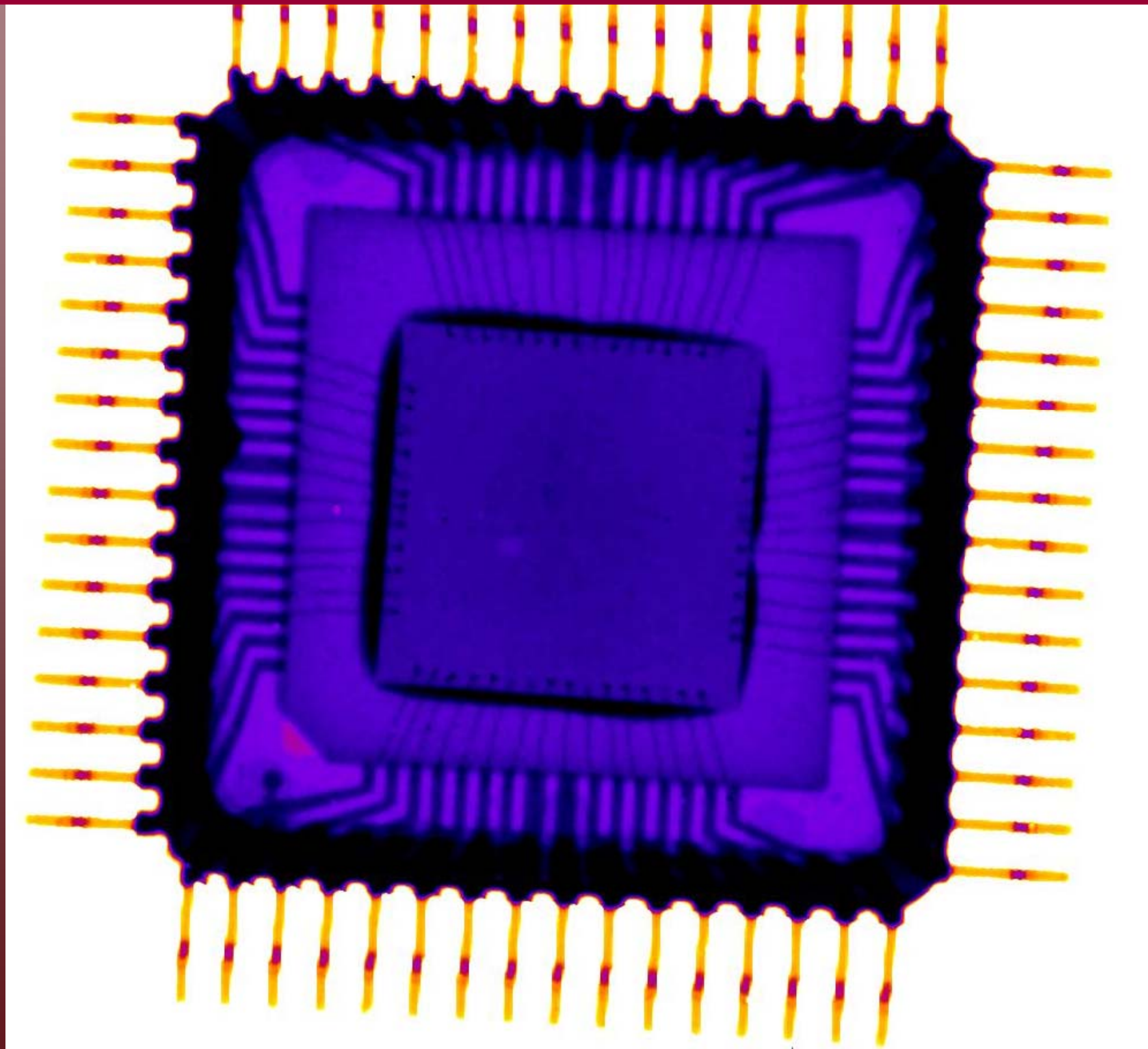

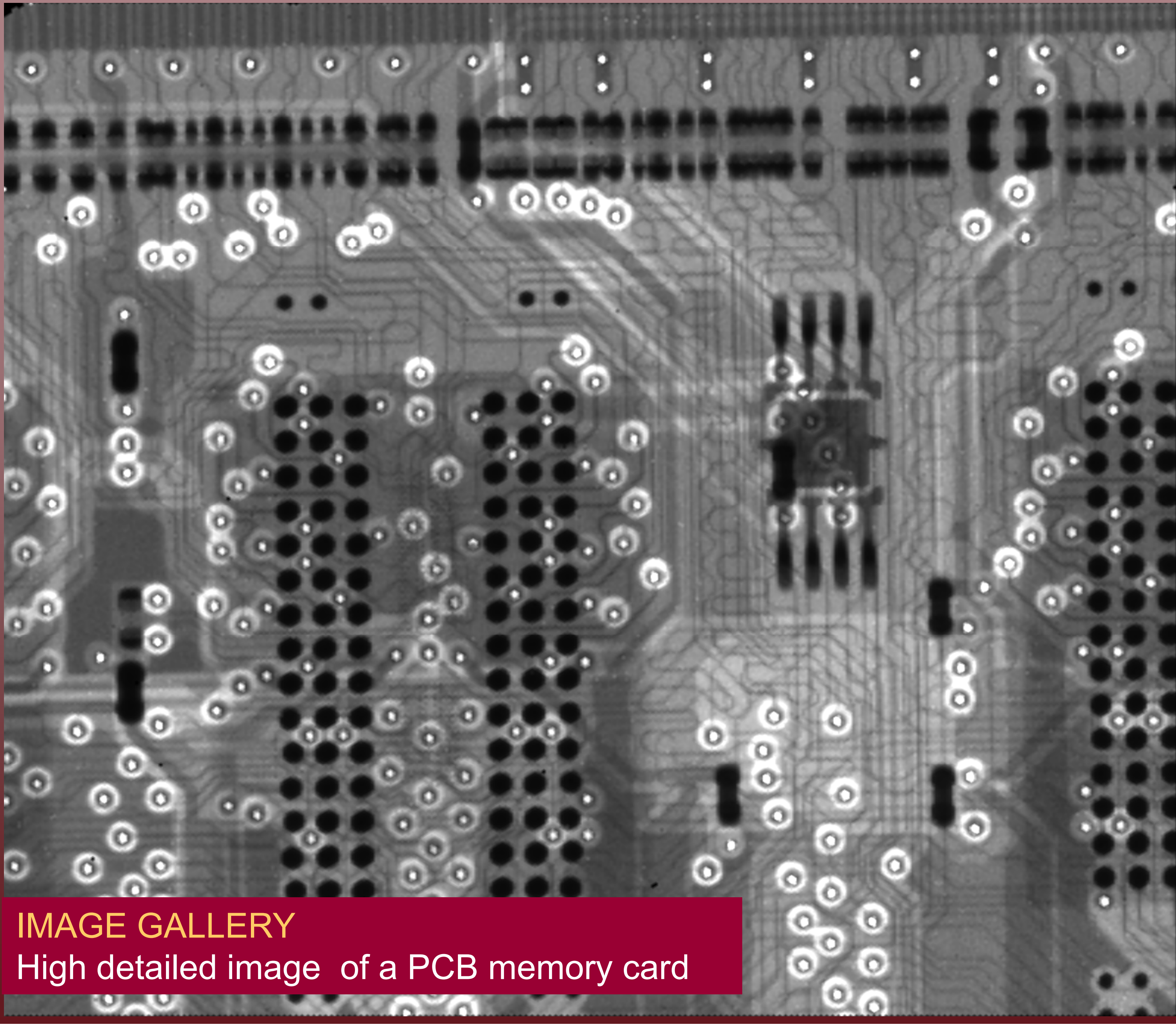

IMAGE GALLERY

High detailed image of a PCB memory card

IMAGE GALLERY

High resolution imaging of a biological sample (high statistics)

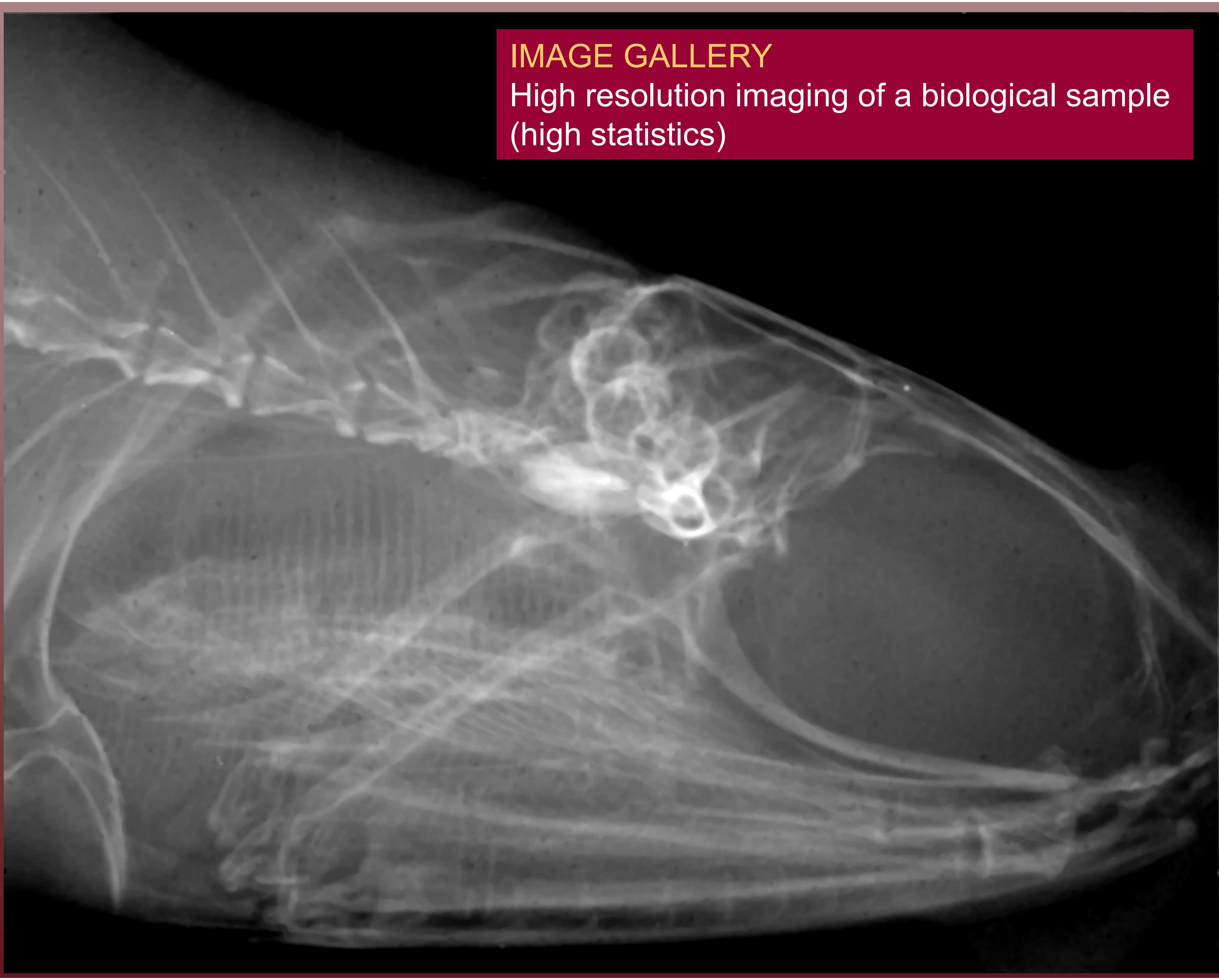

IMAGE GALLERY

High resolution imaging of a biological sample

Statistics acquired in 800 ms, typical mammography exposure time

Average pixel counting rate: 15 kHz - Cr-tube @25 kV

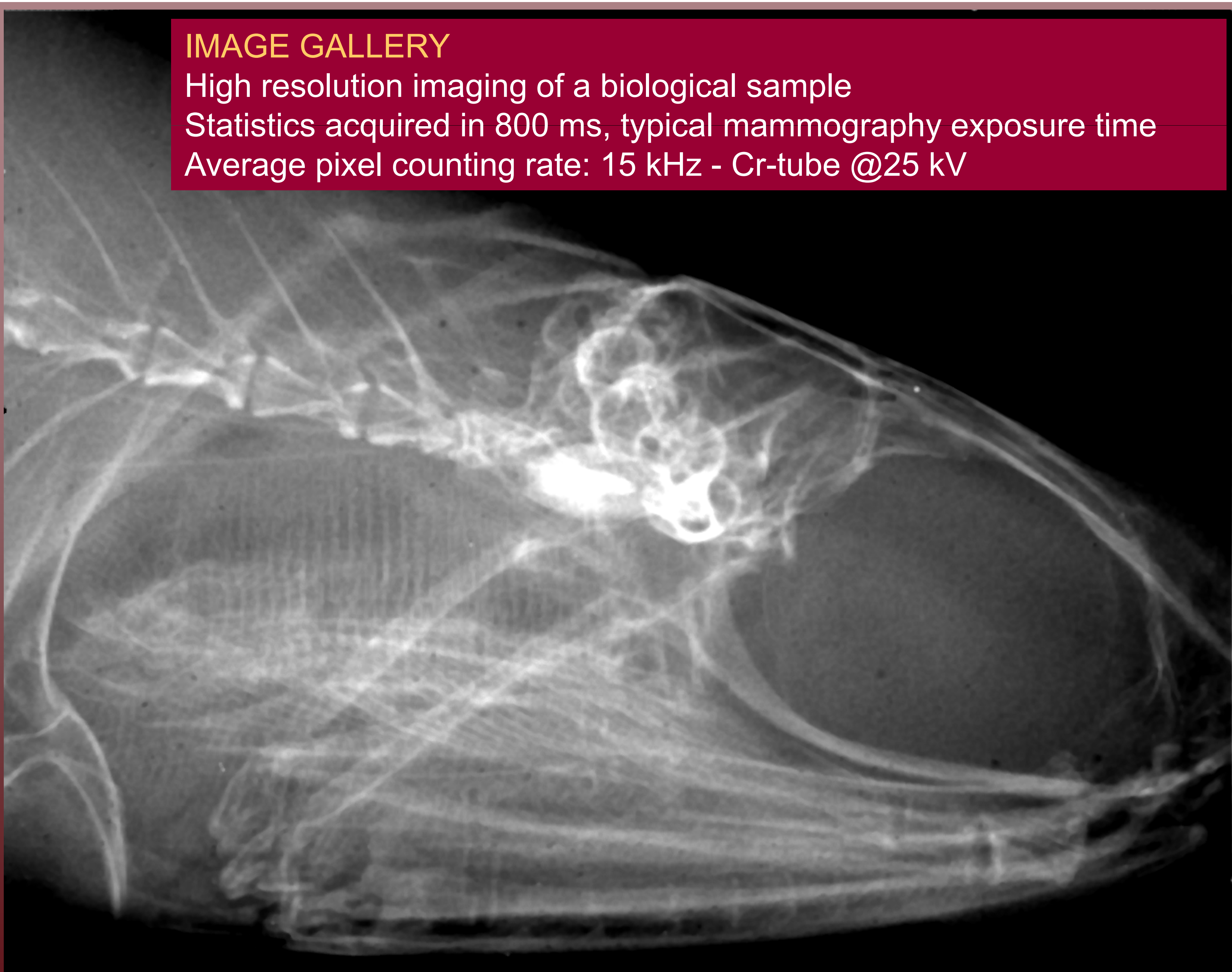

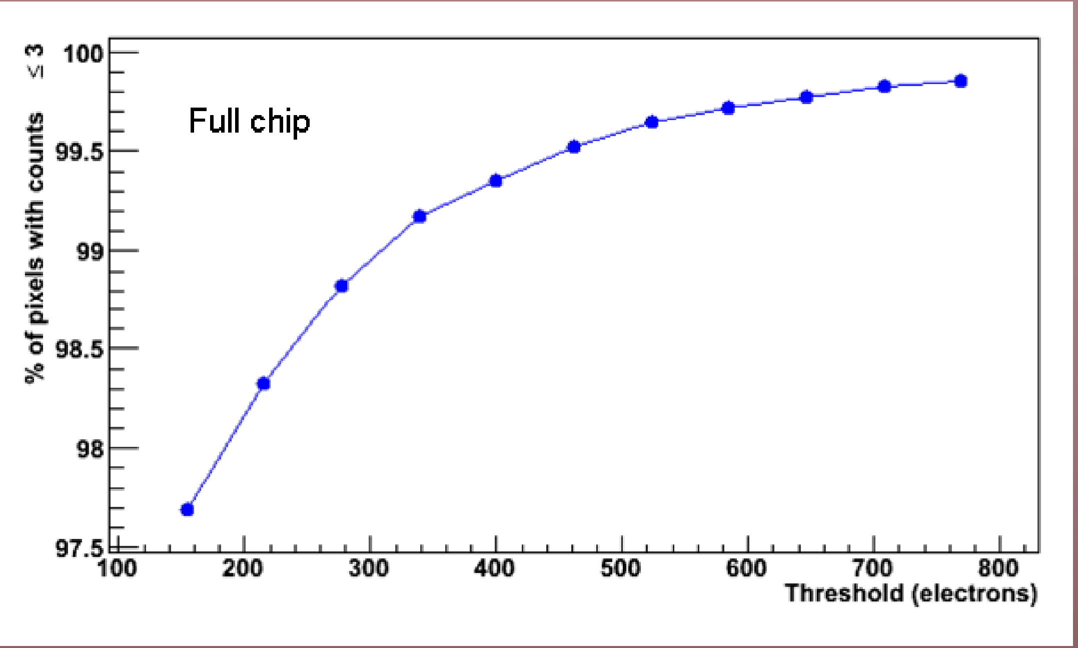
Full chip
% of pixels with counts ≤ 3
100
99.5
99
98.5
98
97.5
100
200
300
400
500
600
700
800
Threshold (electrons)

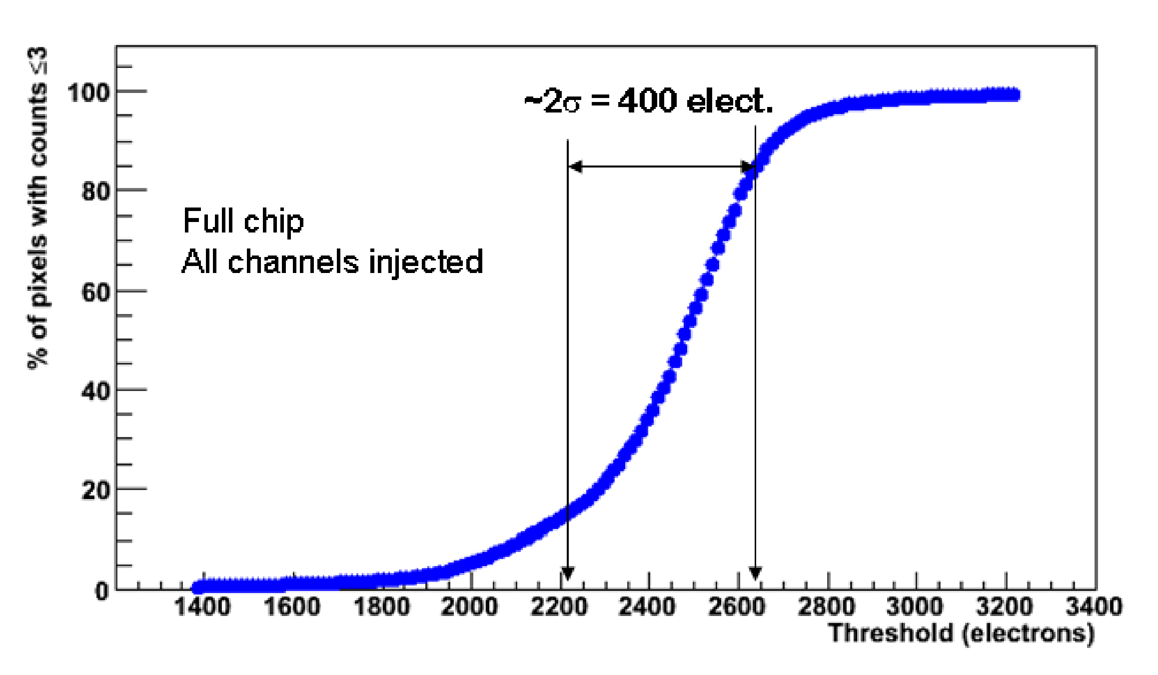
~2σ = 400 elect.
Full chip
All channels injected
% of pixels with counts ≤3
100
80
60
40
20
0
1400
1600
1800
2000
2200
2400
2600
2800
3000
3200
3400
Threshold (electrons)

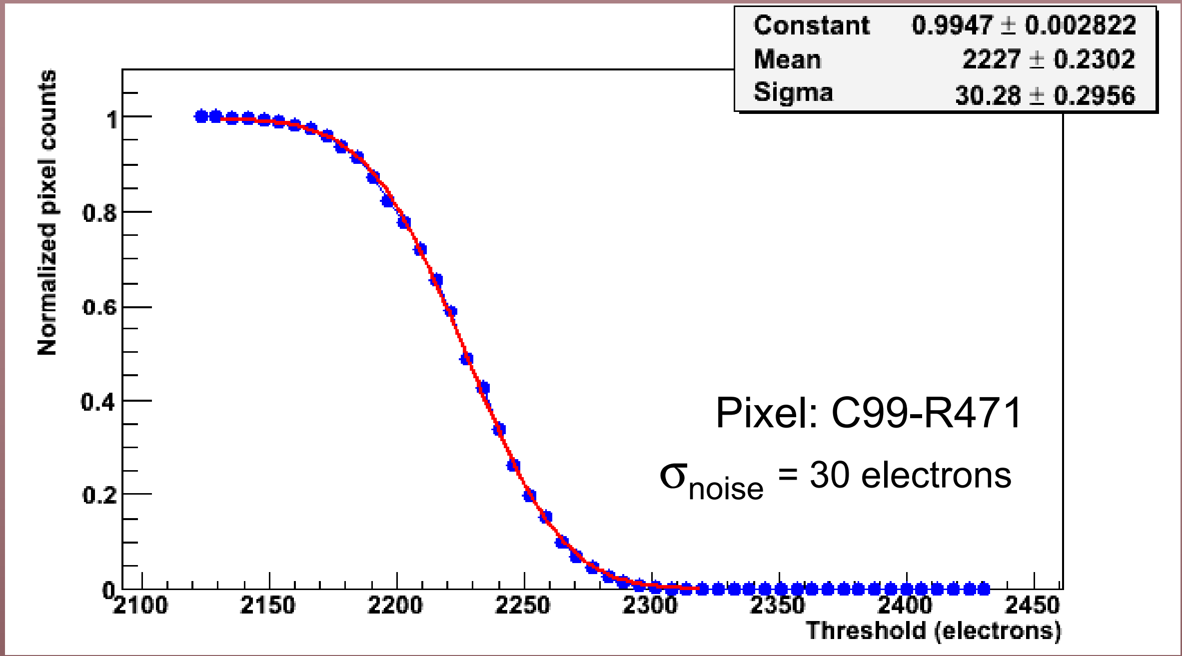

Constant 0.9947 ± 0.002822
Mean 2227 ± 0.2302
Sigma 30.28 ± 0.2956
Normalized pixel counts
0
0.2
0.4
0.6
0.8
1
2100
2150
2200
2250
2300
2350
2400
2450
Threshold (electrons)
Pixel: C99-R471
σnoise = 30 electrons

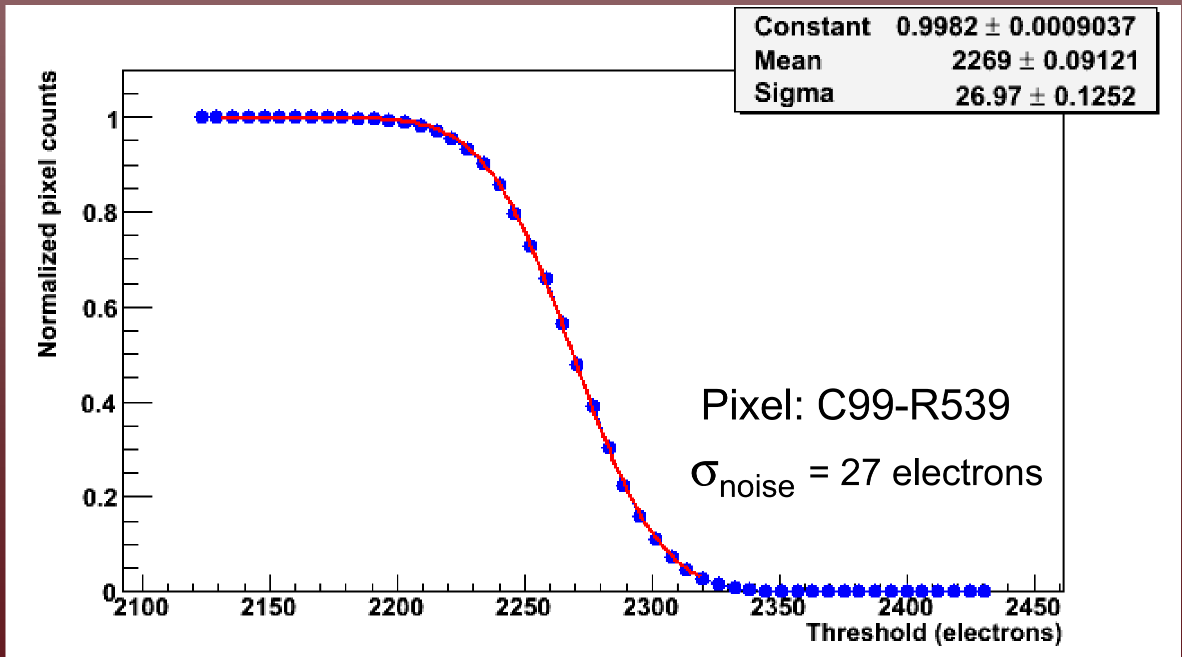

Constant 0.9982 ± 0.0009037
Mean 2269 ± 0.09121
Sigma 26.97 ± 0.1252
Normalized pixel counts
0
0.2
0.4
0.6
0.8
1
2100
2150
2200
2250
2300
2350
2400
2450
Threshold (electrons)
Pixel: C99-R539
σnoise = 27 electrons

Reflective Photocathode

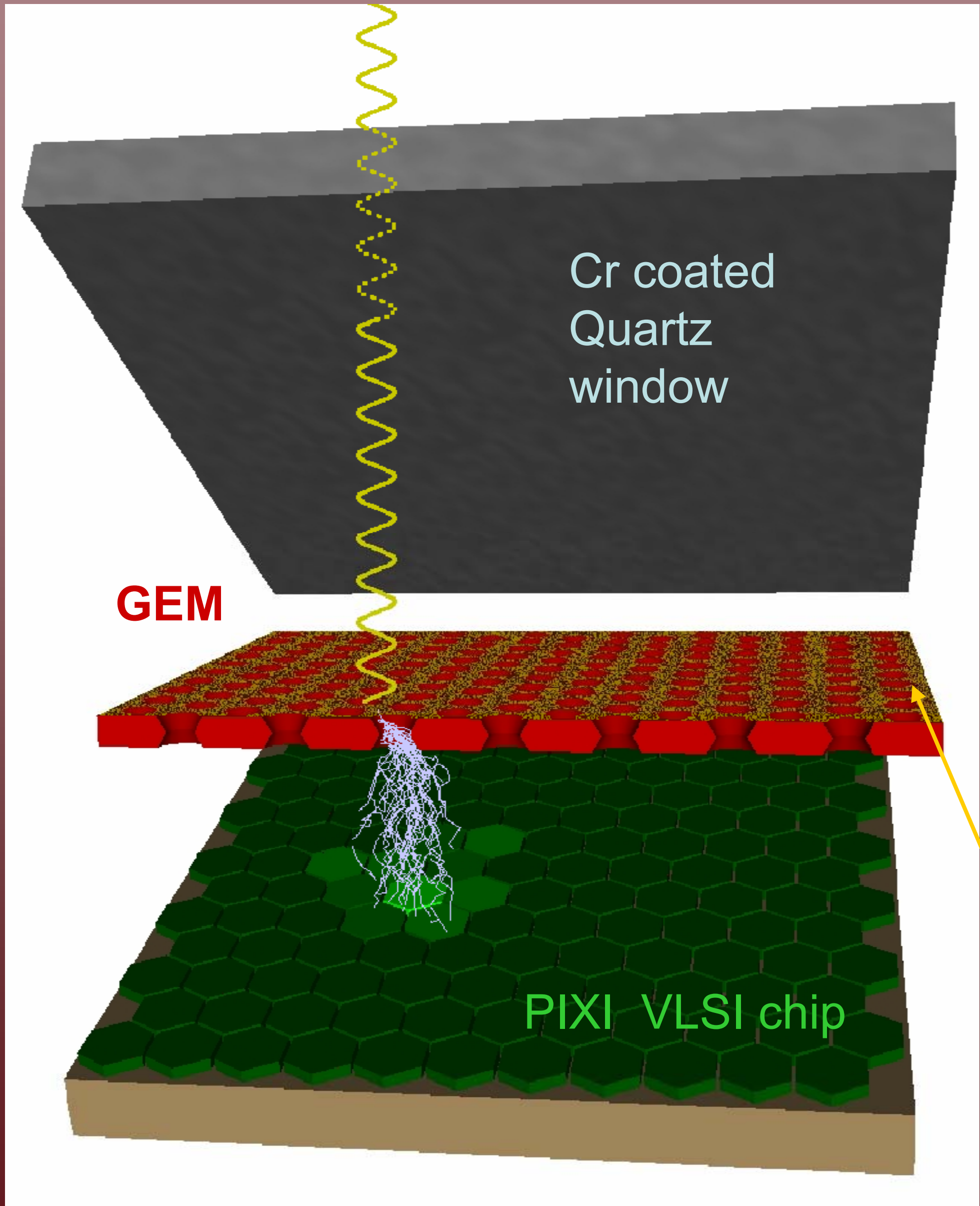

Drift gap = 1 mm
Transfer gap = 1mm
GEM thickness = 50 μm
GEM pitch = 50 μm

Pros:
- Thick film → high Q.E. (10-20%)

Cons:
- More complicated to build
- Special gold coating on the GEM
- Low geometrical efficiency (in our case 50%)
- Lower gas gain

CsI photocathode

0.18 μm ASIC features

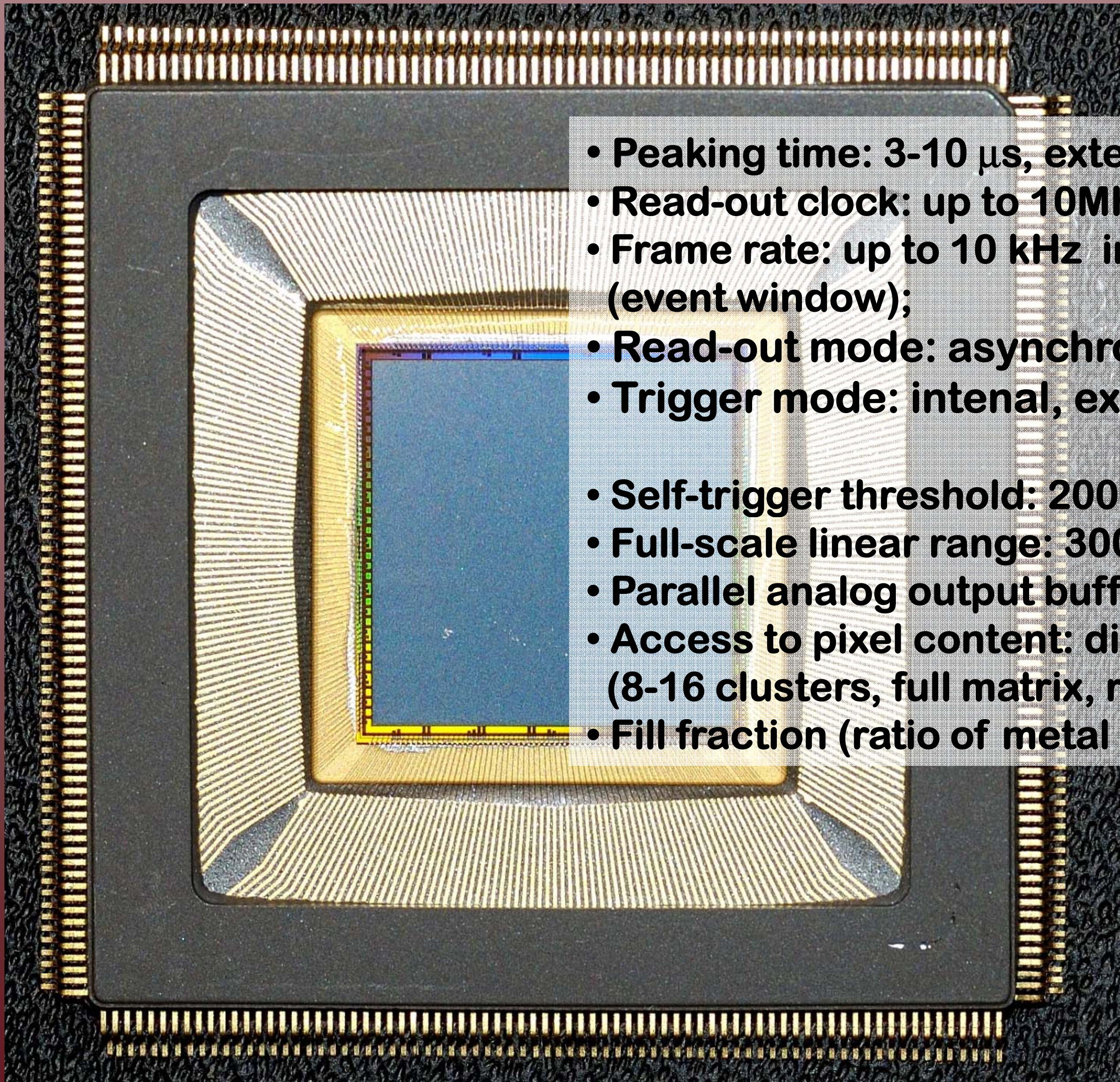

- Peaking time: 3-10 μs, externally adjustable;
- Read-out clock: up to 10MHz;
- Frame rate: up to 10 kHz in self-trigger mode (event window);
- Read-out mode: asynchronous or synchronous;
- Trigger mode: intenal, external or self-trigger;

- Self-trigger threshold: 2000 electrons;
- Full-scale linear range: 30000 electrons;
- Parallel analog output buffers: 1, 8 or 16;
- Access to pixel content: direct (single pixel) or serial (8-16 clusters, full matrix, region of interest);
- Fill fraction (ratio of metal area to active area): 92%

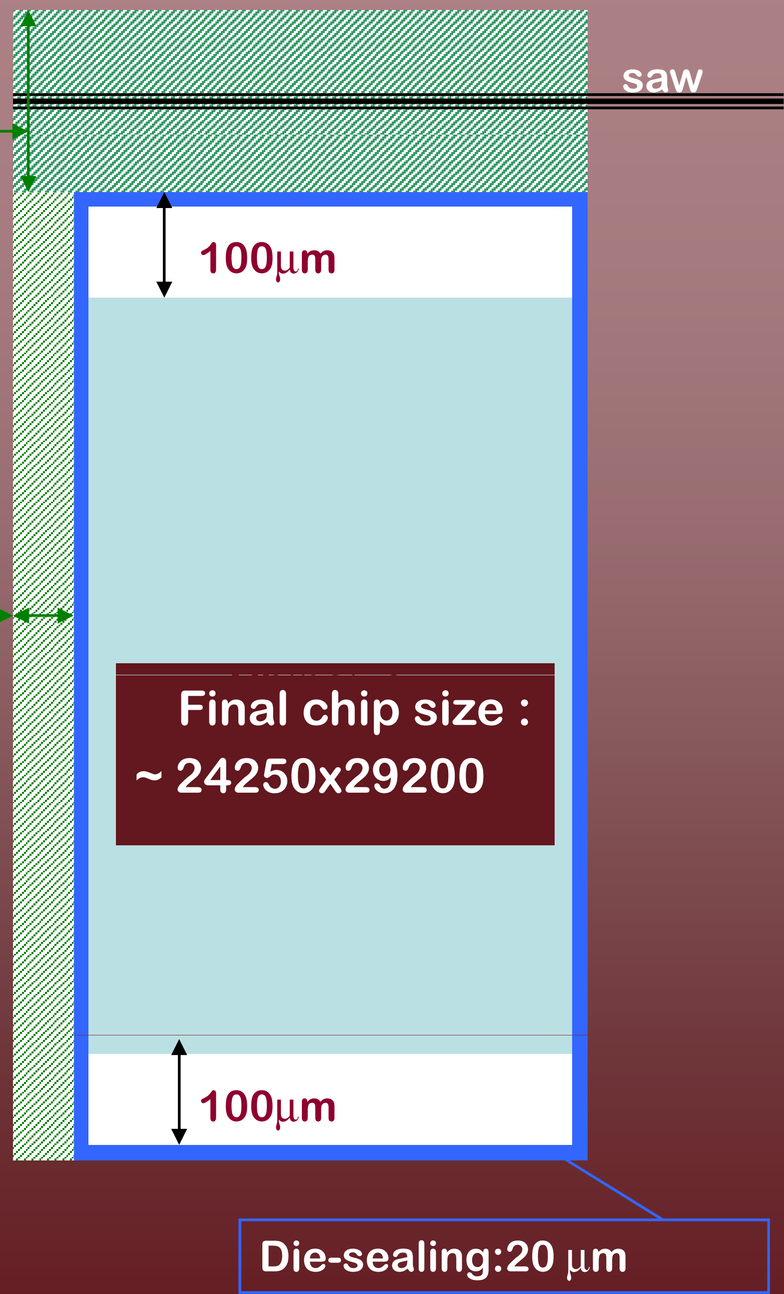

The ASIC mask has been laid out by using *scanner technology* instead of stepper technology

The counting ASIC features

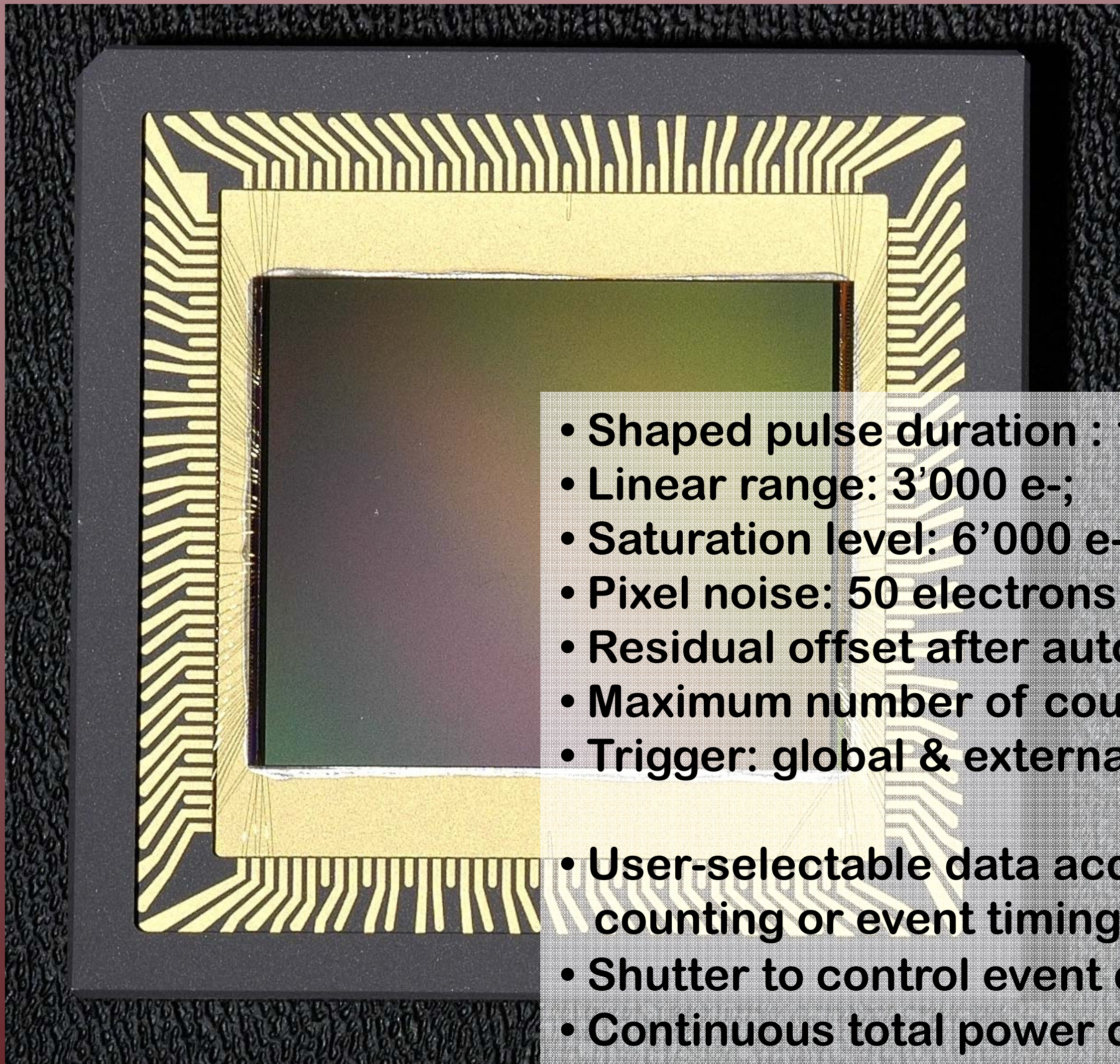

- Shaped pulse duration : 1μs (externally adjustable) ;
- Linear range: 3'000 e-;
- Saturation level: 6'000 e-;
- Pixel noise: 50 electrons ENC;
- Residual offset after auto-calibration: +/-30 e-;
- Maximum number of counts before reading: 32'768;
- Trigger: global & externally adjustable to > 200 e-;

- User-selectable data acquisition mode (per column): counting or event timing;
- Shutter to control event capture time slots;
- Continuous total power dissipation: < 3000 mW

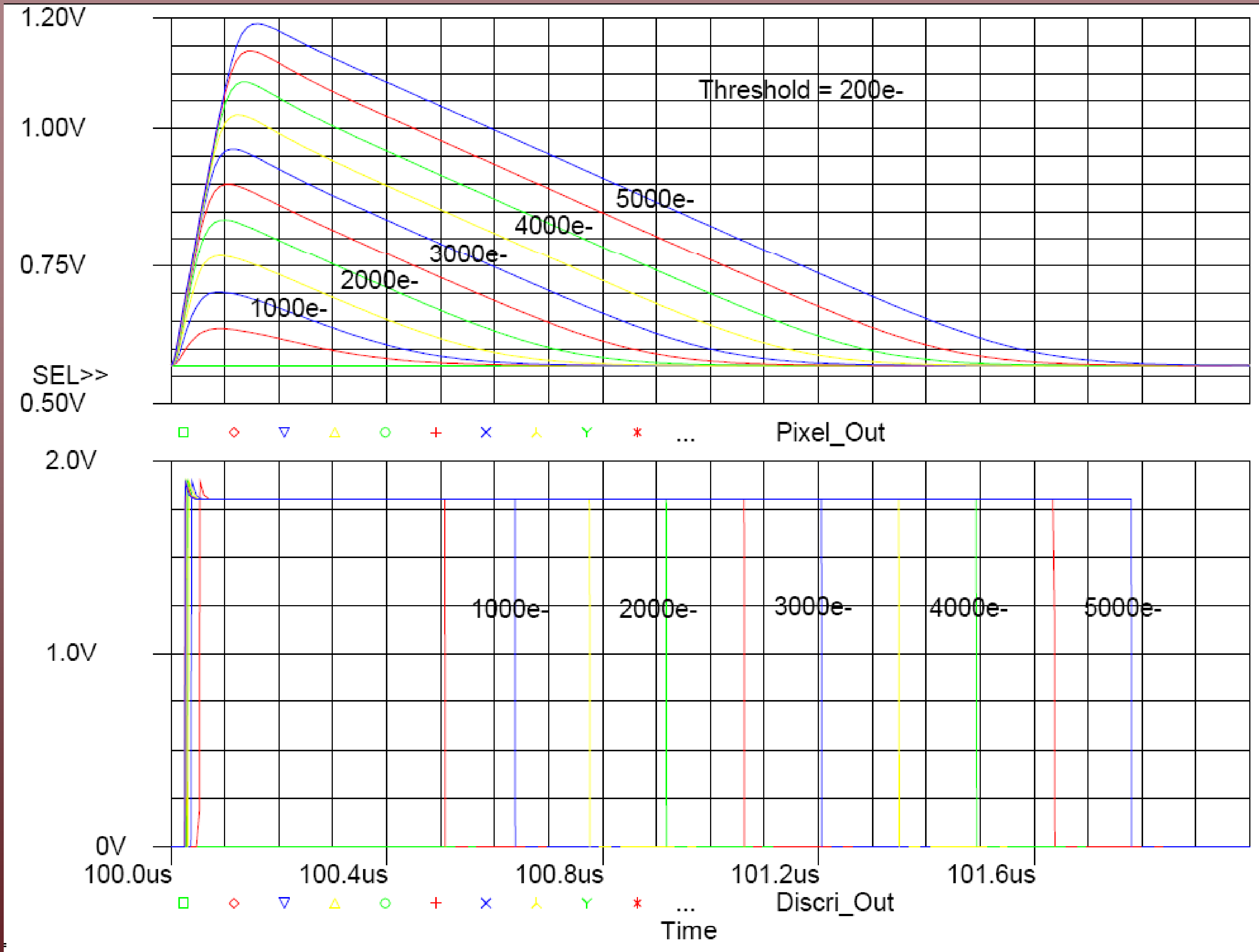

Pixel response to negative input charge

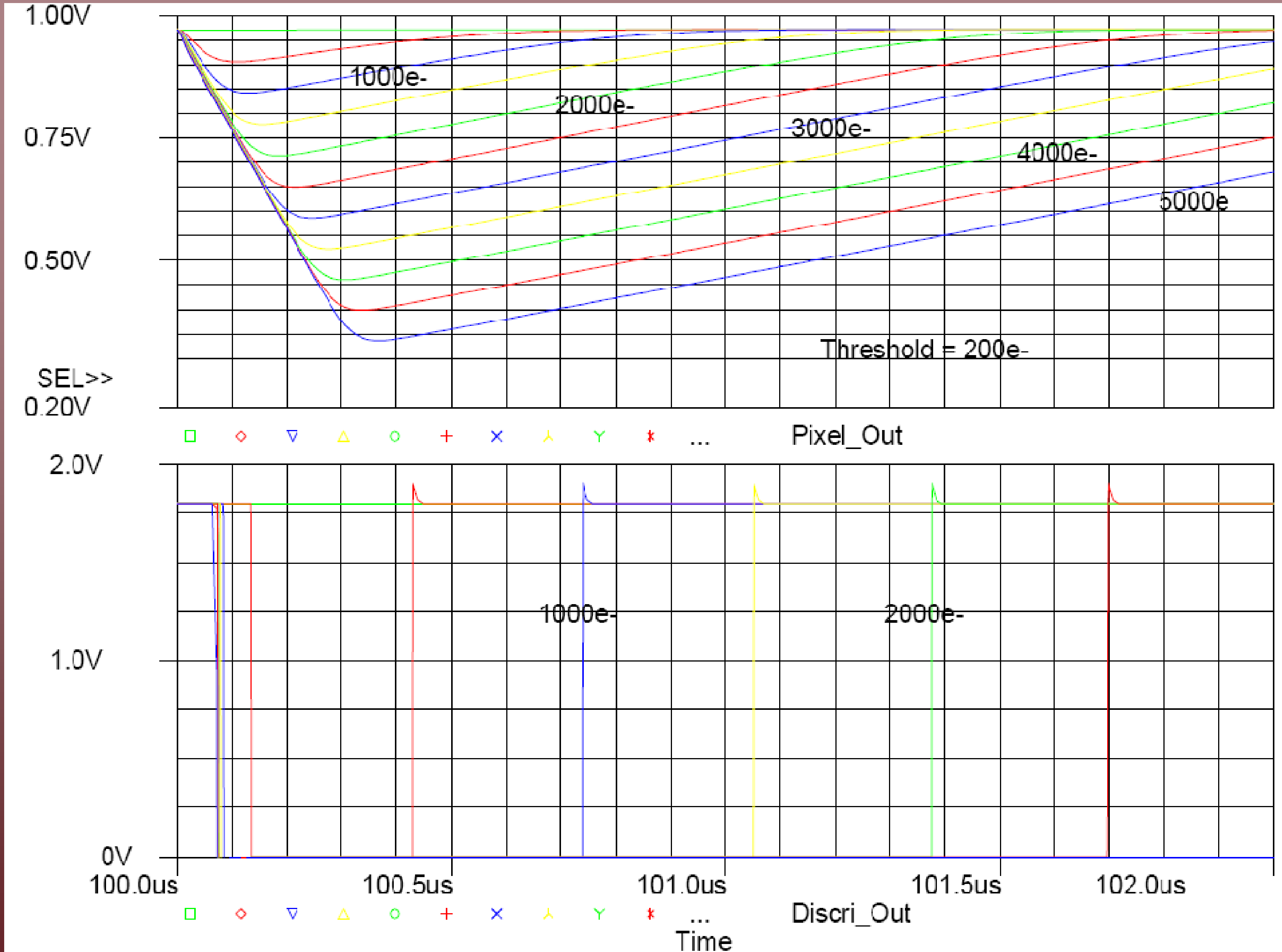

Pixel response to positive input charge

Autocalibration

Problem: in the case of very small pixels, i.e. pixels with extremely low parasitic capacitance, CSA/shaping amplifier & discriminators offsets become more important than noise.

Solution: on chip autocalibration circuit. A single sequencer is used to calibrate simultaneously all pixels in < 10ms.

Implementation *(30% of the pixel cell area):*

- 5-bit current DAC & autocal code storage register
- 120fF MOSFET & analog switches for CSA and discr
- some combinational logic

Autocal algorithm: a successive approximation algorithm.
The 5-bit DAC is a binary-weighted current source realizing the function
*Iout = (B4*1/2 + B3*1/4 + B2*1/8 + B1*1/16 + B0*1/32) * Iref*
The DAC output current Iout is added to the output current of the first stage of the discriminator equivalent to a programmable offset voltage at the discri input.

– The discr threshold is set to Vref (=AGnd).
– All bits are successively tried starting with the MSB (B4). If the discr output is high, B4 is returned to 0 (otherwise B4 is set to 1) and the related value is stored, then the procedure continues with next bit (B3), and so on.
– At the end the discr switching point is AGnd ±0.5LSB.
– Then the discr threshold level and the CSA gain are returned back to normal,